Title
Distributed Cooperative Spectrum Sensing for Overlay Self-organizing Dynamic Cognitive Radios Network Systems

Author
Chen, Chih-Kai

Publication Date
2012

Peer reviewed|Thesis/dissertation

UNIVERSITY OF CALIFORNIA

Los Angeles

Distributed Cooperative Spectrum Sensing for Overlay Self-organizing Dynamic Cognitive Radios Network Systems

A dissertation submitted in partial satisfaction of

the requirements for the degree Doctor of

Philosophy in Electrical Engineering

by

Chih-Kai Chen

2012

ABSTRACT OF THE DISSERTATION

Distributed Cooperative Spectrum Sensing for

Overlay Self-organizing Dynamic Cognitive Radios

Network Systems

by

Chih-Kai Chen

Doctor of Philosophy in Electrical Engineering

University of California, Los Angeles, 2012

Professor Kung Yao, Chair

Cognitive Radio Network (CRN) is an emerging technology to increase usages of the underutilized spectrum. Since cognitive radios (CR) join and leave CRN at will, as a dynamic secondary overlay network operating in the dynamic scenarios, CRN faces many new practical challenges. Spectrum sensing is a key functionality enabling dynamic spectrum management. Distributed cooperative spectrum sensing can

effectively overcome the hidden primary user issue. The performance of the distributed sensing scheme is affected by the number of collaborative CRs. In this dissertation, we analyze the performance of cooperative spectrum sensing for the dynamic CRN systems, which is a more realistic application scenario. Closed form exact expressions for the dynamic performance of distributed energy-based cooperative spectrum sensing over different fading channels are derived. These expressions enable the calculation of probability of detection and probability of false alarm efficiently tractable, and also provide a feasible approach for optimization of sensing performance. Quick performance evaluation is essential for CRN to achieve real-time adaptation to guarantee optimal system operations. We also study two promising applications for cognitive radio networks technologies: wireless cellular networks and public safety emergency networks. We analyze the performance of cooperative spectrum sensing in these two scenarios and the closed form expressions provide the framework to apply the cognitive radio networks technologies to perform online learning for self-organizing dynamic ad hoc cellular wireless system and public safety emergency networks system.

The dissertation of Chih-Kai Chen is approved.

_____

Lieven Vandenberghe

_____

Danijela Čabrić

_____

Henry Huang

_____

Kung Yao, Committee Chair

University of California, Los Angeles

2012

To my family.

Contents

List of Figures

Acknowledgements

I would like to begin by thanking my advisor, Professor Kung Yao, for his guidance, encouragement and financial support throughput the years of my research, and the members of my committee, Professors Lieven Vandenberghe, Danijela Čabrić, and Henry Huang, for the time they invested in helping me finish this dissertation. I would also like to thank Dr. Ralph E. Hudson and Dr. Flavio Lorenzelli for fruitful discussions and suggestions and Prof. Charles Taylor, Alex Kirschel and Yuan Yao for broadening my research horizon. Additionally, I send many thanks to lab-mates past and present: Bing Hwa Cheng, Chiao-En Chen, Shadnaz Asgari, Jing Z. Stafsudd, Wei-Ho Chung, Andreas M. Ali, Ni-Chun Wang, Juo-Yu Lee and Cheng-An Yang. Finally, to my family, who always asks me, "How are the radios going?" …Thanks, they're going well.

Vita

2001 B.S., Electronics Engineering
National Chiao Tung University, Taiwan

2005 M.S., Electrical Engineering
Stanford University

Publications

C. Chen and K. Yao, "Distributed Energy-based Spectrum Sensing for Cognitive Radio Public Safety Emergency Communications over Shadowed Fading Channels," submitted to *IEEE Transactions on Wireless Communications*.

C. Chen, R. E. Hudson and K. Yao, "Energy-based Cooperative Spectrum Sensing for Emergency Communications over Fading Channels in Cognitive Radio Public Safety Networks," in *Proc. IEEE Global Communications Conference*, Anaheim, California, December 2012.

C. Chen and K. Yao, "Cognitive Radios Methodology for Dynamic Spectrum Allocation in Broadband Wireless Cellular/Public Safety Network Systems," in *Proc. IEEE Global Communications Conference*, Anaheim, California, December 2012.

C. Chen and K. Yao, "Distributed Energy-based Spectrum Sensing with Opportunistic Cooperative Diversity for Cognitive Radio Networks over Non-Identical Fading Channels," in *Proc. IEEE Military Communications Conference*, Orlando, Florida, October 2012.

C. Chen, R. E. Hudson and K. Yao, "Spatially Distributed Energy-based Opportunistic Cooperative Spectrum Sensing in Cognitive Radio Networks," in *Proc. IEEE 2nd International Conference on Consumer Electronics, Communications and Networks*, pp.2866-2869, April 2012.

C. Chen, R. E. Hudson and K. Yao, "Modeling and Theoretical Performance Analysis for Dynamic Spatially Distributed Energy-based Spectrum Sensing in Cognitive Radios over Shadowed Fading Channels in Public Safety Networks," in *Proc. IEEE first International Workshop on Emerging Cognitive Radio Applications and Algorithms*, San Francisco, CA, June 2012. (Best Student Paper Award)

Chap 1
Introduction

The usage of radio spectrum resources and the regulation of radio emissions are coordinated by national regulatory bodies such as the Federal Communications Commission (FCC) in the U.S. The FCC assigns spectrum to licensed holders, also known as primary users, on a long-term basis for large geographical regions. However, a large portion of the assigned spectrum remains under utilized from many field measurements. The inefficient usage of the limited spectrum necessitates the development of dynamic spectrum access techniques, where users who have no spectrum licenses, also known as secondary users, are allowed to use the temporarily unused licensed spectrum. In recent years, the FCC has been considering more flexible and comprehensive uses of the available spectrum through the use of cognitive radio technology [1-1].

1.1 Standardization

The underutilization of the radio spectrum resource is an issue not only for US but also for many other countries. [1-2] Because of the promises of the efficient spectrum utilization,

cognitive radio technologies have already drawn much attention these years. Many experts are dedicated to develop standards related to cognitive radio-based wireless technologies.

1.1.1 IEEE 802.22 WG on Wireless Regional Area Networks [1-3]

The IEEE 802.22 Working Group (WG), the first worldwide wireless air interface standard committee formed in 2004 November, is chartered with the development of a Cognitive Radio-based Wireless Regional Area Network (WRAN) Physical (PHY) and Medium Access Control (MAC) layers for use by license-exempt devices in the spectrum that is currently allocated to the Television (TV) service. Since 802.22 reuses the fallow TV spectrum without causing any harmful interference, cognitive radio techniques are of primary importance in order to sense and measure the spectrum and detect the presence/absence of incumbent signals. Meanwhile, other advanced techniques which facilitate the coexistence are also included in IEEE 802.22 standards.

1.1.2 IEEE Standards Coordinating Committee 41 (IEEE SCC41) [1-4]

IEEE Standards Coordinating Committee 41 (IEEE SCC41), which is formerly recognized as IEEE 1900 Standards Committee jointly established by IEEE Communications Society (ComSoc) and the IEEE Electromagnetic Compatibility (EMC) Society, is currently seeking proposals for standards projects in the areas of dynamic spectrum access, cognitive radio, interference management, coordination of wireless systems, advanced spectrum management, and policy languages for next generation radio systems. The focus is on development of new technologies and methods of dynamic spectrum access to improve use of spectrum.

1.2 Cognitive Radio Concepts

Cognitive radio network is viewed as an intelligent wireless communication system which can dynamically utilize valuable radio spectrum without sacrificing licensed primary users' privileges. Since the primary users have the absolute rights to use licensed frequency bands at any time, cognitive radio networks should continuously monitor the radio spectrum utilization and vacate the frequency bands when the primary users arrive. By scanning the radio spectrum, cognitive radio networks can detect spectrum holes which are frequency bands assigned to primary users but not in use at particular times and geographic locations to construct a spectrum map. Then, based on this temporal-geographical spectrum map, the secondary users belong to the

cognitive radio networks opportunistically transmit data through those spectrum holes. Whenever a primary user resumes the service, the secondary users which may interfere with this primary user must be preempted immediately to guarantee primary users' spectrum utilization privileges. Therefore, spectrum sensing and interference prevention for dynamic spectrum management are key functionalities for the realization of cognitive radio networks.

1.2.1 Interference Control

As we know, the primary users paid to use their licensed frequency bands. They have the absolute privileges to use those resources at any time, even during the idle periods. Hence, cognitive radio users have to guarantee incumbent protection and effective coexistence to be allowed to reutilize these frequency bands as the secondary users. Ideally, these secondary users must provide interference-free environment for primary users. However, this severe restriction won't be able to be accomplished in practical scenarios. Meanwhile, in many cases, this severe restriction is not necessary and obstructs the development of cognitive radio networks to improve precious spectrum utilization efficiency. However, the tolerable interference duration and level have to be promised.

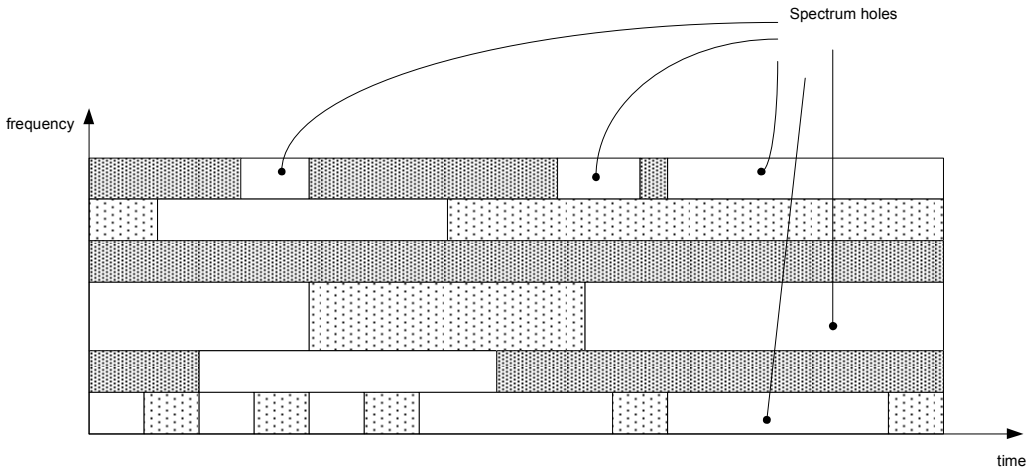

Figure 1-1 Dynamic Spectrum Utilization Map

1.3 Spectrum Sensing

Current wireless communication systems are operated in their own licensed frequency bands without concerns on out-of-the-band activities. However, because of the adaptation nature of cognitive radio networks, the temporal-geographical spectrum utilization map has to be constructed by detecting the spectrum holes [Figure 1-1]. This important functionality is called as spectrum sensing. Spectrum sensing is a key functionality in cognitive radio network to prevent from the interference to the licensed primary users and also to exploit the potential spectrum utilization to improve the spectrum efficiency [1-5]. Spectrum sensing can be classified into three different categorizes:

1.3.1 Matched Filter Detection

This is done by correlator-based pilot detection. This method is shown as the optimal detection scheme for coherent communication systems [1-6]. The performance for this scheme is highly dependent of the synchronization. However, cognitive radio network has to monitor numerous different primary users which are not synchronized to each other. To pursue reliable spectrum sensing requires a corresponding synchronizer to each primary user. Thus, the hardware complexity increases dramatically because of good synchronization constraint and a large number of primary users.

1.3.2 Energy Detection

This is shown as an optimal detection scheme for non-coherent communication systems [1-7]. This method doesn't require synchronization and seems as a good scheme for spectrum sensing. However, the actual noise doesn't follow the theoretical stationary Gaussian assumption and the noise power varies in negative signal-to-noise ratio regime. Meanwhile, without loss of generality, the receiver cannot distinguish which part is signal and which part is noise in the

received signal. The above reasons make the threshold setting very challenging such that reliable spectrum sensing becomes impractical especially in negative SNR scenarios.

1.3.3 Cyclostationary Feature Detection

This method exploits cyclostationary characteristics of received signals. Considering the physical properties of the propagation loss in transmission channel, signals are in general modulated in the transmitter end and then demodulated in the receiver end. The signals are normally modulated by a sinusoidal carrier waveform, pulse trains, or spreading sequences. For OFDM communication systems, the cyclic prefixes are inserted in the transmitted signals. These above operations introduce the transmitted signals built-in periodicity. This embedded periodicity is usually exploited by a receiver to perform detection or parameter estimation [1-8], [1-9], [1-10], and [1-11]. Hence, the original data can be modeled as a wide-sense stationary process, but the modulated transmitted signal is characterized as a cyclostationary process. The cyclostationary feature detector exploits this observation and can provide more robust detection performance than energy-based detector under very low signal-to-noise ratio situations, which is one of the major challenges for cognitive radio networks design.

1.4 Cooperative Spectrum Sensing [1-12]

The performance of spectrum sensing is limited by noise uncertainty, shadowing, and multi-path fading effect. When the received primary SNR is too low, there exists a SNR wall, below which reliable spectrum detection is impossible even with a very long sensing time. If secondary users cannot detect the primary transmitter, while the primary receiver is within the secondary users' transmission range, a hidden primary user problem will occur, and the primary user's transmission will be interfered.

By taking advantage of the independent fading channels (i.e., spatial diversity) and multiuser diversity, cooperative spectrum sensing is proposed to improve the reliability of spectrum sensing, increase the detection probability to better protect a primary user from interference, and reduce false alarm to utilize the idle spectrum more efficiently. In centralized cooperative spectrum sensing, a central controller, e.g., a secondary base station, collects local observations from multiple secondary users, decides the available spectrum channels using some decision fusion rule, and informs the secondary users which channels to access. The theoretical analysis and empirical data in the literatures both demonstrate substantial improvement on the performance of spectrum sensing via exploring the spatial diversity.

1.5 Dynamic Cognitive Radio Networks

Spatially distributed cooperative spectrum sensing schemes can effectively resolve the hidden primary user issue. However, the mobile users opportunistically turn on and off the CR functionalities at will to access the potential spectrum utilizations. Since CRs join and leave a CRN at will, the number of CRs in the cooperative spectrum sensing is indeed random. The probability of miss detection (P_m) is an important reliability metric in CRN. Higher P_m means CRN might cause more interference with the existing primary privileged spectrum utilization, which is not allowed. In this dissertation, we will analyze the performance of spatially distributed cooperative spectrum sensing for the dynamic cognitive radio networks and also study two promising cognitive radio network technology applications: cellular wireless networks and public safety emergency networks.

References

[1-1] "Facilitating opportunities for flexible, efficient and reliable spectrum use employing cognitive radio technologies: Notice of proposed rule making and order," FCC Dec. 2003, FCC Doc. ET Docket No. 03-108.

[1-2] J. Walko, "Cognitive Radio," *IEE Review*, Vol. 51, Issue 5, May 2005.

[1-3] [Online]. Available: http://ieee802.org/22/

[1-4] [Online]. Available: http://www.ieeep1900.org/

[1-5] J. Ma, G. Y. Li, and B. H. Juang, "Signal Processing in Cognitive Radio," *Proceedings of the IEEE*, Vol. 97, Issue 5, May 2009.

[1-6] K. Yao, *EE230A Estimation and Detection in Communication and Radar Engineering Lecture Notes*, UCLA, Fall 2011.

[1-7] J. Proakis, *Digital Communications*, 4th ed. Mc-Graw Hill, 2001.

[1-8] A. V. Dandawate and G. B. Giannakis, "Statistical test for presence of cyclostationarity," *IEEE Transactions on Signal Processing*, vol. 42, September 1994.

[1-9] W. A. Gardner, "Spectral correlation of modulated signals: Part I – analog modulation," *IEEE Transactions on Communications*, vol. 35, June 1987.

[1-10] W. A. Gardner, W. A. Brown, and C. K. Chen, "Spectral correlation of modulated signals: Part II – digital modulation," *IEEE Transactions on Communications*, vol. 35, June 1987.

[1-11] W. A. Gardner, "Signal interception: A unifying theoretical framework for feature detection," *IEEE Transactions on Communications*, vol. 36, August 1986.

[1-12] Y. C. Liang, K. C. Chen, G. Y. Li, and P. Mähönen, "Cognitive radio networking and communications: an overview," *IEEE Trans. on Vehicular Tech.*, Vol. 60, Issue 7, 2011.

Chap 2
Cooperative Spectrum Sensing

In spectrum sensing, statistical hypothesis testing is typically used to test the sensing results for the binary decision on the presence/absence of primary users. To detect the primary signal, energy detection based on the sensed energy is the most popular sensing technology in cooperative sensing, due to its simplicity and no requirement on a priori knowledge of primary user signals. However, detection performance in practice is often compromised with multipath fading, shadowing and receiver uncertainty issues. To mitigate the impact of these problems, cooperative spectrum sensing has been proved to be an effective method to improve the detection performance.

The aim of cooperative spectrum sensing is to enhance the sensing performance by exploiting the spatial diversity in the observations of spatially located CR users. Through sharing sensing information from each other by collaboration, CR users can make a more accurate global decision than individual local decisions [2-1].

2.1 Multipath Fading and Receiver Uncertainty

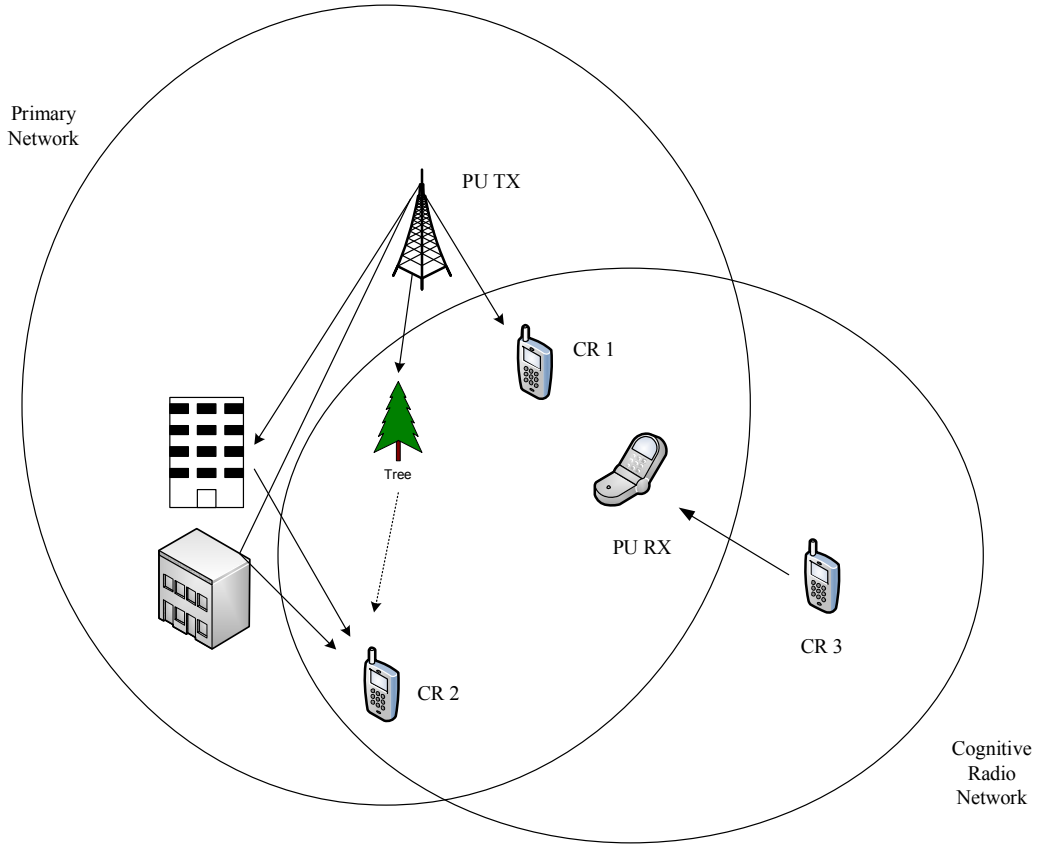

Figure 2-1. Multipath Fading and Receiver Uncertainty

Many factors such as multipath fading, shadowing, and receiver uncertainty problem make detection performance worse in spectrum sensing. In Figure 2-1, a scenario involved multipath fading, shadowing, and receiver uncertainty problem are illustrated. As shown in the figure, secondary users CR1 and CR2 are located inside the transmission range of primary transmitter

(PU TX) while CR3 is outside the range. It is obvious to know that only CR1 is able to accurately detect primary signal. Due to multiple attenuated copies of the PU's signal and the blocking building, CR2 experiences multipath and shadow fading so that the PU's signal may not be correctly detected. Since CR3 is outside the scope of primary network, thus unaware of the PU's transmission and the presence of primary receiver (PU RX), it suffers from receiver uncertainty problem. Therefore, the transmission from CR3 may interfere with the reception of PU RX.

In order to improve the performance of spectrum sensing, collaboration among secondary users have been proposed [2-1], [2-2], and [2-3]. If CR users, which can observe strong PU's signal like CR1 in Figure. 2-1, can share the sensing results with other users, the combined cooperative decision derived from the spatially collected observations can overcome the deficiency of individual detection at each CR user. Therefore, the overall sensing performance greatly improves. It has been proved that cooperative spectrum sensing is an effective approach to resolve multipath fading, shadowing, and the receiver uncertainty problem in previous research [2-4], [2-5].

2.2 Primary Signal Detection

Local spectrum sensing is referred as spectrum sensing individually performed by each CR user. The local spectrum sensing for primary signal is formulated as a binary hypothesis problem as follows:

$$x(t) = \begin{cases} n(t), & H_0 \\ h(t) \cdot s(t) + n(t), & H_1 \end{cases} \quad (2\text{-}1)$$

where $x(t)$ is the received signal by CR user, $s(t)$ denotes the primary transmitted primary user signal, $h(t)$ represents the channel gain of fading channel and $n(t)$ is the zero-mean additive white Gaussian noise (AWGN), H_0 and H_1 respectively represent the hypotheses of absence and presence of primary user in the denoted frequency band.

The detection performance is mainly evaluated by probability of false alarm P_f and probability of detection P_d. Probability of false alarm P_f denotes the rate of a CR user declaring that a primary user is transmitting while the spectrum is actually available, and probability of detection P_d, which denotes the probability of a CR user correctly claims that a

primary user is actually present. These probabilities are defined as

$$P_d = P\{decision = H_1 | H_1\} = P\{Y > \lambda | H_1\} \quad (2\text{-}2)$$

$$P_f = P\{decision = H_1 | H_0\} = P\{Y > \lambda | H_0\} \quad (2\text{-}3)$$

where Y is test statistic and λ is the decision threshold. The value of λ is set depending on the requirements of detection performance. Based on the definition above, the probability of miss detection is defined as

$$P_m = 1 - P_d = P\{decision = H_0 | H_1\} \quad (2\text{-}4)$$

Since a miss in the detection will cause the interference with primary user and a false alarm will reduce the spectral efficiency, it is usually demanded for optimal detection performance of maximizing P_d subject to the constraint of P_f. The plot that shows P_d versus P_f is called the receiver operation characteristic (ROC) curve, which is the metric for performance evaluation of a detector. Theoretical deduction of P_d and P_f over non-fading and fading channels, and the impact of diversity analysis for fading channels will be discussed in the later content.

2.3 Elements of Cooperative Spectrum Sensing

The cooperative spectrum sensing is roughly considered as a three-step process: local spectrum sensing, local test statistic reporting, and data fusion, see Fig. 2-2. In addition to these steps, there are other fundamental and essential components as the elements of cooperative spectrum sensing. The key elements are *cooperation models*, *spectrum sensing techniques*, *hypothesis testing*, *control and reporting channel*, *data fusion rule*, *user selection*, and *knowledge base*.

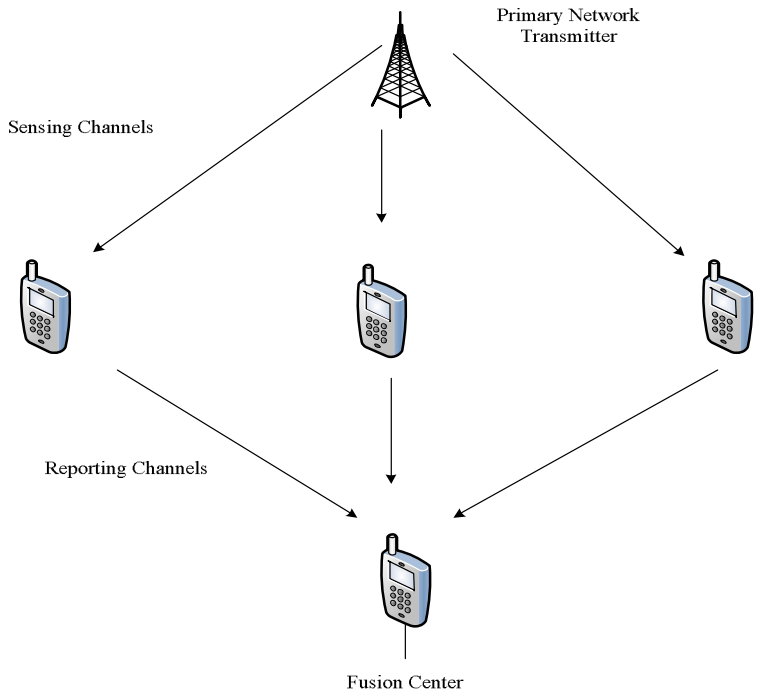

Figure 2-2. Cooperation Model: Parallel Fusion Model

- *Cooperation model* is primarily concerned with how CR users collaborate to perform spectrum sensing and achieve the optimal detection performance. The most popular and dominating method originated from the parallel fusion model in distributed detection and data fusion [2-6]. As can be seen in Figure 2-2, there is some similarity between the parallel fusion model and centralized cooperative spectrum sensing. In this scheme, cooperative model follows the same three-step process: local sensing, data reporting, and data fusion. All cooperating CR users are supposed to be synchronized to sense the primary user signal and report local statistics/decisions to the fusion center. All the fading channels between the collaborative CR users and the primary user are independent. Upon local statistics/decisions received by the fusion center, the fusion center combines the reported local sensing data to make a cooperating decision, then diffusing back. Recent studies provide a cooperation model by using game theory [2-7], [2-8]. Unlike the parallel fusion model aiming to improve overall detection performance by emphasizing sensing part, game theoretical models focus on analyzing the iterations and the cooperative or non-cooperative behaviors of CR users.

- *Sensing techniques* are used to sense the radio frequency environment, take observation samples, and employ signal processing techniques for detecting a primary user signal or

the available spectrum. Similar to traditional spectrum sensing without cooperation, the objective of the local spectrum sensing is primary signal detection. Sensing techniques are critical in cooperative spectrum sensing; what kind of sensing techniques are chosen has a big effect on how CR users collaborate. Basically, sensing techniques can be classified as two broad types: coherent and non-coherent detection. In coherent detection, the primary signal can be coherently detected by comparing a received signal with a priori knowledge of primary signals. Instead, no priori knowledge is needed in non-coherent detection. One of the most popular sensing techniques in cooperative sensing is energy detection, a non-coherent detection method. The issue of energy detection of an unknown signal over a multipath channel will be described in detail in the later content.

- *Hypothesis testing* is a statistic test to make a binary decision on the presence or absence of a primary user signal. The test can be taken solely by each cooperating CR user for local spectrum sensing or performed by the fusion center for a cooperative decision. The *Neyman-Pearson* criteria and the *Bayes* criteria are two basic hypothesis testing methods commonly used in spectrum sensing. The objective of a Neyman-Pearson test is to maximize probability of detection P_d and insure that probability of false alarm P_f is

below a fixed value. In Bayes test, the objective is to minimize the expected cost called the Bayes Risk defined by $R = \Sigma_{i=0}^{1}\Sigma_{j=0}^{1} C_{ij} P(H_i \left| H_j \right.) P(H_j)$, where C_{ij} is the cost of choosing H_i when H_j is true, $P(H_i \left| H_j \right.)$ denotes the probability of declaring H_i when H_j is true, and $P(H_j)$ is the prior probability of hypothesis H_j.

- *Control and reporting channel* concerns with how local decisions sensed by cooperating CR users can be efficiently and accurately transmitted to the fusion center or shared with other CR users via control channel with limited bandwidth and fading problem. In cooperative spectrum sensing, a common control channel (CC) is commonly used by CR user to report local sensing data to the fusion center or share the sensing results with neighboring nodes. The control center can be implemented as a dedicated channel in licensed or unlicensed bands. For reporting sensing data, three major control channel requirements must be satisfied in cooperative spectrum sensing: bandwidth, reliability, and security.

- *Data Fusion* is a process of combining local sensing data for hypothesis testing. According to the requirement of control channel, reported sensing information may be of different types, forms and sizes. In general, the sensing results reported to the fusion

center or shared with neighboring users can be processed in three ways as (I) *soft combining*: CR users can transmit the entire local sensing samples or the complete local test statistics for soft decision; (II) *quantized soft combining*: CR user can quantize local sensing data, then only send quantized data for soft combining to alleviate control channel overhead; (III) *hard combining*: CR users make a local decision and transmit the one-bit decision for hard combining. Based on the schemes, it is obvious that using soft combining can achieve the best sensing performance because all the information is kept, while using the rest combining methods can save bandwidth of control channel at the risk of degraded sensing performance.

- *User selection* concerns with how to optimally select the cooperating CR users and decide proper cooperation range to maximize the cooperative gain and minimize the cooperation overhead. The selection of CR users for cooperative spectrum sensing plays a key role in determining the quality of cooperative spectrum sensing because it can be utilized to improve cooperative gain and address the overhead issues.

- *Knowledge base* stores the information and facilitates the cooperative sensing process to improve the detection performance. The performance of cooperative spectrum sensing

depends closely on the information of primary user' characteristics such as traffic patterns, location, and transmit power. If the knowledge base has such information, it will greatly facilitate primary user detection. Since knowledge base can be used to assist, complement or even replace cooperative spectrum sensing for detecting primary user signal, it is a indispensable component in cooperative spectrum sensing.

2.4 Local Spectrum Sensing

2.4.1 AWGN channels

Energy detectors have been extensively studied in the past. Early in 1967, Urkowitz [2-9] firstly addressed the issue of energy detection of an unknown deterministic signal over an additive white Gaussian noise (AWGN) channel. He proposes that the receiver is employed with an energy detector that measures the energy in the received waveform over an observation time window. In his work, the energy output y follows the distributions,

$$y \sim \begin{cases} \chi^2_{2TW}, & H_0 \\ \chi^2_{2TW}(2\gamma), & H_1 \end{cases}$$

(2-5)

where χ^2_{2TW} and $\chi^2_{2TW}(2\gamma)$ denote central and non-central chi-square distributions respectively, each with $2TW$ degrees of freedom, and 2γ is a non-centrality parameter. For simplicity, the time bandwidth TW is assumed as an integer number denoted by m.

Based on the statistics of y, the probability of detection P_d and the probability of false alarm P_f, defined as $P_d = P\left(y > \lambda \middle| H_1\right)$ and $P_f = P(y > \lambda | H_0)$ respectively, where λ is a decision threshold, can be evaluated as [2-10]

$$P_f = \frac{\Gamma(m, \lambda/2)}{\Gamma(m)}, \tag{2-6}$$

$$P_d = Q_m(\sqrt{2\gamma}, \sqrt{\lambda}), \tag{2-7}$$

where γ is the signal-to-noise ratio (SNR), $\Gamma(.)$ and $\Gamma(.,.)$ are complete and upper incomplete gamma functions respectively, and Q_m is the generalized Marcum Q-function. Complete and upper incomplete gamma functions [2-11] are defined as

$$\Gamma(s) = \int_0^{\infty} t^{s-1} e^{-t}\, dt, \tag{2-8}$$

$$\Gamma(s,x) = \int_x^{\infty} t^{s-1} e^{-t}\, dt, \tag{2-9}$$

respectively. The generalized Marcum Q-function [2-12] is defined as follows

$$Q_m(a,b) = \int_b^{\infty} \frac{x^m}{a^{m-1}} e^{-\frac{x^2+a^2}{2}} I_{m-1}(ax)\, dx \tag{2-10}$$

where $I_{m-1}(.)$ is the modified Bessel function of (m-1)-th order.

The receiver operating characteristic (ROC) curves, a plot of P_d versus P_f is a primary criterion to quantify the sensing performance. Equivalently, we sometimes use complementary ROC curves (probability of miss detection P_m versus P_f) for different situations of interest. The fundamental tradeoff between P_m and P_f has different implications in the case of spectrum sensing. A high P_m would cause miss the presence of primary user with high probability that in return increases interference to the licensed primary network. On the other hand, a high P_f would waste more opportunities of free spectrum that leads to inefficient spectrum utilization, which degrades the CRN throughput.

2.4.2 Rayleigh Fading Channels

In mobile radio channels, the Rayleigh distribution is commonly used to describe the statistical time-varying nature of the received envelope of a flat fading signal, or the envelope of an individual multipath component. It is well known that the envelope of the sum of two quadrature Gaussian noise signals obeys a Rayleigh distribution [2-13]. The Rayleigh distribution has a probability density function (PDF) given by

$$p(r) = \begin{cases} \frac{r}{\sigma^2} \exp\left(-\frac{r^2}{2\sigma^2}\right), (0 \le r \le \infty) \\ 0, (r < 0) \end{cases} \tag{2-11}$$

where r is the *root-mean-squared* value of the received voltage signal before envelope detection, and σ^2 is the time-averaged power of the received signal before envelope detection. The probability that the envelope of the received signal does not exceed a specified value R is given by the corresponding cumulative distribution function (CDF)

$$P(R) = \Pr(r \le R) = \int_0^{\infty} p(r)\,dr = 1 - \exp\left(-\frac{R^2}{2\sigma^2}\right) \tag{2-12}$$

The mean value r_{mean} of the Rayleigh distribution is given by

$$r_{mean} = E(r) = \int_0^\infty rp(r)\,dr = \sigma\sqrt{\frac{\pi}{2}} = 1.2533\sigma, \qquad (2\text{-}13)$$

and the variance of the Rayleigh distribution is given by σ_r^2, which represents the ac power in the signal envelope

$$\sigma_r^2 = E(r^2) - E^2(r) = \int_0^\infty r^2 p(r)\,dr - \frac{\sigma^2\pi}{2} = \sigma^2\left(2 - \frac{\pi}{2}\right) = 0.4292\sigma^2 \qquad (2\text{-}14)$$

Often, the gain and phase elements of a channel's distortion are conveniently represented as a complex number. In this case, Rayleigh fading is exhibited by the assumption that the real and imaginary parts of the response are modeled by independently and identically distributed (i.i.d.) zero-mean Gaussian process so that the amplitude of the response is the sum of two such processes. Rayleigh fading can be a useful model in heavily built-up city centers where there is no direct line-of-sight between the transmitter and receiver, and large number of buildings and other objects attenuate, reflect, refract, and diffract transmitted signals.

Under Rayleigh fading channel, the average detection probability $P_{d,Ray}$ can be obtained as [2-10]

$$P_{d,Ray} = e^{-\frac{\lambda}{2}} \sum_{k=0}^{m-2} \frac{1}{k!} \left(\frac{\lambda}{2} \right)^k + \left(\frac{1+\bar{\gamma}}{\bar{\gamma}} \right)^{m-1} \times \left(e^{-\frac{\lambda}{2(1+\bar{\gamma})}} - e^{-\frac{\lambda}{2}} \sum_{k=0}^{m-2} \frac{1}{k!} \left(\frac{\lambda\bar{\gamma}}{2(1+\bar{\gamma})} \right)^k \right) \quad (2\text{-}15)$$

where $\bar{\gamma}$ is the average SNR. Notice that P_f in (2-6) is independent with SNR, thus $P_{f,Ray}$ remains the same as P_f. Rayleigh fading degrades spectrum sensing performance of energy detector significantly, compared to AWGN channel scenario. Therefore, cooperative spectrum sensing is crucial to improve the spectrum sensing performance in fading channel environments.

2.5 Cooperative Spectrum Sensing over Fading Channels

In this section, *Square-law combining* (SLC) and *Square-law selection* (SLS) diversity schemes are introduced. Here, the two diversity schemes are employed into parallel fusion model. In Chapter 4, we will use either fusion model to fuse the local CR statistics to perform the final spectrum sensing decisions.

2.5.1 Square-law Combining (SLC)

In this scheme, each cooperating CR user experiences an independent Rayleigh fading channel, then simultaneously reported sensing data, also known as the output of energy detector $\{y_i\}_{i=1}^{L}$, where L is the number of cooperative CR users, to the fusion center. The fusion center combines the reported local sensing data to yield a fused decision statistic $y_{SLC} = \sum_{i=1}^{L} y_i$, and then compares this fused data against with a testing threshold λ to make final decisions.

Under H_0 in AWGN channels, adding L i.i.d. central chi-square varieties, each with $2m$ degrees of freedom, will result in another chi-square varieties with $2Lm$ degrees of freedom. Therefore, we have [2-10]

$$P_{f,SLC} = \frac{\Gamma(Lm, \frac{\lambda}{2})}{\Gamma(Lm)}, \qquad (2\text{-}16)$$

which is similar to (2-6) for AWGN channel without cooperation.

Likewise, under H_1, y_{SLC} will be a non-central chi-square variety with $2Lm$ degrees of

freedom, non-centrality parameter $\sum_{i=1}^{L} 2\gamma_i$, denoted by $2\gamma_t$. Thus, $P_{d,SLC}$ can be evaluated by analogy to (2-7) as

$$P_{d,SLC} = Q_{Lm}\left(\sqrt{2\gamma_t}, \sqrt{\lambda}\right). \qquad (2\text{-}17)$$

2.5.2 Square-law Selection (SLS)

In the SLS diversity scheme, instead of adding all the sensing results of cooperating CR users, the fusion center selects the maximum received local statistic, which denotes as $y_{SLS} = \max\{y_i\}_{i=1}^{L}$. Under H_0, $P_{f,SLS}$ can be evaluated by using CDF of y_{SLS} given H_0 defined as $F_{y_{SLS}} = \left(y|H_0\right)$, yielding as

$$P_{f,SLS} = 1 - F_{y_{SLS}}\left(\lambda|H_0\right) = 1 - \left(1 - \frac{\Gamma(m,\lambda)}{\Gamma(m)}\right)^{L} . \qquad (2\text{-}18)$$

Similarly,

$$P_{d,SLS} = 1 - \prod_{i=1}^{L}\left(1 - Q_m\left(\sqrt{2\gamma_i}, \sqrt{\lambda}\right)\right) . \qquad (2\text{-}19)$$

Averaging this $P_{d,SLS}$ over L independent Rayleigh branches, we can have

$$P_{d,SLS,Ray} = 1 - \prod_{i=1}^{L}(1 - P_{d,Ray}(\overline{\gamma}_i, m)), \qquad (2\text{-}20)$$

where $P_{d,Ray}$ is provided in (2-15).

2.6 Summary

Spatially distributed cooperative spectrum sensing methodology can significantly improves the performance of spectrum sensing [2-14]. As the number of CR users increases, the sensing results are more reliable. However, the number of CR users in cognitive radio networks is time varying. CR users come and go. Cognitive radio networks cannot hold the CR users when the CR users decide to leave. Therefore, in the following chapters, we will study the dynamic behaviors of CR users and the performance of cooperative spectrum sensing due to the dynamic behavior of CR users.

References

[2-1] D. Cabric, S. Mishra, and R. Brodersen, "Implementation issues in spectrum sensing for cognitive radios," in *Proc. of Asilomar Conf. on Signals, Systems, and Computers*, 2004.

[2-2] J. Hillenbrand, T. A. Weiss, and F. Jondral, "Calculation of detection and false alarm probabilities in spectrum pooling systems," *IEEE Communications Letters*, vol. 9, no. 4, 2005.

[2-3] S. Haykin, "Cognitive Radio: Brain-Empowered Wireless Communications," *IEEE Journal on Selected Areas in Communications*, vol. 23, no. 2, 2005.

[2-4] A. Ghasemi and E. Sousa, "Collaborative spectrum sensing for opportunistic access in fading environments," in *Proc. of IEEE DySPAN 2005*, 2005.

[2-5] S. Mishra, A. Sahai, and R. Brodersen, "Cooperative sensing among cognitive radios," in *Proc. of IEEE ICC 2006*, 2006.

[2-6] P. K. Varshney, *Distributed Detection and Data Fusion*. SpringerVerlag, New York, 1997.

[2-7] W. Saad, Z. Han, M. Debbah, A. Hjorungnes, and T. Basar, "Coalitional games for distributed collaborative spectrum sensing in cognitive radio networks," in *Proc. of IEEE INFOCOM 2009*, 2009.

[2-8] B. Wang, K. Ray Liu, and T. Clancy, "Evolutionary cooperative spectrum sensing game: how to collaborate?" *IEEE Transactions on Communications*, vol. 58, no. 3, 2010.

[2-9] H. Urkowitz, “Energy detection of unknown deterministic signals,” P*roceedings of IEEE*, 1967.

[2-10] F. F. Digham, M.S. Alouini, and M. K. Simon, “On the energy detection of unknown signals over fading channels,” *IEEE Transactions on Communications*, vol. 55, no. 1, 2007.

[2-11] I. S. Gradshteyn and I. M. Ryzhik, *Table of Integrals, Series, and Products*. Academic Press, 1994.

[2-12] A. H. Nuttall, “Some integrals involving the QM function,” *IEEE Transactions on Information Theory*, vol. 23, no. 1, 1975.

[2-13] S.Rappaport, *Wireless communications: Principles and Practice*. Prentice Hall PTR, 2002.

[2-14] K. B. Letaief and W. Zhang, “Cooperative Communications for Cognitive Radio Networks,” *Proceedings of the IEEE*, vol. 97, no. 5, May 2009.

Chap 3
User Dynamics

Exploring the spatial diversity, the spectrum sensing can make more reliable decisions [3-1]. However, since the CR users can turn on/off the CR functionalities at will, CRN is not a static network but a dynamic network. Thus, the number of spatial diversity in the distributed spectrum sensing is not constant but time-varying. The dynamics of CRs impact the spectrum sensing performance. To guarantee not to violate the privileges of the licensed primary users and also to optimize CRN its own throughput, CRN has to adapt the system parameters to the dynamics of CR accordingly. Therefore, CRN cannot ignore the dynamics of CRs and the dynamics of CRs is an important topic for the CRN system operations. In this chapter, we study the dynamic behavior of the CR users and hence the dynamics of the collaborative CRs in the network.

3.1 Dynamic Behaviors

People use their mobile wireless devices at will. For example, people use their cell phones

to make calls to other people and hang up whenever they finish the conversations. People turn on the Wi-Fi functionality in the laptops to access the Internet and leave when they finish or when they need to go to the following schedules. Similarly, the CR users also turn on/off the CR functionalities embedded in their mobile devices to attempt to use the available wireless spectrum at will. Therefore, the CRN is not a static network but a dynamic network. The CRN network size is changing over time. Since the number of collaborative CRs in the PHY-layer cooperative spectrum sensing is time-varying, the number of available spatial diversity is also changing, see Fig. 3-1. The performance of cooperative spectrum sensing is hence fluctuating accordingly.

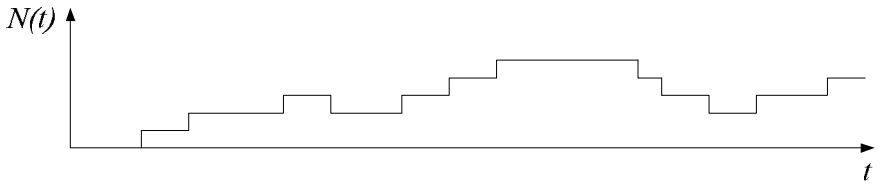

Fig. 3-1 One Realization of {*N(t)*}

3.2 Semi-Markov Processes

When the CR users turn on the CR functionalities, the mobile devices equipped with the CR functionalities join the cooperative spectrum sensing immediately. These CRs form an ad hoc

cognitive radio network. They collaborate all together to monitor the primary users' activities and seek for the spectrum opportunities. Suppose the CRs join this network by Poisson arrival random process with rate λ. After a certain amount of time, a CR will leave the network and thus leave the distributed cooperative spectrum sensing. Based on the different application scenarios and also different amount of information regarding the dynamic behaviors of the CR users, we can use different distributions to model this amount of time. For example, in the cellular systems application, several and significantly different probability distribution functions (e.g., exponential, Erlang, Gamma, uniform, deterministic, hyper-Erlang, sum of hyper-exponentials, log-normal, Pareto, Weibull, general phase-type distributions, generalized Pareto, and generalized Coxian) are proposed to model Cell Dwell Time (CDT) which is the amount of time a mobile device stays within a cell, see [3-2], [3-3], [3-4], and the references therein. These CDT distributions can be used to model the amount of time $T_i(t)$ the i-th CR stays in the cooperation for the cognitive radio ad hoc cellular network systems. After this amount of time, the CR leaves the system and thus leaves the collaboration in spectrum sensing.

The random departure process {D(t)} is formed by the given Poisson arrival process {A(t)} and the amount of time {T(t)} a CR stays in the network, see Fig. 3-2. Thus, the number of CRs in the network can be modeled by a semi-Markov stochastic process {*N(t)*} over infinity countable space {0, 1, 2, …} [3-5]. This semi-Markov process consists of Poisson arrival process

$\{A_i(t)\}$, cooperation time $\{T_i(t)\}$, and the associated random departure process

$\{D_i(t)\}=\{A_i(t)+T_i(t)\}$.

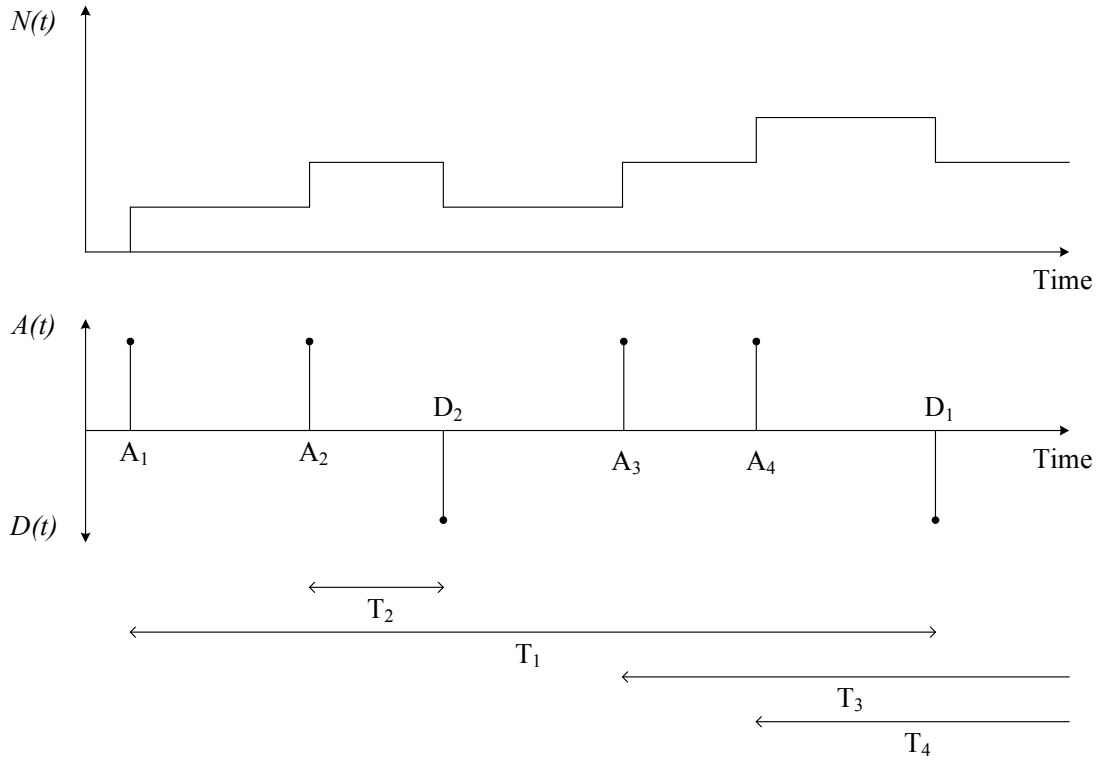

Fig. 3-2 The Semi-Markov Random Process $\{N(t)\}$, Arrival/Departure Random Processes $\{A(t)\}/\{D(t)\}$, and Cooperation Times $\{T_i\}$

This nonstationary random process can capture the number of CRs in the network at any time instance t by the time-varying probability mass function (PMF) of $N(t)$ according to the

dynamic arrivals and departures of CRs. Therefore, based on different cognitive radio network technology application scenarios, we can derive the dynamic probability mass function accordingly as follows.

3.2.1 Persistent Cognitive Radios

CRs arrive in a CRN following the Poisson process with rate λ. They join the cooperative spectrum sensing immediately and they do not leave before PU stops transmitting. Therefore, during this PU busy period, the dynamic probability mass function of the number of CRs in the network, N(t), is

$$P(N(t)=n)=\frac{(\lambda t)^n}{n!}e^{-\lambda t}, \quad \text{n} = 0,1,2,.... \qquad (3\text{-}1)$$

Since they don't leave and thus there is no departure process, after a long period of time, there will have huge number of CRs in the system. For the cooperative spectrum sensing, this definitely enhance the detection performance. However, from the system operation point of view, too many CRs waiting for the potential spectrum opportunities is a huge burden for the network

because of the communications costs between the central controller to all these CRs and also the related fairness-related network management.

3.2.2 Deterministic Cooperation Time with Parameter c > 0

Given the PU is using its own licensed band, the CRs in the system are collaborating to monitor the possible frequency utilization opportunities, i.e. the PU leaves. CRs arrive in a CRN following the Poisson process with rate λ. They join the cooperative spectrum sensing immediately and wait for the opportunities. They lose the patience after a period of time c > 0 and leave the system immediately. In this scenario, we can obtain the dynamic PMF of N(t) as

$$P(N(t)=n)=\begin{cases}(n!)^{-1}\lambda^{n}t^{n}e^{-\lambda t}, & 0 \le t < c,\\ (n!)^{-1}\lambda^{n}c^{n}e^{-\lambda c}, & t \ge c.\end{cases} \qquad (3\text{-}2)$$

This is a simplified scenario. There is no uncertainty for the amount of time a CR stays in the network. However, the arrival process is random and thus the departure process is still random. This model can give us a preliminary insight on how the performance of cooperative spectrum sensing varies with time. While we collect more information regarding the CR users'

behavior, we can migrate to a more complete and sophisticated model to evaluate the spectrum sensing performance.

3.2.3 Uniform Random Cooperation Time over (0, c]

In the PU busy period, suppose the arrival process for CRs follows Poisson with rate λ. CRs immediately join the distributed spectrum sensing when they arrive. The amount of time a CR is willing to wait before the PU leaves is independent. Given the upper limit for the waiting time as c, while we don't have any further information regarding how patient for each CR, we can use independent and identically distributed uniform waiting time to model the random amount of time a CR stays in the cooperation. The associated probability density function for uniform random cooperation time is given by:

$$f(x)=\begin{cases}\dfrac{1}{c}, & 0<x\le c\\ 0, & \text{otherwise}\end{cases} \qquad (3\text{-}3)$$

They leave randomly after they lose the patience. Hence, the dynamic PMF of N(t) for this scenario can be obtained by

$$P(N(t)=n)=\begin{cases}(n!)^{-1}\lambda^n t^n[1-(t/2c)]^n e^{-\lambda t[1-(t/2c)]}, 0\le \mathrm{t}<\mathrm{c},\\ (2^n n!)^{-1}(\lambda c)^n e^{-\lambda c/2}, \qquad \mathrm{t}\ge \mathrm{c}.\end{cases} \tag{3-4}$$

In this scenario, not all CRs stay the same amount of time c which is the upper limit of the cooperation time information. Considering the probability of miss detection drops substantially faster than the linear relationship with respect to the number of spatial diversity, we know the spectrum sensing performance with the deterministic cooperation time is better than the spectrum sensing performance with the uniform random cooperation time under the same parameter value c.

3.2.4 Pareto Random Cooperation Time with Parameters $x_m > 0$ and $\alpha > 0$

The associated probability density function for Pareto random cooperation time is given by

$$f(x)=\begin{cases}\dfrac{\alpha {x_m}^{\alpha}}{x^{\alpha+1}}, & x\ge x_m\\ 0, & \text{otherwise}\end{cases} \tag{3-5}$$

CRs arrive at the system following the Poisson process with rate λ. When a CR joins the cooperation to look for the potential spectrum opportunities, it is willing to wait at least x_m amount of time, e.g. 10 seconds or 3 minutes, but, after that, it loses the patience α-exponentially and leaves the system. Thus, the dynamic PMF of N(t) can be obtained by, for $0 \le t < x_m$,

$$P(N(t)=n) = (n!)^{-1}(\lambda t)^n e^{-\lambda t}. \tag{3-6}$$

For $t \ge x_m$,

$$P(N(t)=n) = (n!)^{-1}\lambda^n x_m{}^n \left(x_m^{\alpha-1}t^{-\alpha+1}-1\right)^n (1-\alpha)^{-n} \times \exp\left\{-\lambda x_m\left(x_m^{\alpha-1}t^{-\alpha+1}-1\right)/1-\alpha\right\}. \tag{3-7}$$

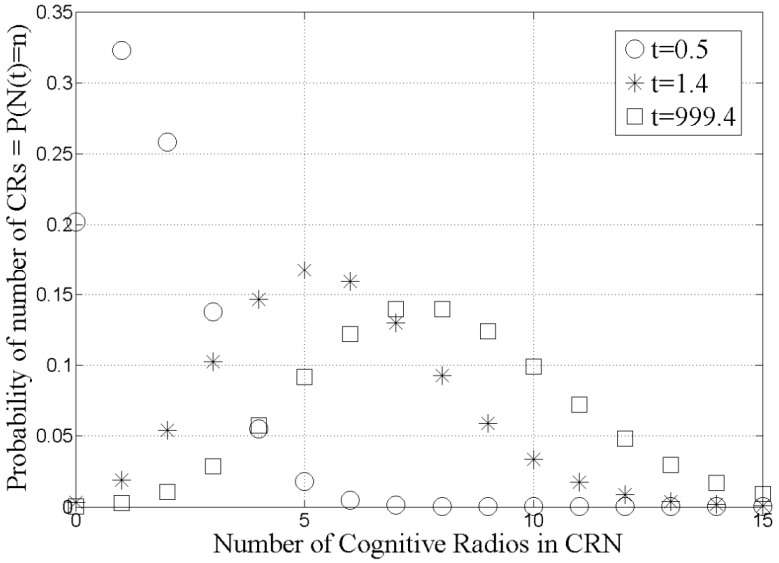

Fig. 3-3 Probability Mass Function of the Number of CRs in the Cooperation at Different Time Instants under Pareto Random Cooperation Time Scenario

Fig. 3-4 plots the probability mass functions of the number of CRs {N(t)} in the network at different time instants. We can see the probability mass function is changing and thus {N(t)} is not a stationary random process. The derived analytical expression for the probability mass function of the number of CRs can help us to evaluate the dynamic performance of the cooperative spectrum sensing in the next chapter.

3.2.5 Gamma Random Cooperation Time with Parameters $k > 0$ and $\theta > 0$

Suppose the arrival process for CRs follows Poisson with rate λ. CRs immediately join the distributed spectrum sensing when they arrive. The amount of time a CR is willing to wait before the PU leaves is independent. Gamma distribution is widely used to model the random amount of time a customer in a system and the associated probability density function is given by

$$f(x) = \frac{1}{\Gamma(k)\theta^k} x^{k-1} e^{-\frac{x}{\theta}}, \quad x \geq 0. \tag{3-8}$$

If we use gamma distribution to model the random amount of time a CR stays in the collaboration, the random departure process is composed of the arrival random process and also this random amount of cooperation time. We can derive the dynamic probability mass function of the number of CRs in the network as

$$P(N(t)=n)=\frac{\left(\lambda t-\frac{\lambda t^{k+1}}{\Gamma(k)\theta^{k}}\sum_{i=0}^{\infty}\frac{(-t/\theta)^{i}}{(i+k)i!}\right)^{n} e^{-\lambda t+\frac{\lambda t^{k+1}}{\Gamma(k)\theta^{k}}\sum_{i=0}^{\infty}\frac{(-t/\theta)^{i}}{(i+k)i!}}}{n!} \quad (3\text{-}9)$$

3.2.5 Weibull Random Cooperation Time with Parameters $\mu > 0$ and $k > 0$

Given CRs' arrivals follow the Poisson random process with rate λ. CRs join the cooperative spectrum sensing immediately when they arrive. Since some CRs are carried by more patient users and some are carried by impatient users, the amount of time a CR is willing to wait can be modeled by Weibull distribution and its associated probability density function is given by:

$$f(x)=\begin{cases}\dfrac{k}{\mu}\left(\dfrac{x}{\mu}\right)^{k-1} e^{-\left(x/\mu\right)^{k}}, & x\geq 0\\ 0, & x<0\end{cases} \qquad (3\text{-}10)$$

When a CR loses the patience, it leaves the system and spectrum sensing cooperation. Therefore, we can derive the dynamic PMF of N(t) as

$$P(N(t)=n)=\frac{\lambda^{n}t^{n}}{n!}\left(\sum_{i=0}^{\infty}\left(-t/\mu\right)^{ki}\left[i!(ki+1)\right]^{-1}\right)^{n} e^{\lambda\sum_{i=0}^{\infty}\frac{(-t)^{ki+1}\mu^{-ki}}{i!(ki+1)}}. \quad (3\text{-}11)$$

3.2.7 Log-normal Random Cooperation Time with Parameters μ and $\sigma^2 \geq 0$

Given CRs' arrivals follow the Poisson process with rate λ. CRs join the cooperative spectrum sensing immediately when they arrive. Log-normal distribution is widely used to describe the random amount of time for each person stays and waits for services in many different scientific studies. Moreover, log-normal distribution has been used in the literatures to model cell dwell time (CDT), which is the amount of time a mobile terminal stays within a cell. The associated probability of log-normal distribution is given by

$$f(x)=\frac{1}{x\sqrt{2\pi\sigma^2}}e^{-\frac{(\ln x-\mu)^2}{2\sigma^2}},\quad x\geq 0 \tag{3-12}$$

where *log(x)* is the logarithm function to the base *e*. Hence, the dynamic probability mass function of the number of CRs in the network can be derived as

$$\begin{aligned}
&P(N(t)=n)= \\
&\exp\{-\lambda\kappa(t)\}\times\left(\frac{\lambda t}{n!}+\left(2\lambda^{-2}\pi\right)^{-1/2}\left\{e^{-t^2/2}-\sum_{i=1}^{\infty}\left[\mu^i\left(i^3+3i^2+2i\right)^{-1}\right.\right.\\
&\left.\left.\sum_{j=0}^{i}B(j+2,i-j+1)^{-1}\left(\sqrt{2}\sigma/\mu\right)^j\left\{\Gamma(1+\frac{j}{2},\frac{t^2}{2})-\Gamma(1+\frac{j}{2})\right\}\right]-1\right\}\\
&\times(n!)^{-1}-\frac{\lambda\Phi(\mathrm{t})}{n!}\left\{\sum_{\mathrm{i}=1}^{\infty}\frac{1}{i(i+1)}\left[\left(\sigma t+\mu\right)^{i+1}-\mu^{i+1}\right]-\sigma t\right\}\Bigg),
\end{aligned} \tag{3-13}$$

$$\begin{aligned}
\kappa(t)=t+&\left(\sqrt{2\pi}\right)^{-1}\left\{e^{-t^2/2}-1-\sum_{i=1}^{\infty}\sum_{j=0}^{i}\left[\Gamma(1+\frac{j}{2},\frac{t^2}{2})-\Gamma(1+\frac{j}{2})\right]\right.\\
&\left.\times\frac{2^{j/2}(i-1)!\sigma^j\mu^{i-j}}{(j+1)!(i-j)!}\right\}-\Phi(\mathrm{t})\left\{\sum_{\mathrm{i}=1}^{\infty}\frac{1}{i(i+1)}\left[\left(\sigma t+\mu\right)^{i+1}-\mu^{i+1}\right]-\sigma t\right\},
\end{aligned}$$

where $B(x,y)=\int_0^1 t^{x-1}(1-t)^{y-1}\,dt.$ is the beta function, $\Phi(t)=(2\pi)^{-1/2}\int_{-\infty}^{x}e^{-t^2/2}dt.$ is the cumulative distribution function of the Gaussian distribution with zero mean and unit variance, $\Gamma(s,x)=\int_x^{\infty}t^{s-1}e^{-t}dt.$ is the upper incomplete gamma function, and $\Gamma(s)=\int_0^{\infty}t^{s-1}e^{-t}dt.$ is the gamma function.

3.3 Asymptotic Time-averaged Dynamic Behaviors

The time-averaged probability mass function can be obtained by $\overline{P_N}(n) = \lim_{T\to\infty} T^{-1}\int_0^T P(N(t)=n)\,dt$. [3-6]. When we take T to infinity, the asymptotic long-term time-averaged probability distribution for the number of CRs in the network can be obtained as follows.

3.3.1 Deterministic Cooperation Time with Parameter $c > 0$

CRs lose the patience after a period of time c and leave the system immediately. In this scenario, we can obtain the asymptotic probability mass function of the number of CRs in the network, N(t), as

$$P_N(n) = \lim_{T\to\infty}\frac{1}{T}\int_0^T P(N(t)=n)dt = \frac{(\lambda c)^n e^{-\lambda c}}{n!} \qquad (3\text{-}14)$$

Hence, we can see that the probability of the number of CRs in the system in this deterministic cooperation time scenario depends on the parameter c value. If CRs are willing to stay longer in the network, it's more probable to have more CRs in the network after a long period of time. This analytical result does agree with the engineer intuition. However, in a more practical setting,

cognitive radio network cannot hold the CR user in the system in order to achieve better spectrum sensing performance.

3.3.2Uniform Random Cooperation Rime with Distribution over (0, c]

Given the upper limit for the waiting time as c, while we don't have any further information regarding how patient for each CR, we can use independent and identically distributed uniform waiting time to model the random amount of time a CR stays in the cooperation. After taking T to infinity, we can obtain the asymptotic long-term probability mass function for the number of CRs in the network as

$$P_N(n) = \lim_{T\to\infty} \frac{1}{T} \int_0^T P(N(t) = n)dt = \frac{(\lambda c)^n e^{-\lambda c/2}}{2^n n!} \qquad (3\text{-}15)$$

From the above result, we can also conclude that while the upper limit of the amount of time for a CR is willing to wait is larger, it's more probable to have more CRs in the system after a long period of time, which is consistent with the result for the deterministic cooperation time scenario.

Moreover, if the upper limit c for the uniform random cooperation time scenario is twice of the amount of time a CR stays in the system for the deterministic cooperation time scenario, the asymptotic probability mass functions of the number of CRs in the system are the same for the both scenarios.

3.3.3Pareto Random Cooperation Time with Parameters $x_m > 0$ and $\alpha > 0$

In this scenario, a CR is willing to wait at least x_m amount of time, but, after that, it loses the patience α-exponentially and leaves the system. As T goes to infinity, the long-term time-averaged probability mass function for the number of CRs in the network can be obtained by

$$P_N(n) = \lim_{T\to\infty} \frac{1}{T} \int_0^T P(N(t) = n)dt = \frac{(\lambda\alpha x_m)^n \, e^{-\left(\lambda\alpha x_m / \alpha - 1\right)}}{(\alpha - 1)^n \, n!} \qquad (3\text{-}16)$$

From the above equation, we can understand the parameter x_m is more important than the other parameter α. While either x_m and/or α is larger, it's more probable to have large number of CRs in

the system. However, the increase in x_m can move the peak of the probability mass function further to the right than the increase in α does.

3.3.4 Gamma Random Cooperation Time with Parameters $k > 0$ and $\theta > 0$

While the amount of time a CR stays in the network can be described by the Gamma distribution, if we take T to infinity to evaluate the long-term time-averaged probability mass function of the number of CRs in the network, we can obtain the following asymptotic probability mass function as

$$P_N(n) = \lim_{T\to\infty} \frac{1}{T} \int_0^T P(N(t) = n)dt = \frac{(\lambda k\theta)^n e^{-\lambda k\theta}}{n!} \qquad (3\text{-}17)$$

From the above result, we can understand the increase in either the parameter k or the parameter θ can move the asymptotic probability mass function of the number of CRs in the system to the right. They are equally important in determining the shape of the probability mass function. Furthermore, their effects are multiplicative.

3.3.5Weibull Random Cooperation Time with Parameters $\mu > 0$ and $k > 0$:

With Weibull random cooperation time, the asymptotic time-averaged probability mass function of the number of CRs in the network can be obtained by

$$P_N(n) = \lim_{T\to\infty} \frac{1}{T} \int_0^T P(N(t) = n)dt = \frac{\left(\lambda\mu\Gamma(1+1/k)\right)^n e^{-\lambda\mu\Gamma(1+1/k)}}{n!} \quad (3\text{-}18)$$

From the above equation, we know the shape parameter μ is much more important than the scaling parameter k for the asymptotic probability mass function of the number of CRs in the system.

3.3.6 Log-normal Random Cooperation Time with Parameters μ and $\sigma^2 \geq 0$,

When the CRs in the system behave log-normally, the long-term time-averaged probability mass function for the number of CRs in the network can be obtained by taking T

to infinity as follows.

$$P_N(n) = \lim_{T\to\infty} \frac{1}{T} \int_0^T P(N(t) = n)dt = \frac{\lambda^n}{n!} e^{n\mu + n\sigma^2/2 - \lambda \exp(\mu + \sigma^2/2)} \quad (3\text{-}19)$$

Both parameters μ and σ^2 are exponentially important in determining the shape of asymptotic probability mass function of the number of CRs in the system. Therefore, a small amount of increase in either μ or σ^2 can lead to substantially increase in the average number of CRs in the system while T goes to infinity.

3.4 System Capacity

Due to many dynamic spectrum management reasons, such as Qualify-of-Service (QoS) constraints, collision avoidance, interference control, throughput controls, and etc, CRN usually can only keep up to *L* CRs in the pool waiting for the possible spectrum utilization opportunities [3-7] [3-8].

3.4.1 Deterministic Cooperation Time with Parameter $c > 0$:

CRs lose the patience after a period of time c and leave the system immediately. In this scenario, considering the CRN size limitation L, we can obtain the asymptotic probability mass function for the number of CRs in the network as follows,

$$P_N^L(n) = \frac{L!(\lambda c)^n e^{-\lambda c}}{\Gamma(L+1,\lambda c)n!},\ \text{n=0,1,2,…,L} \quad (3\text{-}20)$$

where Γ(x,y) is the upper incomplete Gamma function as $\Gamma(x, y) = \int_y^\infty t^{x-1}e^{-t}dt$

3.4.2 Uniform Random Cooperation Time with Distribution over (0, c]:

Given the upper limit for the waiting time as c, while we don't have any further information regarding how patient for each CR, we thus use independent and identically distributed uniform waiting time to model the random amount of time a CR stays in the cooperation. In this scenario, considering the CRN size limitation L, we can obtain the asymptotic probability mass function

for the number of CRs in the network as follows,

$$P_N^L(n) = \frac{L!(\lambda c)^n e^{-\lambda c/2}}{\Gamma(L+1, \lambda c/2) 2^n n!}, \text{ n=0,1,2,…,L} \quad (3\text{-}21)$$

3.4.3 Pareto Random Cooperation Time with Parameters $x_m > 0$ and $\alpha > 0$:

In this scenario, a CR is willing to wait at least x_m amount of time, but, after that, it loses the patience α-exponentially and leaves the system. Considering the CRN size limitation L, we can obtain the asymptotic probability mass function for the number of CRs in the network as follows,

$$P_N^L(n) = \frac{L!(\lambda \alpha x_m)^n e^{-\left(\lambda \alpha x_m/\alpha - 1\right)}}{\Gamma(L+1, \lambda \alpha x_m/\alpha - 1)(\alpha - 1)^n n!}, \text{ n=0,1,2,…,L} \quad (3\text{-}22)$$

3.4.4 Gamma Random Cooperation Time with Parameters $k > 0$ and $\theta > 0$

While the amount of time a CR stays in the network can be described by the Gamma

distribution, considering the CRN size limitation L, we can obtain the asymptotic probability mass function for the number of CRs in the network as follows,

$$P_N^L(n) = \frac{L!(\lambda k\theta)^n e^{-\lambda k\theta}}{\Gamma(L+1,\lambda k\theta)n!},\ \text{n=0,1,2,…,L} \qquad (3\text{-}23)$$

3.4.5 Weibull Random Cooperation Time with Parameters $\mu > 0$ and $k > 0$:

With Weibull random cooperation time, considering the CRN size limitation L, we can obtain the asymptotic probability mass function for the number of CRs in the network as follows,

$$P_N^L(n) = \frac{L!(\lambda\mu\Gamma(1+1/k))^n e^{-\lambda\mu\Gamma(1+1/k)}}{\Gamma(L+1,\lambda\mu/k)n!},\ \text{n=0,1,2,…,L} \qquad (3\text{-}24)$$

3.4.6 Log-normal Random Cooperation Time with Parameters μ and $\sigma^2 \geq 0$,

When the CRs in the system behave log-normally, considering the CRN size limitation L, we can obtain the asymptotic probability mass function for the number of CRs in the network as follows,

$$P_N^L(n) = \frac{L!\lambda^n}{\Gamma(L+1, \lambda\exp(\mu+\sigma^2/2))n!} e^{n\mu+n\sigma^2/2-\lambda\exp(\mu+\sigma^2/2)},\ \text{n=0,1,2,…,L} \tag{3-25}$$

3.5 Summary

In this chapter, we investigate the dynamics of CR users in the network and thus the dynamic number of spatial diversity in the cooperative spectrum sensing. Under different CR dynamics, we obtain different dynamic probability mass function of the number of CRs in system for any time instant t. Moreover, considering several network operation constraints, the dynamic probability mass function with the system size limitation is also studied for different cooperation time scenarios. The long-term time-averaged probability mass functions of the number of CRs in the system are also analyzed under different scenarios. With this information, we can analyze the performance of the cooperative spectrum sensing in the dynamic cognitive radio networks in the following chapter.

References

[3-1] B. Wang and K. J. R. Liu, “Advances in Cognitive Radio Networks: a survey,” *IEEE Journal of Selected Topics in Signal Processing*, Vol. 5, NO.1 Feb. 2011.

[3-2] A. L. E. Corral-Ruiz, F. A. Cruz-Perez, and G. Hernandez-Valdez, “Channel holding time in mobile cellular networks with heavy-tailed distributed cell dwell time,” *in Proc. IEEE Wireless Commun. Netw. Conf. (WCNC)*, 2011.

[3-3] A. L. E. Corral-Ruiz, F. A. Cruz-Perez, and G. Hernandez-Valdez, “Channel holding time in mobile cellular networks with generalized coxian distributed cell dwell time,” in *Procc. IEEE Intl. Sym. On Personal, Indoor and Mobile Radio Comm. (PIMRC)*, 2010.

[3-4] S. Pattaramalai, V.A. Aalo, and G. P. Efthymoglou, “Evaluation of call performance in cellular networks with generalized cell dwell time and call-holding time distributions in the presence of channel fading,” *IEEE Transations on Vehicular Technology.*, vol. 58, no. 6, July 2009.

[3-5] R. G. Gallager, *Discrete Stochastic Processes*. Kluwer Academic Publishers, 1995.

[3-6] J. G. Proakis, *Digital Communications*. McGraw-Hill, 2008.

[3-7] T. Braun, M. Diaz, J. E. Gabeiras, and T. Staub, *End-to-End Quality of Service Over Heterogeneous Networks*. Springer, 2008.

[3-8] M. Marchese, *QoS Over Heterogeneous Networks*. Wiley, 2007.

Chap 4
Performance Analysis

We formulate the spectrum sensing as a binary hypothesis testing problem. H_1 means the PU is using its own licensed frequency band; H_0 represents the PU is idle. Spectrum sensing makes the binary decisions, $\hat{H}_0$: the band is vacant and $\hat{H}_1$: the band is occupied. The probability of detection $P_d = P\left(\hat{H}_1 \mid H_1\right)$ represents the probability that the band occupancy can be correctly detected. The probability of miss detection $P_m = P\left(\hat{H}_0 \mid H_1\right) = 1 - P\left(\hat{H}_1 \mid H_1\right) = 1 - P_d$ is an important performance metric for controlling the interference to the primary user. Higher P_m means CRN might cause interference with the existing primary privileged spectrum utilization, which is not allowed. The probability of false alarm $P_{FA} = P\left(\hat{H}_1 \mid H_0\right)$ denotes the probability that CRN makes a false alarm on the primary user's occupancy. This is another important performance metric for spectrum sensing because the larger P_{FA} implies that CRN is more likely to miss the opportunities to exploit the available spectrum, which lead to the CRN throughput degradation.

4.1 Energy-based Spectrum Sensing

Each CR monitors the primary user spectrum utilization by obtaining the energy statistic as in Fig. 4-1. The received signal waveform at a CR at each I/Q component is first passed through a band-pass filter (BPF) to remove out-of-band noises and then followed by the full-wave rectifier and the square–law circuit. Then *M*/2 samples are taken over a period of time T both at the I and Q components respectively. After summing over *M*/2 samples from both components, the output yields the energy statistic Y. Then, based on the output of a comparator device, the local CR sensing module could make the local decisions.

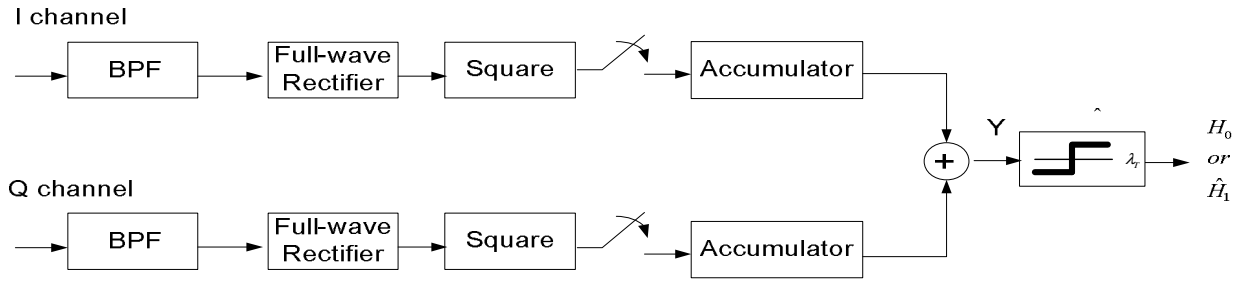

Fig. 4-1 Energy Detector Block Diagram

If the energy statistic Y is greater than a threshold λ_T, $\hat{H}_1$ decision is reached; otherwise, $\hat{H}_0$ decision is made. Let γ be the instantaneous signal-to-noise ratio (SNR). Given H_1, Y follows a noncentral chi-square distribution with noncentrality 2γ and *M* degrees of freedom;

under H_0, Y has a central chi-square distribution with M degrees of freedom. With additive white Gaussian noise (AWGN) with variance σ^2 and mean zero, the average probability of detection can be obtained as [4-1]

$$P_{d,AWGN} = P(\hat{H}_1 \mid H_1) = Q_{M/2}\left(\sqrt{2\gamma/\sigma^2}, \sqrt{\lambda_T/\sigma^2}\right), \quad (4\text{-}1)$$

where $Q_x(a,b)$ denotes the generalized Marcum Q-function. The average probability of false alarm is given by [4-1]

$$P_{FA,AWGN} = P(\hat{H}_1 \mid H_0) = \Gamma(u, \lambda_T/2)/\Gamma(u), \qquad (4\text{-}2)$$

where $\Gamma(x,y)$ is the upper incomplete gamma function, $\Gamma(x)$ is the gamma function, and u = TW is the time bandwidth product with T as the observation time interval and W as the one-sided bandwidth. The threshold λ_T can be determined based on the overlay CRN design concerns. For example, the recent work [4-2] bounds the queue occupancy based on some statistical Quality-of-Service (QoS) constraints and interference constraint to dynamically adjust the threshold. After λ_T value is decided, P_d and P_{FA} can be calculated by (4-1) and (4-2) respectively.

However, the instantaneous SNR, γ, is random over a fading channel. Therefore, the probability of detection over a fading channel can be obtained by averaging over the probability density function of γ as follows:

$$P_d = \int_0^{\infty} Q_{M/2}\left(\sqrt{2\gamma/\sigma^2}, \sqrt{\lambda_T/\sigma^2}\right) f_\gamma(\gamma) d\gamma. \qquad (4\text{-}3)$$

Since the probability of false alarm is independent of the instantaneous SNR, the probability of false alarm over a fading channel is still equal to (4-2).

4.2 Dynamic Spectrum Sensing Performances

Due to the wireless fading channel, a CR faces the hidden primary user issue in spectrum sensing. From the previous chapter, we know that through the collaboration among spatially distributed CRs, the hidden primary user issue can be effectively combated. The cooperative spectrum sensing performance is varying because of fading, shadowing, etc. On the other hand, since the number of CRs in CRN is also dynamically changing, the cooperative spectrum sensing performance is varying accordingly. We assume that there is a dedicated error-free channel for all spatially distributed CRs to send the collected energy statistics to the fusion center. The fusion

center performs the hypothesis testing based on the fused energy statistic, Z, from all concurrent n CRs against a testing threshold λ_T to reach the final decisions. The dynamic probability of detection can be obtained by

$$P_d(t) = \sum_{n=1}^{\infty} P(N(t)=n) \int_0^{\infty} Q_{M/2}\left(\sqrt{2\gamma_Z/\sigma^2}, \sqrt{\lambda_T/\sigma^2}\right) f_\gamma(\gamma_Z) d\gamma_Z, \quad (4\text{-}4)$$

where the probability density function of SNR for the fused energy statistic Z, $f_\gamma(\gamma_Z)$, depends on the number of CRs, channel model, and the energy statistic fusion scheme. The dynamic probability of false alarm can be calculated by

$$P_{FA}(t) = \sum_{n=1}^{\infty} P(N(t)=n) P(Z > \lambda_T \mid H_0), \quad (4\text{-}5)$$

where Z is the fused energy statistic based on n CRs. Therefore, the probability of false alarm depends on the number of CRs, and also the energy statistic fusion scheme.

4.2.1 AWGN Channels

4.2.1.1 Square-law Combining

Suppose the arrival process follows Poisson with rate λ. All CRs join the cooperative spectrum sensing immediately when they arrive. The random amount of time a CR stays in the cooperation follows Pareto distribution with parameters $x_m > 0$ and $\alpha > 0$. After this amount of time, it leaves immediately and thus leaves the collaboration. CRs collect the local energy statistics through the independent AWGN channels. Then, all these local energy statistics are transmitted via a dedicated error-free reporting channel to the fusion center. The fusion center combines the local statistics by summing over all energy statistics from all concurrent CRs in the network. Based on the fused statistic, the fusion center makes final sensing decisions. Therefore, we can obtain the dynamic probability of detection, for $0 \le t < x_m$,

$$P_d(t) = \sum_{n=1}^{\infty} (n!)^{-1} (\lambda t)^n e^{-\lambda t} Q_{M/2}\left(\sqrt{2\sum_{i=1}^{n} \gamma_i \Big/ \sigma^2}, \sqrt{\frac{\lambda_T}{\sigma^2}} \right). \quad (4\text{-}6)$$

For $t \ge x_m$,

$$P_d(t) = \sum_{n=1}^{\infty} (n!)^{-1} \lambda^n x_m{}^n \left(x_m^{\alpha-1} t^{-\alpha+1} - 1 \right)^n (1-\alpha)^{-n} \times \exp\left\{ -\lambda x_m \left(x_m^{\alpha-1} t^{-\alpha+1} - 1 \right) / 1-\alpha \right\} (n!)^{-1} (\lambda t)^n e^{-\lambda t} Q_{M/2}\left(\sqrt{2\sum_{i=1}^{n} \gamma_i \Big/ \sigma^2}, \sqrt{\frac{\lambda_T}{\sigma^2}} \right). \quad (4\text{-}7)$$

The dynamic probability of false alarm of the distributed cooperative spectrum sensing is given by

For $0 \le t < x_m$,

$$P_{FA}(t) = \sum_{n=1}^{\infty} \frac{\Gamma(nu, \lambda_T / 2)}{n!\Gamma(nu)} (\lambda t)^n e^{-\lambda t}. \quad (4\text{-}8)$$

For $t \ge x_m$,

$$P_{FA}(t) = \sum_{n=1}^{\infty} \frac{\Gamma(nu, \lambda_T / 2)}{n!\Gamma(nu)} \left[\frac{\lambda x_m}{1-\alpha_m} \left(x_m^{\alpha_m - 1} t^{-\alpha_m + 1} - 1 \right) \right]^n e^{-\left[\frac{\lambda x_m}{1-\alpha_m} \left(x_m^{\alpha_m - 1} t^{-\alpha_m + 1} - 1 \right) \right]}. \quad (4\text{-}9)$$

4.2.1.2 Square-law Selection

Suppose the arrival process follows Poisson with rate λ. All CRs join the cooperative spectrum sensing immediately when they arrive. The random amount of time a CR stays in the cooperation follows Pareto distribution with parameters $x_m > 0$ and $\alpha > 0$. After this amount of time, it leaves immediately and thus leaves the collaboration. CRs collect the local energy statistics through the independent AWGN channels. Then, all these local energy statistics are transmitted via a dedicated error-free reporting channel to the fusion center. The fusion center

combines them by adopting the largest energy statistic among all received local statistics from concurrent CRs in the network. Based on this fused statistic, the fusion center makes final sensing decisions. Therefore, we can obtain the dynamic probability of detection, for $0 \leq t < x_m$,

$$P_d(t) = 1 - \exp\left\{-\lambda t\left[1 - Q_{M/2}\left(\sqrt{2\gamma/\sigma^2}, \sqrt{\lambda_T/\sigma^2}\right)\right]\right\}. \quad (4\text{-}10)$$

For $t \geq x_m$,

$$P_d(t) = 1 - \exp\left\{-\lambda x_m\left(x_m^{\alpha-1}t^{-\alpha+1} - 1\right)\left[1 - Q_{M/2}\left(\sqrt{2\gamma/\sigma^2}, \sqrt{\lambda_T/\sigma^2}\right)\right]\Big/(1-\alpha)\right\}. \quad (4\text{-}11)$$

On the other hand, the dynamic probability of false alarm, for $0 \leq t < x_m$, can be obtained by

$$P_{FA}(t) = 1 - \exp\left[-\lambda t\Gamma(u, \lambda_T/2)/\Gamma(u)\right]. \quad (4\text{-}12)$$

and for $t \geq x_m$, the dynamic probability of false alarm can be obtained by

$$P_{FA}(t) = 1 - \exp\left[-\frac{\lambda x_m}{1-\alpha}\left(x_m^{\alpha-1}t^{-\alpha+1} - 1\right)\Gamma(u, \lambda_T/2)\Big/\Gamma(u)\right]. \quad (4\text{-}13)$$

4.2.2Log-normal Shadowing Channel

4.2.2.1 Dynamic Performances

Suppose the local cognitive radio network is within a certain short distance and hence the deterministic path-loss is negligible. However, the surrounding environment clutter may be vastly different from the primary user to each CR. This leads to the fluctuation of the received signal power. The empirical measurements showed this fluctuation is random and distributed log-normally [4-3] for various outdoor and indoor environments. This phenomenon is termed as log-normal shadowing. Therefore, the dynamic probability of detection of the distributed cooperative spectrum sensing can be obtained by

$$P_d(t) = \int_0^{\infty} \sum_{n=1}^{L} P_{N(t)}(n,t) \times Q_{M/2}\left(\sqrt{2\gamma/\sigma^2}, \sqrt{n\lambda_T/\sigma^2}\right) f(\gamma) d\gamma, \tag{4-14}$$

where M is the number of samples taken over a period of time T, σ^2 is the variance for zero-mean additive white Gaussian noise (AWGN), λ_T is the detection threshold, γ is the instantaneous fused energy statistic from local energy statistic affected by shadowing, and f(γ) is the probability

density function of the fused energy statistic. Suppose CRs arrive at CRN by a Poisson random process with parameter λ. CRs join the collaboration immediately while they arrive. The random amount of time they stay in the system follows Pareto distribution with parameters $x_m > 0$ and $\alpha > 0$. After this amount of time, they leave the network and thus the cooperative spectrum sensing. Therefore, based on $P_{N(t)}(n)$ in the previous chapter and with the aid of [4-4], we can obtain the closed-form expression for the dynamic probability of detection as

for $0 \le t < x_m$,

$$P_d(t) = \sum_{n=1}^{\infty} \frac{1}{n!} \sqrt{\frac{2n\eta}{\pi}} e^{\frac{\eta}{\theta}} (\lambda t)^n e^{-\lambda t} \sum_{m=0}^{\infty} \frac{\Gamma(m+nu, \lambda_T/2)}{\Gamma(m+nu)m!} \left(\frac{\eta\theta^2 n^2}{2n\theta^2+\eta} \right)^{m-\frac{1}{2}} K_{m-\frac{1}{2}} \left(\frac{\sqrt{\eta(2n\theta^2+\eta)}}{\theta} \right) \quad (4\text{-}15)$$

For $t \ge x_m$,

$$P_d(t) = \sum_{n=1}^{\infty} \frac{1}{n!} \sqrt{\frac{2n\eta}{\pi}} e^{\frac{\eta}{\theta}} \left(\frac{\lambda x_m}{1-\alpha_m} \left(x_m^{\alpha_m - 1} t^{-\alpha_m + 1} - 1 \right) \right)^n e^{-\frac{\lambda x_m}{1-\alpha_m} \left(x_m^{\alpha_m - 1} t^{-\alpha_m + 1} - 1 \right)}$$

$$\sum_{m=0}^{\infty} \frac{\Gamma(m+nu, \lambda_T/2)}{\Gamma(m+nu)m!} \left(\frac{\eta\theta^2 n^2}{2n\theta^2+\eta} \right)^{m-\frac{1}{2}} K_{m-\frac{1}{2}} \left(\frac{\sqrt{\eta(2n\theta^2+\eta)}}{\theta} \right) \quad (4\text{-}16)$$

If we only numerically calculate the first N_B terms in the summation for the dummy variable n and also the first N_M terms in the summation for the dummy variable m, by the Markov inequality and some mathematical manipulations, we can find the truncation error is upper bounded by

$$Te(t) \le \frac{e^{N_B}}{N_B^{\,N_B}} \times \left[\frac{\lambda x_m}{1-\alpha_m} \left(x_m^{\alpha_m - 1} t^{-\alpha_m + 1} - 1 \right) \right]^{N_B} e^{-\frac{\lambda x_m}{1-\alpha_m} \left(x_m^{\alpha_m - 1} t^{-\alpha_m + 1} - 1 \right)} \tag{4-17}$$

On the other hand, the dynamic probability of false alarm of the distributed cooperative spectrum sensing is given by

For $0 \le t < x_m$,

$$P_{FA}(t) = \sum_{n=1}^{\infty} \frac{\Gamma(nu, \lambda_T / 2)}{n! \Gamma(nu)} (\lambda t)^n e^{-\lambda t}. \tag{4-18}$$

For $t \ge x_m$,

$$P_{FA}(t) = \sum_{n=1}^{\infty} \frac{\Gamma(nu, \lambda_T / 2)}{n! \Gamma(nu)} \left[\frac{\lambda x_m}{1-\alpha_m} \left(x_m^{\alpha_m - 1} t^{-\alpha_m + 1} - 1 \right) \right]^n e^{-\left[\frac{\lambda x_m}{1-\alpha_m} \left(x_m^{\alpha_m - 1} t^{-\alpha_m + 1} - 1 \right) \right]}. \tag{4-19}$$

where *Γ(x,y)* is the upper incomplete gamma function, Γ(x) is the gamma function, and u = TW is the time bandwidth product with T as the observation time interval and W as the one-sided bandwidth.

4.2.2.2 Asymptotic Performances

The time-averaged asymptotic performance can be obtained by $\bar{P} = \lim_{T\to\infty} T^{-1} \int_0^T P(t)dt.$ Therefore, the asymptotic time-averaged probability of detection is given by

$$\bar{P}_d = \sum_{n=1}^{\infty} \frac{1}{n!} \sqrt{\frac{2n\eta}{\pi}} e^{\frac{\eta}{\theta}} \left[\lambda \alpha_m x_m / (\alpha_m - 1) \right]^n e^{-\left[\lambda \alpha_m x_m / (\alpha_m - 1) \right]} \sum_{m=0}^{\infty} \frac{\Gamma(m+nu, \lambda_T / 2)}{\Gamma(m+nu) m!} \left(\frac{\eta \theta^2 n^2}{2n\theta^2 + \eta} \right)^{m-\frac{1}{2}} K_{m-\frac{1}{2}} \left(\frac{\sqrt{\eta(2n\theta^2 + \eta)}}{\theta} \right) \quad (4\text{-}20)$$

Similarly, the asymptotic time-averaged probability of false alarm can be obtained by

$$\bar{P}_{FA} = \sum_{n=1}^{\infty} \frac{(-1)^{n+1} \Gamma(nu, \lambda_T / 2)}{n! \Gamma(nu)} \left[\lambda \alpha_m x_m / (\alpha_m - 1) \right]^n e^{-\left[\lambda \alpha_m x_m / (\alpha_m - 1) \right]} \quad (4\text{-}21)$$

4.2.3 Rayleigh Fading Channels

4.2.3.1 IID Rayleigh Fading Channels

Suppose CRs' arrivals follow Poisson random process with rate λ. While CRs arrive at CRN, they immediately collaborate with the other CRs concurrently in the network to perform the cooperative spectrum sensing. Assume the time of CRs stays in the network follows Pareto distribution with parameters $x_m > 0$ and $\alpha > 0$ and CRs leave the network after this amount of

time. The channels between the primary user to each CR are independent and identically distributed (i.i.d.) Rayleigh fading channels. The fusion center calculates the fused energy statistic by summing the received energy statistics from all CRs currently in the network. With the aid of the conditional probability of detection in [4-5], after some mathematical manipulations, the dynamic probability of detection and the dynamic probability of false alarm can be obtained by, for $0 \leq t < x_m$,

$$P_d(t) =$$

$$\left(1-e^{-\lambda t}\right)e^{\frac{-\lambda_T}{2\sigma^2}} + \sum_{n=1}^{\infty}\frac{(\lambda t)^n e^{-\lambda t}}{n!}\left\{\sum_{i=0}^{\frac{M}{2}-2}\frac{1}{i!}\left(\frac{\lambda_T}{2\sigma^2}\right)^i + \left[\left(\sigma^2+n\overline{\gamma}\right)/n\overline{\gamma}\right]^{\frac{M}{2}-1}\right.$$

$$\left.\left[e^{-\frac{\lambda_T}{2(\sigma^2+n\overline{\gamma})}} - e^{-\frac{\lambda_T}{2\sigma^2}}\sum_{i=0}^{M/2-2}(i!)^{-1}\left(n\lambda_T\overline{\gamma}/2\sigma^2(\sigma^2+n\overline{\gamma})\right)^i\right]\right\}. \qquad (4\text{-}22)$$

$$P_{FA}(t) = \sum_{n=1}^{\infty}(\lambda t)^n e^{-\lambda t}\Gamma(nu, \lambda_T/2)\left[n!\Gamma(nu)\right]^{-1}. \qquad (4\text{-}23)$$

For $t \geq x_m$,

$$P_d(t)=\left(1-e^{\frac{-\lambda x_m}{1-\alpha}\left(x_m^{\alpha-1}t^{-\alpha+1}-1\right)}\right)e^{\frac{-\lambda_T}{2\sigma^2}}+\sum_{n=1}^{\infty}\frac{1}{n!}\left[\frac{\lambda x_m}{1-\alpha}\left(x_m^{\alpha-1}t^{-\alpha+1}-1\right)\right]^n e^{\frac{-\lambda x_m}{1-\alpha}\left(x_m^{\alpha-1}t^{-\alpha+1}-1\right)}$$
$$\left\{\sum_{i=0}^{\frac{M}{2}-2}(i!)^{-1}\left(\frac{\lambda_T}{2\sigma^2}\right)^i+\left[\left(\sigma^2+n\overline{\gamma}\right)/n\overline{\gamma}\right]^{\frac{M}{2}-1}\right.$$
$$\left.\left[e^{-\frac{\lambda_T}{2(\sigma^2+n\overline{\gamma})}}-e^{-\frac{\lambda_T}{2\sigma^2}}\sum_{i=0}^{M/2-2}(i!)^{-1}\left(n\lambda_T\overline{\gamma}/\left[2\sigma^2(\sigma^2+n\overline{\gamma})\right]\right)^i\right]\right\}. \quad (4\text{-}24)$$

$$P_{FA}(t)=$$
$$\sum_{n=1}^{\infty}\left(\frac{\lambda x_m}{1-\alpha}\left(x_m^{\alpha-1}t^{-\alpha+1}-1\right)\right)^n\frac{\Gamma(nu,\lambda_T/2)}{n!\Gamma(nu)}\exp\left\{\frac{-\lambda x_m}{1-\alpha}\left(x_m^{\alpha-1}t^{-\alpha+1}-1\right)\right\}. \quad (4\text{-}25)$$

4.2.3.2 Independent but Non-identical Rayleigh Fading Channels

4.2.3.2.1 Dynamic Performances

Since CR users are spatially located in different places in the network coverage area, the received primary user signals by cooperating CR users may experience a variety of fading conditions. The fading channels from the primary user to CRs are not necessary identical. Considering the cooperative spectrum sensing over independent but not identically distributed fading channels, with the help of the conditional probability of detection in [4-6] and the

log-normal random cooperation time, the dynamic probability of detection over independent non-identical Rayleigh fading channels can be obtained by

$$P_d(t)=\sum_{n=1}^{\infty}\sum_{i=1}^{n}A_i\left\{\frac{\Gamma(nu-1,\lambda_T/2)}{\Gamma(nu-1)}+\exp\left[-\frac{\lambda_T}{2(1+\overline{\gamma}_i)}\right]\Upsilon\left(nu-1,\frac{\lambda_T}{2}\frac{\overline{\gamma}_i}{(1+\overline{\gamma}_i)}\right)\left[\Gamma(nu-1)\right]^{-1}\left(1+\frac{1}{\overline{\gamma}_i}\right)^{nu-1}\right\}$$
$$\exp\{-\lambda\kappa(t)\}\left(\frac{\lambda t}{n!}+\left(2\lambda^{-2}\pi\right)^{-1/2}\left\{e^{-t^2/2}-\sum_{i=1}^{\infty}\left[\mu^i\left(i^3+3i^2+2i\right)^{-1}\sum_{j=0}^{i}B(j+2,i-j+1)^{-1}\left(\sqrt{2}\sigma/\mu\right)^j\right.\right.\right.$$
$$\left.\left.\left.\left\{\Gamma(1+\frac{j}{2},\frac{t^2}{2})-\Gamma(1+\frac{j}{2})\right\}\right]\right\}(n!)^{-1}-\frac{\lambda\Phi(t)}{n!}\left\{\sum_{i=1}^{\infty}\frac{1}{i(i+1)}\left[(\sigma t+\mu)^{i+1}-\mu^{i+1}\right]-\sigma t\right\}-\frac{\lambda}{\sqrt{2\pi}n!}\right), \quad (4\text{-}26)$$
$$A_i=M_\gamma(s)(1-\overline{\gamma}_i s)|_{s=1/\overline{\gamma}_i},$$

where $\Upsilon(M,x)=\Gamma(M)-\Gamma(M,x)=\int_0^x t^{M-1}e^{-t}dt.$ is the lower incomplete gamma function and $M_\gamma(s)$ can be obtained by

$$M_\gamma(s)=\left\{\prod_{i=1}^{n}(1-\overline{\gamma}_i s)\right\}^{-1}. \quad (4\text{-}27)$$

When we only numerically calculate the first N_B terms in the summation for the dummy variable n in (4-26), by the Markov inequality and some mathematical manipulations, we can find the truncation error is upper bounded by

$$T_e(t) \le \lambda^{N_B}\left(N_B\right)^{-N_B}\left[\kappa(t)\right]^{N_B} e^{N_B-\lambda\kappa(t)}\left(\lambda t+\left(2\lambda^{-2}\pi\right)^{-1/2}\left\{e^{-t^2/2}-\sum_{i=1}^{\infty}\left[\mu^i\left(i^3+3i^2+2i\right)^{-1}\times\right.\right.\right.$$

$$\left.\left.\left.\sum_{j=0}^{i}B(j+2,i-j+1)^{-1}\left(\sqrt{2}\sigma\right)^j\mu^{-j}\left\{\Gamma(1+\frac{j}{2},\frac{t^2}{2})-\Gamma(1+\frac{j}{2})\right\}\right]\right\}\right.$$

$$\left.\text{-}\lambda\Phi(\text{t})\left\{\sum_{\text{i=1}}^{\infty}\frac{1}{i(i+1)}\left[\left(\sigma t+\mu\right)^{i+1}-\mu^{i+1}\right]-\sigma t\right\}-\frac{\lambda}{\sqrt{2\pi}}\right). \qquad (4\text{-}28)$$

On the other hand, the dynamic probability of false alarm can be obtained by

$$P_{FA}(t)=\sum_{n=1}^{\infty}\Gamma(nu,\lambda_T/2)\left[\Gamma(nu)\right]^{-1}\exp\{-\lambda\kappa(t)\}\left(\frac{\lambda}{n!}\right)\left(t+\left(2\pi\right)^{-1/2}\left\{e^{-t^2/2}-\sum_{i=1}^{\infty}\left[\mu^i\right.\right.\right.$$

$$\left.\left.\left.\left(i^3+3i^2+2i\right)^{-1}\sum_{j=0}^{i}B(j+2,i-j+1)^{-1}\left(\sqrt{2}\sigma\Big/\mu\right)^j\left\{\Gamma(1+\frac{j}{2},\frac{t^2}{2})-\Gamma(1+\frac{j}{2})\right\}\right]\right\}\right.$$

$$\left.\text{-}\Phi(\text{t})\left\{\sum_{\text{i=1}}^{\infty}\frac{1}{i(i+1)}\left[\left(\sigma t+\mu\right)^{i+1}-\mu^{i+1}\right]-\sigma t\right\}-1\Big/\sqrt{2\pi}\right). \quad (4\text{-}29)$$

If we only numerically compute the first N_B terms in the above equation, similarly, by the Markov inequality and some mathematical manipulations, the upper bounded truncation error can be evaluated by

$$T_e(t)\le\left(N_B\right)^{-N_B}\left[\lambda e\kappa(t)\right]^{N_B}\times\left[\lambda t+\lambda\sigma t\Phi(\text{t})+\lambda\left(2\pi\right)^{-1/2}\left\{e^{-t^2/2}-1-\sum_{i=1}^{\infty}\sum_{j=0}^{i}\frac{2^{j/2}(i-1)!\sigma^j\mu^{i-j}}{(j+1)!(i-j)!}\right.\right.$$

$$\left.\left.\left[\Gamma(1+\frac{j}{2},\frac{t^2}{2})-\Gamma(1+\frac{j}{2})\right]\right\}\text{-}\lambda\Phi(\text{t})\left\{\sum_{\text{i=1}}^{\infty}\frac{1}{i(i+1)}\left[\left(\sigma t+\mu\right)^{i+1}-\mu^{i+1}\right]\right\}\right]\times e^{-\lambda\kappa(t)}. \quad (4\text{-}30)$$

4.2.3.2.2 Asymptotic Performances

The time-averaged probability of detection can be obtained by $\overline{P_d} = T^{-1}\int_0^T P_d(t)\,dt$. If we take T to infinity, the asymptotic long-term time-averaged probability of detection for distributed cooperative spectrum sensing with log-normal random cooperation time over independent non-identical distributed Rayleigh fading channels can be obtained by

$$\begin{aligned}\overline{P}_d &= \lim_{T\to\infty}\frac{1}{T}\int_{t=0}^{T} P_d(t)dt \\ &= \sum_{n=1}^{\infty}\sum_{i=1}^{n}\lambda^n A_i\left\{\frac{\Gamma(nu-1,\lambda_T/2)}{\Gamma(nu-1)}+\exp\left[-\frac{\lambda_T}{2\left(1+\overline{\gamma}_i\right)}\right]\Upsilon\left(nu-1,\frac{\lambda_T}{2}\frac{\overline{\gamma}_i}{\left(1+\overline{\gamma}_i\right)}\right)\left[\Gamma\left(nu-1\right)\right]^{-1}\right. \\ &\left.\left(1+\frac{1}{\overline{\gamma}_i}\right)^{nu-1}\right\}\exp\left\{n\mu+n\sigma^2/2-\lambda\exp(\mu+\sigma^2/2)\right\}\Big/n!. \qquad (4\text{-}31)\end{aligned}$$

If we only numerically evaluate (4-31) with the first N_B terms, by using the Markov inequality, the associated truncation error can be upper-bounded by

$$T_e(t)\le\left(\lambda/N_B\right)^{N_B}\exp\left\{N_B\left(1+\mu+\sigma^2/2\right)-\lambda e^{\mu+\sigma^2/2}\right\}. \qquad (4\text{-}32)$$

Similarly, the asymptotic probability of false alarm can be obtained by

$$\overline{P}_{FA} = \lim_{T\to\infty} \frac{1}{T} \int_{t=0}^{T} P_{FA}(t)dt$$
$$= \sum_{n=1}^{\infty} \lambda^n \Gamma(nu, \lambda_T/2)\left[n!\Gamma(nu)\right]^{-1} \times \exp\left\{n\mu + n\sigma^2/2 - \lambda\exp(\mu + \sigma^2/2)\right\}. \quad (4\text{-}33)$$

If we only numerically calculate the first N_B finite terms for the above equation, with the aid of Markov inequality, after some mathematical manipulations, the upper bounded truncation error is given by

$$T_e(t) \le N_B^{-N_B} \left(\lambda e^{\mu+\sigma^2/2}\right)^{N_B} \exp\left\{N_B + \lambda e^{\mu+\sigma^2/2}\right\}. \quad (4\text{-}34)$$

4.2.4 Nakagami-*m* Fading Channels

Assume the sensing channels from the primary user to each CR are independent Nakagami-*m* fading channels. CRs form an ad-hoc network and randomly choose one of them as a leader to be the fusion center. Assume CRs arrive at CRN by Poisson random process with rate λ. When a CR joins the network, it immediately collaborates with the other CRs in the network until it leaves. The random amount of time a CR stays in cooperation follows Pareto distribution

with parameters $x_m > 0$ and $\alpha > 0$. After this amount of time, it leaves the system and thus leaves the cooperative spectrum sensing. Each CR collects the local energy statistic and transmits this energy statistic via a dedicated error-free channel to the fusion center. The fusion center combines all local energy statistics by summing them together to yield the fused energy statistic and then performs the binary hypothesis testing against a testing threshold λ_T for the spectrum sensing decisions. When the fused energy statistic is greater than or equal to λ_T, $\widehat{H}_1$ decision is reached; otherwise, $\widehat{H}_0$ is claimed. With the aid of the conditional probabilities in [4-7], after routine mathematical manipulations, for $0 \le t < x_m$, the dynamic probability of miss detection can be obtained by

$$P_m(t) = 1 - e^{-\lambda t} \sum_{n=1}^{\infty} \frac{(\lambda t)^n}{n!} \left[A + \beta^m e^{-\frac{\lambda_T}{2\sigma^2}} \sum_{i=1}^{Mn/2-1} \frac{\left(\frac{\lambda_T}{2\sigma^2}\right)^i}{i!} {}_1F_1\left(m; i+1; \frac{\lambda_T(1-\beta)}{2\sigma^2} \right) \right],$$

$$A = e^{-\frac{\lambda_T \beta}{2m\sigma^2}} \left[\beta^{m-1} L_{m-1}\left(\frac{-\lambda_T(1-\beta)}{2\sigma^2} \right) + (1-\beta) \sum_{i=1}^{m-2} \beta^i L_i\left(\frac{-\lambda_T(1-\beta)}{2\sigma^2} \right) \right], \tag{4-35}$$

$$\beta = \left(m\sigma^2\right) \Big/ \left(m\sigma^2 + \sum_{i=1}^{n} \overline{\gamma}_i \right),$$

where M is the number of samples taken over a period of time T in each CR to yield the accumulated local energy statistic, λ_T is the binary hypothesis testing threshold for the fused

energy statistic, σ^2 is the variance for the zero-mean additive noise, the integer m is the Nakagami-m parameter, $\overline{\gamma}_i$ is the average SNR at the i-th Nakagami-m fading sensing channel, ${}_1F_1(.;.;.)$ is the confluent hypergeometric function, and $L_i(.)$ is the Laguerre polynomial of degree i. On the other hand, the dynamic probability of false alarm, for $0 \le t < x_m$, can be obtained by

$$P_{FA}(t) = \sum_{n=1}^{\infty} \frac{(\lambda t)^n e^{-\lambda t} \Gamma(nu, \lambda_T/2)}{n! \Gamma(nu)}. \qquad (4\text{-}36)$$

where u = TW is the time bandwidth product with T as the observation time interval and W as the one-sided bandwidth, $\Gamma(x)$ is the gamma function, and $\Gamma(x,y)$ is the upper incomplete Gamma function. For $t \ge x_m$, the dynamic probability of miss detection can be obtained by

$$P_m(t) = 1 - e^{\frac{-\lambda x_m}{1-\alpha}\left(x_m^{\alpha-1} t^{-\alpha+1} - 1\right)} \sum_{n=1}^{\infty} \left(\frac{\lambda x_m}{1-\alpha} \left(x_m^{\alpha-1} t^{-\alpha+1} - 1 \right) \right)^n \times \frac{1}{n!} \left[A + \beta^m e^{-\frac{\lambda_T}{2\sigma^2}} \sum_{i=1}^{Mn/2-1} \frac{\left(\frac{\lambda_T}{2\sigma^2} \right)^i}{i!} \right.$$

$$\left. \times {}_1F_1\left(m; i+1; \frac{\lambda_T (1-\beta)}{2\sigma^2} \right) \right], \qquad (4\text{-}37)$$

and the dynamic probability of false alarm can be obtained by

$$P_{FA}(t)=\sum_{n=1}^{\infty}\left(\frac{\lambda x_m}{1-\alpha}\left(x_m^{\alpha-1}t^{-\alpha+1}-1\right)\right)^n\times\frac{\Gamma(nu,\lambda_T/2)}{n!\Gamma(nu)}\exp\left\{\frac{-\lambda x_m}{1-\alpha}\left(x_m^{\alpha-1}t^{-\alpha+1}-1\right)\right\}. \quad (4\text{-}38)$$

If CRN has the system size limitation and can only keep up to L CRs in system at the same time, for $0 \le t < x_m$, the dynamic probability of miss detection can be obtained by

$$P_m(t)=1-\frac{e^{-\lambda t}L!}{\Gamma(L+1,\lambda t)}\sum_{n=1}^{L}\frac{(\lambda t)^n}{n!}\left[A+\beta^m e^{-\frac{\lambda_T}{2\sigma^2}}\times\sum_{i=1}^{Mn/2-1}\frac{\left(\frac{\lambda_T}{2\sigma^2}\right)^i}{i!}{}_1F_1\left(m;i+1;\frac{\lambda_T(1-\beta)}{2\sigma^2}\right)\right], \quad (4\text{-}39)$$

and the dynamic probability of false alarm can be obtained by

$$P_{FA}(t)=\sum_{n=1}^{L}\frac{(\lambda t)^n e^{-\lambda t}\Gamma(nu,\lambda_T/2)L!}{n!\Gamma(nu)\Gamma(L+1,\lambda t)}. \quad (4\text{-}40)$$

For $t \ge x_m$, the dynamic probability of miss detection can be obtained by

$$P_m(t)=1-e^{\frac{-\lambda x_m}{1-\alpha}\left(x_m^{\alpha-1}t^{-\alpha+1}-1\right)}\left[\Gamma(L+1,\frac{\lambda x_m}{1-\alpha}\left(x_m^{\alpha-1}t^{-\alpha+1}-1\right))\right]^{-1}\times L!\sum_{n=1}^{L}\frac{1}{n!}\left(\frac{\lambda x_m}{1-\alpha}\left(x_m^{\alpha-1}t^{-\alpha+1}-1\right)\right)^n \quad (4\text{-}41)$$
$$\times\left[A+\beta^m e^{-\frac{\lambda_T}{2\sigma^2}}\sum_{i=1}^{Mn/2-1}\frac{\left(\frac{\lambda_T}{2\sigma^2}\right)^i}{i!}{}_1F_1\left(m;i+1;\frac{\lambda_T(1-\beta)}{2\sigma^2}\right)\right]$$

and the dynamic false alarm probability can be obtained by

$$P_{FA}(t)=\frac{L!\exp\left\{\frac{-\lambda x_m}{1-\alpha}\left(x_m^{\alpha-1}t^{-\alpha+1}-1\right)\right\}}{\Gamma\left(L+1,\frac{\lambda x_m}{1-\alpha}\left(x_m^{\alpha-1}t^{-\alpha+1}-1\right)\right)}\times\sum_{n=1}^{\infty}\left(\frac{\lambda x_m}{1-\alpha}\left(x_m^{\alpha-1}t^{-\alpha+1}-1\right)\right)^n\frac{\Gamma(nu,\lambda_T/2)}{n!\Gamma(nu)}. \tag{4-42}$$

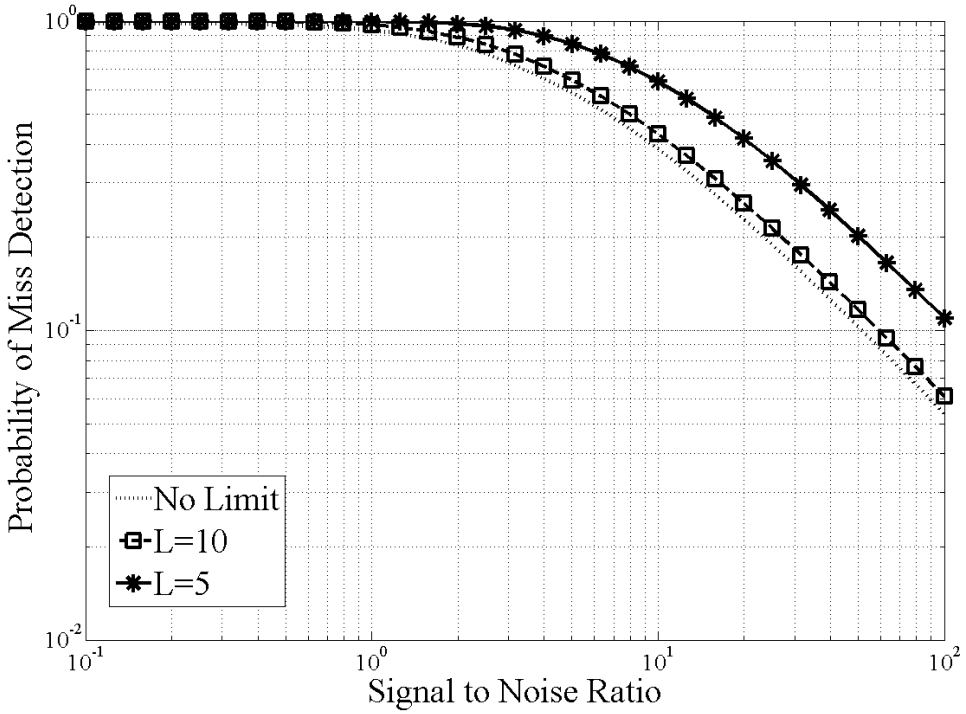

Fig. 4-2 Probability of Miss Detection under Different System Size Limitation

When the system size is limited up to L=10, from Fig. 4-2, the system performance does degrade slightly. However, if this limit becomes too aggressive, i.e. L=5, there is significant performance loss in the distributed cooperative spectrum sensing. Hence, if CRN wants to split

CRs into several groups to monitor several primary users simultaneously, from Fig. 4-2, we can see a group of 10 only loses the sensing reliability slightly but a group of 5 might lead to too much harmful interference with the primary users, which is not allowed

4.5 Shadowed Nakagami-*m* Fading Channels

A composite shadowed fading wireless fading environment consists of multipath fading superimposed on shadowing. In this environment, the wireless receiver does not average out the envelope fading due to multipath but rather reacts to the instantaneous composite multipath/shadowed signal. This is often the scenario in congested downtown areas with slow pedestrians and vehicles [4-8]. When the CRs are carried by slow pedestrians and or people in slow vehicles in congested downtown areas, these CRs are only moving slowly or even almost stationary. Therefore, the wireless links for CRs in such areas can be described by a composited shadowed Nakagami-*m* channel model introduced by Ho and Stüber [4-9]. The received signal-to-noise ratio for this composite shadowed fading channel has the Gamma-log-normal probability density function as follows:

$$f(\gamma)=\int_0^{\infty}\left(\frac{m}{w}\right)^m\frac{\gamma^{m-1}}{\Gamma(m)}e^{-m\gamma/w}\frac{10}{\sqrt{2\pi}\ln(10)\sigma_\Omega w}\times\exp\left\{-\left[10\log_{10}(w)-\mu_\Omega\right]^2\Big/2\sigma_\Omega{}^2\right\}dw, \quad (4\text{-}43)$$

where m is the Nakagami-m parameter and μ_Ω and σ_Ω are the parameters for the log-normal shadowing. By [4-10], we can obtain the well approximated moment generating function for the Gamma-log-normal probability density function as

$$M_\gamma(s)\cong\frac{1}{\sqrt{\pi}}\sum_{j=1}^{N_p}H_{x_j}(1-10^{\left(\sqrt{2}\sigma_\Omega x_j+\mu_\Omega\right)/10}\times\frac{s}{m})^{-m}. \quad (4\text{-}44)$$

Therefore, after carrying out routine mathematical manipulations, the average probability of detection over the composite shadowed Nakagami-m fading channel can be obtained by

$$P_d=\sum_{k=0}^{\infty}\frac{(-1)^k\Gamma(m+k)\Gamma(Nu+k,\lambda_Z/2)}{k!\sqrt{\pi}m^{k+1}\Gamma(m)\Gamma(Nu+k)}\times\sum_{j=1}^{N_p}H_{x_j}10^{\left(\sqrt{2}\sigma_\Omega x_j+\mu_\Omega\right)/10}\left(m-10^{\left(\sqrt{2}\sigma_\Omega x_j+\mu_\Omega\right)/10}\right)^{-(m+k)}, \quad (4\text{-}45)$$

where x_j are the zeros of the N_p-order polynomial and H_{xj} are the weight factors of the N_p-order Hermite polynomial [4-11].

Suppose CRs' arrivals follow Poisson random process with rate λ. While CRs arrive at CRN, they immediately collaborate with the other CRs concurrently in the network to perform the cooperative spectrum sensing. Assume the time of CRs stays in the network follows Pareto distribution with parameters $x_m > 0$ and $\alpha > 0$ and, after this amount of time, CRs leave the network and thus leave the collaboration for distributed spectrum sensing immediately. The channels between the primary user to each CR are independent and identically distributed shadowed Nakagami-m fading channels. The fusion center calculates the fused energy statistic by summing the received energy statistics from all CRs currently in the network. Therefore, the dynamic probability of false alarm can be obtained by, for $0 \le t < x_m$ and n=0, 1, 2, …,

$$P_{FA}(t) = \sum_{n=1}^{\infty} \frac{t^n \Gamma(nu, \lambda_Z/2)}{n!\Gamma(nu)} \times \lambda^n e^{-\lambda t}. \quad (4\text{-}46)$$

For $t \ge x_m$ and n=0,1, 2, …,

$$P_{FA}(t) = \sum_{n=1}^{\infty} \frac{\Gamma(nu, \lambda_Z/2)}{n!\Gamma(nu)(1-\alpha_m)} [\lambda x_m \left({x_m}^{\alpha_m - 1} t^{-\alpha_m + 1} - 1 \right)]^n e^{-\left[\frac{\lambda x_m}{1-\alpha_m} \left({x_m}^{\alpha_m - 1} t^{-\alpha_m + 1} - 1 \right) \right]} \quad (4\text{-}47)$$

Similarly, the dynamic probability of detection can be obtained by, for $0 \le t < x_m$ and n = 0, 1, 2, …,

$$P_d(t)=\sum_{n=1}^{\infty}\sum_{k=0}^{\infty}\lambda^n e^{-\lambda t}\ t^n\Gamma(m+k)\Gamma(Nu+k,\lambda_Z/2)\left[n!k!\sqrt{\pi}m^{k+1}\Gamma(m)\Gamma(Nu+k)\right]^{-1}$$

$$\sum_{j=1}^{N_p}H_{x_j}10^{\left(\sqrt{2}\sigma_\Omega x_j+\mu_\Omega\right)/10}\left(m-10^{\left(\sqrt{2}\sigma_\Omega x_j+\mu_\Omega\right)/10}\right)^{-(m+k)} \quad (4\text{-}48)$$

For $t \geq x_m$,

$$P_d(t)$$

$$=\sum_{n=1}^{\infty}\sum_{k=0}^{\infty}\frac{(-1)^k\,\Gamma(m+k)\Gamma(Nu+k,\lambda_Z/2)\left[\lambda x_m\left({x_m}^{\alpha_m-1}t^{-\alpha_m+1}-1\right)\right]^n}{n!k!\sqrt{\pi}m^{k+1}\Gamma(m)\Gamma(Nu+k)(1-\alpha_m)}\times \quad (4\text{-}49)$$

$$\sum_{j=1}^{N_p}H_{x_j}10^{\left(\sqrt{2}\sigma_\Omega x_j+\mu_\Omega\right)/10}\left(m-10^{\left(\sqrt{2}\sigma_\Omega x_j+\mu_\Omega\right)/10}\right)^{-(m+k)}e^{-\left[\frac{\lambda x_m}{1-\alpha_m}\left({x_m}^{\alpha_m-1}t^{-\alpha_m+1}-1\right)\right]}$$

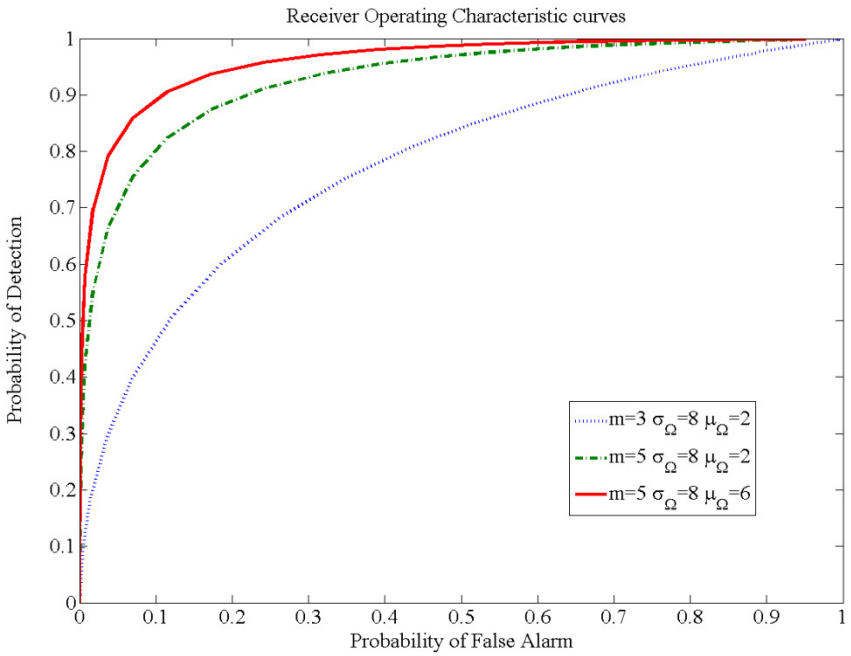

Fig. 4-3. Receiver Operating Characteristic (ROC) Curves for Cooperative Spectrum Sensing over Shadowed Nakagami-m Fading Channels

Performance of a detector is often described through its receiver operating characteristic (ROC) curves (P_d versus P_{FA}). In figure 4-3, the ROC curves for energy-based spectrum sensing over shadowed Nakagami-*m* fading channel are plotted with different combinations of Nakagami-*m* fading parameter, *m*, and log-normal shadowing parameters, μ_Ω and σ_Ω. Smaller *m* means more severe the fading effect, e.g., Nakagami-*m* fading degenerates to Rayleigh fading when *m* = 1. Since σ_Ω is typically observed between 5 to 12 dB in macrocellular applications and between 4 to 13 dB in microcellular applications, we use σ_Ω = 8 dB to generate the curves in Fig. 4. When the channels are more benign, the receiver yields better detection results.

References

[4-1] M. K. Simon and M. Alouini, *Digital Communication over Fading Channels*. John Wiley & Sons, 2005.

[4-2] Q. Du and X. Zhang, " Queue-aware spectrum sensing for interference-constrained transmissions in cognitive radio networks," in *Proc. IEEE Inter. Conf. on Communications (ICC),* Cape Town, May 2010.

[4-3] T. S. Rappaport, *Wireless Communications: Principles and Practice*. Prentice Hall, 2002.

[4-4] H. Sun, D. I. Laurenson, and C. X. Wang, "Computationally tractable model of energy

detection performance over slow fading channels," *IEEE Communications Letters*, vol. 14, no. 10, October 2010.

[4-5] F. F. Digham, M. Alouini, and M. K. Simon, "On the energy detection of unkown signals over fading channels," *IEEE Trans. Communications*, Vol. 55, NO.1, Jan. 2007.

[4-6] A. Rao and M. Alouini, "Performance of cooperative spectrum sensing over non-identical fading environments," *IEEE Trans. on Communications*, Vol. 59, No. 12, Dec. 2011.

[4-7] F. F. Digham, M. Alouini, and M. K. Simon, "On the energy detection of unkown signals over fading channels," *IEEE Trans. Communications*, Vol. 55, NO.1, Jan. 2007.

[4-8] H. Suzuki, "A statistical model for urban multipath propagation," *IEEE Trans. Commun.*, vol. COM-25, July 1977.

[4-9] M. Ho and G. Stüber, "Co-channel interference of microcellular systems on shadowed Nakagami fading channels," *Proc. IEEE Veh. Technol. Conf. (VTC'93)*, Secaucus, NJ, May 1993.

[4-10] M. K. Simon and M. Alouini, *Digital Communication over Fading Channels*. John Wiley & Sons, 2005.

[4-11] M. Abramowitz and I. Stegun, *Handbook of Mathematical Functions With Formulas, Graphs, and Mathematical Tables*, National Bureau of Standards, U.S. Department of Commerce, Dec. 1972.

Chap 5
Applications in Cellular Wireless Systems

Wireless technology has greatly influenced the human society. The demand for the wireless spectrum resources substantially increases with the growth of population. Especially, portable wireless devices, such as smart phones, have been very popular in people's daily lives. People use their smart phones taking pictures and uploading these pictures to the social network websites. People also can watch video streaming or have videoconferencing on their portable devices through the wireless communications. These popular wireless applications have posed great demand for the precious radio spectrum. Especially, there are usually a huge number of audiences in big events, such as superstar's concerts, NFL football games, the Presidential candidate speech, and etc. If a certain percentage of these audiences take pictures and upload them to the social network websites at the same time, this will overwhelm the cellular wireless systems. Therefore, the cellular wireless systems urgently need new technologies to be able to explore extra spectrum utilization opportunities for this type of sudden bursty spectrum demand in certain local areas.

On the other hand, a large portion of the licensed spectrum remains underutilized [5-1]. In recent years, the Federal Communications Commission (FCC) has been considering more

flexible and comprehensive usages of the available spectrum via the use of cognitive radio networks (CRN) technology [5-2]. The cognitive radio network technology is a promising solution for cellular wireless systems to seek for geographically temporal spectrum opportunities for bursty spectrum demand.

As a secondary overlay network, CRN technologies have to guarantee not to cause harmful interference to the licensed primary users [5-3]. Spectrum sensing is one of key components in CRN to monitor the licensed primary users' activities [5-4]. When the primary users are not using their licensed frequency bands, cellular cognitive radio networks (CCRN) is allowed to temporarily exploit these frequency bands. Due to the fading and shadowing phenomena of the wireless channels, CCRN should explore the spatial diversity through the cooperation among CRs to overcome the hidden primary user issue [5-5]. Various spectrum sensing algorithms are proposed in the literatures [5-6]. They can be classified into the following categories: energy detection, matched filter coherent detection, feature-based detection, and eigenvalue-based detection [5-7], [5-8]. Among these existing spectrum sensing schemes, energy-based spectrum sensing is the most widely adopted one in the current CRN prototype systems due to the simplicity and relatively low computational costs [5-9]. Therefore, from the practical perspective, we focus on the energy-based cooperative spectrum sensing scheme in this chapter.

Exploring the spatial diversity, the spectrum sensing can make more reliable decisions [5-10]. However, since the cellular users can turn on/off the CR functionalities at will, the associated CCRN is not a static network but a dynamic network. Thus, the number of spatial diversity in the distributed spectrum sensing is not constant but time-varying. The dynamics of CRs impact the spectrum sensing performance. To guarantee not to violate the privileges of the licensed primary users and also to optimize CCRN its own throughput, CCRN has to adapt the system parameters to the dynamics of CR accordingly. Furthermore, since the surroundings for each CR in the collaboration might be different, the received primary user signals by spatially distributed CRs may experience a variety of random phenomena in the wireless transmissions [5-11]. Hence, in this chapter, considering a more appropriate and practical scenario, we investigate distributed spectrum sensing over non-identical distributed wireless channels.

5.1 User Dynamics

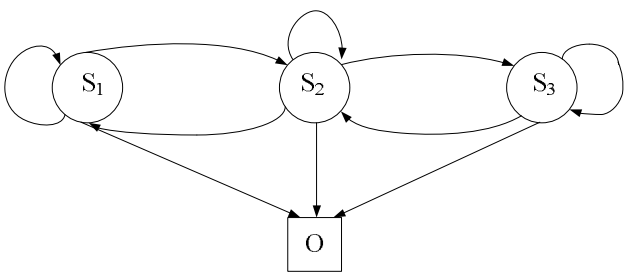

Fig. 5-1. Hidden Markov Model

People move based on their schedules and their needs. For example, there are more people around the dining facilities around the meal times than the other time. More students are on campus in the day time than night time. The high way traffic is congested in the morning and evening times when people go to work/return. Therefore, the number of people in a location is usually fluctuating. Thus, the number of CRs in any specific location is also time-varying. We can model the CRs' arrivals by a Hidden-Markov Model (HMM) [5-12] which consists of 3 hidden state nodes, S_1, S_2, and S_3, and one observation node, O, see Fig. 5-1. State 1 represents CRs arrive at low rate; state 2 represents CRs' arrivals are at regular rate; state 3 means CRs are at high arrival rate. The transition from state S_i to state S_j is denoted by a directed edge $\{S_i, S_j\}$ and the associated transition probability $P(S_j|S_i)$ is short-handed by p_{ij}. The transition probability matrix is given by

$$P = \begin{bmatrix} 1-p_{12} & p_{12} & 0 \\ p_{21} & 1-p_{21}-p_{23} & p_{23} \\ 0 & p_{32} & 1-p_{32} \end{bmatrix}. \qquad (5\text{-}1)$$

However, due to the weather and some other random factors, e.g. the traffic, social events, etc, CRs' arrival rate is usually not a constant but randomly fluctuating. Hence, we can indeed model the CRs' arrivals by a doubly stochastic process, called Cox process [5-13]. The

fluctuating arrival rate can be model by another random process $\{\lambda(t)\}$. Given any specific time instance t_1 with the rate $\{\lambda(t_1)=\lambda_1\}$, the arrival process is the Poisson random process with rate λ_1. Hence, Cox process can be viewed as a Poisson random process with fluctuating rate modeled by another stochastic process.

After a person turns on the mobile device equipped with CR functionalities, the CR module immediately joins the ad hoc network formed by the other CRs to seek for the spectrum opportunities. However, people might lose the patience and leave before they are allowed to use the wireless spectrum. In current cellular wireless systems, Gamma distribution can well model Cell Dwell Time (CDT) which is the amount of time a mobile device stays within a cell, see [5-14], [5-15], [5-16], and the references therein. Suppose, in CCRN, the random amount of time a CR stays in cooperation and waits for the spectrum opportunities follows the Gamma distribution. After this random amount of time, the user loses the patience and turns off the CR. Thus, the equipped CR leaves the spectrum sensing collaboration.

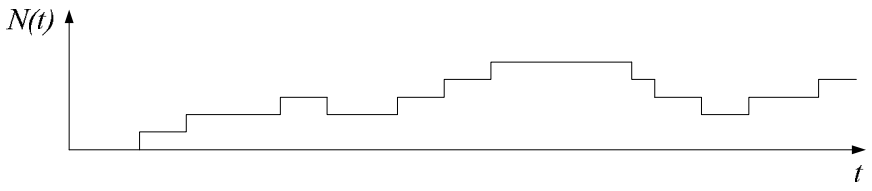

Fig. 5-2. One Realization of Semi-Markov Process

The number of CRs in a CCRN based on the above mentioned random arrivals and random departures is indeed a semi-Markov process, $\{N(t)\}$ over infinitely countable space $\{0,1,2,\ldots\}$ [5-17], see Fig. 5-2. Assume state 1 is associated with stationary arrival rate process $\{\lambda_1(t)\}$ uniformly distributed over $(b_1-\Delta_1, b_1+\Delta_1]$; state 2 has stationary arrival rate process $\{\lambda_2(t)\}$ uniformly distributed over $(b_2-\Delta_2, b_2+\Delta_2]$; state 3 is associated with stationary arrival rate process $\{\lambda_3(t)\}$ uniformly distributed over $(b_3-\Delta_3, b_3+\Delta_3]$. Suppose all CRs in the network join the cooperative spectrum sensing until they leave. Suppose the random amount of time for each CR stays in the collaboration for CCRN is independent and identically Gamma distributed with parameters, $k > 0$ and $\theta > 0$. The probability density function of the Gamma distribution is given by

$$f(x) = \frac{1}{\Gamma(k)\theta^k} x^{k-1} e^{-\frac{x}{\theta}}, \qquad x \in [0,\infty), \qquad (5\text{-}2)$$

where $\Gamma(.)$ is the gamma function. Hence, the dynamic probability mass function of the number of CRs in the network at any time t can be derived as follows:

$$P(N(t)=n)=\left[2\left(p_{32}p_{21}+p_{32}p_{12}+p_{23}p_{12}\right)n!\right]^{-1}\left\{p_{32}p_{21}\left(\left[t-\frac{t^{k+1}}{\Gamma(k)\theta^{k}}\sum_{z=0}^{\infty}\frac{\left(-t/\theta\right)^{z}}{(z+k)z!}\right]\left[b_1+\Delta_1\right]\right)^{n}\right.$$

$$\Delta_1^{-1}\left(b_1+\Delta_1\right)\sum_{i=0}^{\infty}\left[i!(n+i+1)\right]^{-1}\left(-\left[t-\frac{t^{k+1}}{\Gamma(k)\theta^{k}}\sum_{z=0}^{\infty}\frac{\left(-t/\theta\right)^{z}}{(z+k)z!}\right]\times\left[b_1+\Delta_1\right]\right)^{i}+p_{32}p_{12}\Delta_2^{-1}\left(b_2+\Delta_2\right) \quad (5\text{-}3)$$

$$\left(\left[t-\frac{t^{k+1}}{\Gamma(k)\theta^{k}}\sum_{z=0}^{\infty}\frac{\left(-t/\theta\right)^{z}}{(z+k)z!}\right]\left[b_2+\Delta_2\right]\right)^{n}\sum_{i=0}^{\infty}\left[i!(n+i+1)\right]^{-1}\left(\left[t-\frac{t^{k+1}}{\Gamma(k)\theta^{k}}\sum_{z=0}^{\infty}\frac{\left(-t/\theta\right)^{z}}{(z+k)z!}\right]\left[-b_2-\Delta_2\right]\right)^{i}$$

$$+p_{23}p_{12}\Delta_3^{-1}\left(\left[b_3+\Delta_3\right]\left[t-\frac{t^{k+1}}{\Gamma(k)\theta^{k}}\sum_{z=0}^{\infty}\frac{\left(-t/\theta\right)^{z}}{(z+k)z!}\right]\right)^{n}\sum_{i=0}^{\infty}\left(-\left[t-\frac{t^{k+1}}{\Gamma(k)\theta^{k}}\sum_{z=0}^{\infty}\frac{\left(-t/\theta\right)^{z}}{(z+k)z!}\right]\left[b_3+\Delta_3\right]\right)^{i}$$

$$\left(b_3+\Delta_3\right)p_{32}p_{21}\Delta_1^{-1}\left(b_1-\Delta_1\right)\sum_{i=0}^{\infty}\left[i!(n+i+1)\right]^{-1}\left(-\left[b_1-\Delta_1\right]\left[t-\frac{t^{k+1}}{\Gamma(k)\theta^{k}}\sum_{z=0}^{\infty}\frac{\left(-t/\theta\right)^{z}}{(z+k)z!}\right]\right)^{i}-p_{32}p_{12}$$

$$\Delta_2^{-1}\left(b_2-\Delta_2\right)\left(\left[t-\frac{t^{k+1}}{\Gamma(k)\theta^{k}}\sum_{z=0}^{\infty}\frac{\left(-t/\theta\right)^{z}}{(z+k)z!}\right]\left[b_2-\Delta_2\right]\right)^{n}\sum_{i=0}^{\infty}\left(-\left[t-\frac{t^{k+1}}{\Gamma(k)\theta^{k}}\sum_{z=0}^{\infty}\frac{\left(-t/\theta\right)^{z}}{(z+k)z!}\right]\left[b_2-\Delta_2\right]\right)^{i}$$

$$\left[i!(n+i+1)\right]^{-1}-\left(\left[b_3-\Delta_3\right]\left[i!(n+i+1)\right]^{-1}-\left(\left[t-\frac{t^{k+1}}{\Gamma(k)\theta^{k}}\sum_{z=0}^{\infty}\frac{\left(-t/\theta\right)^{z}}{(z+k)z!}\right]\left[b_1-\Delta_1\right]\right)^{n}\left(b_3-\Delta_3\right)\right.$$

$$\left.\left.\left[t-\frac{t^{k+1}}{\Gamma(k)\theta^{k}}\sum_{z=0}^{\infty}\frac{\left(-t/\theta\right)^{z}}{(z+k)z!}\right]\right)^{n}\sum_{i=0}^{\infty}\left[i!(n+i+1)\right]^{-1}\left(-\left[t-\frac{t^{k+1}}{\Gamma(k)\theta^{k}}\sum_{z=0}^{\infty}\frac{\left(-t/\theta\right)^{z}}{(z+k)z!}\right]\left[b_3-\Delta_3\right]\right)^{i}\Delta_3^{-1}p_{23}p_{12}\right\}.$$

Based on the above dynamic probability mass function, we can evaluate the time-varying probability of detection and time-varying probability of false alarm in the following section.

5.2 Performance Analysis

We consider that spatially distributed CRs form a local CCRN to collaborate with each other in sensing the spectrum utilization to seek for the opportunities using available wireless channels to communicate. The base station of the cellular wireless system is the fusion center for this ad hoc CCRN to seek for extra spectrum opportunities. Each CR senses the spectrum and sends the collected local energy information through a dedicated error-free reporting channel to the fusion center. The fusion center makes final sensing decisions based on the collected local statistics.

5.2.1 System Model

Consider the received signal at the *i*-th CR is given by

$$\begin{aligned} H_0 &: r_i(t) = n_i(t), \\ H_1 &: r_i(t) = h_i(t)x_i(t) + n_i(t), \end{aligned} \tag{5-4}$$

where $x_i(t)$ is the primary user's complex-valued signal waveform received at the *i*-th CR, $h_i(t)$ is a slow fading channel, and $n_i(t)$ is the additive white Gaussian noise (AWGN). H_1 is when the primary user is using its own licensed band; H_0 means the licensed band is vacant. The *i*-th CR collects the energy by taking $M/2$ samples of the received waveform $r_i(t)$ both at the I and Q

components respectively over a period of time T, and then takes the absolute values, squares, and sums the samples to yield the corresponding collected received signal energy statistic $y_i = \sum_{k=1}^{M/2} | r_i(k) |^2$. Under H_1, y_i has a noncentral chi-square distribution with noncentrality $2\gamma_i$ and M degrees of freedom and, under H_0, y_i has a central chi-square distribution with M degrees of freedom. Then all N CRs transmit the encoded collected energy statistics through a dedicated error-free channel to the fusion center. The fused energy statistics Z is obtained by summing y_i over all N CRs. To make a spectrum sensing decision, the fusion center compares the energy statistic Z to a threshold λ_Z, and then declares $\hat{H}_0$ when $Z < \lambda_Z$ and declares $\hat{H}_1$ when $Z \geq \lambda_Z$. The probability of false alarm, $P(\hat{H}_1 | H_0, \gamma)$, and probability of detection, $P(\hat{H}_1 | H_1, \gamma)$, conditioned on the Signal-to-Noise Ratio (SNR), γ, are given by [5-18]

$$P_{FA|\gamma} = \frac{\Gamma(Nu, \lambda_Z/2)}{\Gamma(Nu)}, \tag{5-5}$$

$$P_{d|\gamma} = Q_{Nu}\left(\sqrt{2\gamma}, \sqrt{\lambda_Z}\right), \tag{5-6}$$

where $Q_M(a,b)$ is the generalized Marcum Q-function, $\Gamma(x,y)$ is the upper incomplete gamma function, $\Gamma(x)$ is the gamma function, u = TW is the time bandwidth product with T as the observation time interval and W as the one-sided bandwidth. From (5-5), we know the

conditional probability of false alarm is indeed independent of SNR, γ. Therefore, the average probability of false alarm over any fading channels is fully characterized by (5-5). The average probability of detection over a fading channel can be obtained by

$$P_d = \int_0^\infty Q_{Nu}\left(\sqrt{2\gamma}, \sqrt{\lambda_Z}\right) f_\gamma(\gamma) d\gamma. \qquad (5\text{-}7)$$

The detection threshold λ_Z can be decided under the Neyman-Pearson criterion. Under the given desired probability of false alarm, $P_{FA} = \alpha$, λ_Z can be determined and the average probability of detection can be calculated by (5-7).

5.2.2 Composite Fading/Shadowing Channels

We consider the scenario in congested downtown areas with slow pedestrians and vehicles. The CRs are carried by the people who are only moving slowly or even almost stationary within an area. In this environment, the wireless receiver does not average out the envelope fading due to multipath but rather reacts to the instantaneous composite multipath/shadowed signal. Therefore, the wireless links for CRs in these areas can be modeled by a composited shadowed Nakagami-*m*

fading channel model introduced by Ho and Stüber [5-19]. A composite shadowed fading wireless environment consists of multipath fading superimposed on shadowing. This composite shadowed fading channel has the Gamma-log-normal probability density function as follows:

$$f(\gamma)=\int_0^\infty \left(\frac{m}{w}\right)^m \frac{\gamma^{m-1}}{\Gamma(m)} e^{-m\gamma/w} \frac{10}{\sqrt{2\pi}\ln(10)\sigma_\Omega w} \exp\left\{-\left[10\log_{10}(w)-\mu_\Omega\right]^2 \Big/ 2\sigma_\Omega{}^2\right\} dw, \qquad (5\text{-}8)$$

where *m* is the Nakagami-*m* parameter and μ_Ω and σ_Ω are the parameters for the log-normal shadowing. By [5-20], we can obtain the well approximated moment generating function for the Gamma-log-normal probability density function as

$$M_\gamma(s) \cong \frac{1}{\sqrt{\pi}} \sum_{j=1}^{N_p} H_{x_j} (1-10^{\left(\sqrt{2}\sigma_\Omega x_j+\mu_\Omega\right)/10} \times \frac{s}{m})^{-m}. \qquad (5\text{-}9)$$

Therefore, after carrying out routine mathematical manipulations, the average probability of detection over the composite shadowed Nakagami-*m* fading channel can be derived as

$$P_d = \sum_{y=0}^{\infty} \frac{(-1)^y \Gamma(m+y)\Gamma(Nu+y,\lambda_Z/2)}{y!\sqrt{\pi}m^{y+1}\Gamma(m)\Gamma(Nu+y)} \sum_{j=1}^{N_p} H_{x_j} 10^{\left(\sqrt{2}\sigma_\Omega x_j+\mu_\Omega\right)/10} \left(m-10^{\left(\sqrt{2}\sigma_\Omega x_j+\mu_\Omega\right)/10}\right)^{-(m+y)}, \qquad (5\text{-}10)$$

where x_j are the zeros of the N_p-order polynomial and H_{xj} are the weight factors of the N_p-order Hermite polynomial [5-21].

5.2.3 Dynamic Performance Analysis

The cooperative spectrum sensing performance is varying because of fading, shadowing, etc. On the other hand, since the number of CRs in CRN is also dynamically changing, the cooperative spectrum sensing performance is varying accordingly. The average probability of false alarm and the average probability of detection in the above subsections are under some fixed number of CRs in the cooperation. In this subsection, we consider the dynamic of the number of CRs in the network to analyze the dynamic performances. We consider the case that the primary user is using its own licensed frequency band (H_1 is true) and the CRs have to collaborate to perform spectrum sensing to wait for the spectrum opportunities. Hence, the dynamic probability of detection, $P(\hat{H}_1 \mid H_1)$, can be obtained by

$$P_d(t)=\sum_{n=1}^{\infty}\sum_{y=0}^{\infty}\frac{(-1)^y\,\Gamma(m+y)\Gamma(nu+y,\lambda_Z/2)}{y!\sqrt{\pi}m^{y+1}\Gamma(m)\Gamma(nu+y)}\sum_{j=1}^{N_p}H_{x_j}10^{\left(\sqrt{2}\sigma_\Omega x_j+\mu_\Omega\right)/10}\left(m-10^{\left(\sqrt{2}\sigma_\Omega x_j+\mu_\Omega\right)/10}\right)^{-(m+y)}$$

$$\times\left[2\left(p_{32}p_{21}+p_{32}p_{12}+p_{23}p_{12}\right)n!\right]^{-1}\left\{p_{32}p_{21}\Delta_1^{-1}\left(b_1+\Delta_1\right)\left(\left[t-\frac{t^{k+1}}{\Gamma(k)\theta^k}\sum_{z=0}^{\infty}\frac{(-t/\theta)^z}{(z+k)z!}\right]\left[b_1+\Delta_1\right]\right)^n\right.$$

$$\times\sum_{i=0}^{\infty}\left[i!(n+i+1)\right]^{-1}\left(\left[t-\frac{t^{k+1}}{\Gamma(k)\theta^k}\sum_{z=0}^{\infty}\frac{(-t/\theta)^z}{(z+k)z!}\right]\left[-b_1-\Delta_1\right]\right)^i+p_{32}p_{12}\Delta_2^{-1}\left(b_2+\Delta_2\right)\left(\left[b_2+\Delta_2\right]\times\right.$$

$$\left.\left[t-\frac{t^{k+1}}{\Gamma(k)\theta^k}\sum_{z=0}^{\infty}\frac{(-t/\theta)^z}{(z+k)z!}\right]\right)^n\times\sum_{i=0}^{\infty}\left[i!(n+i+1)\right]^{-1}\left(-\left[t-\frac{t^{k+1}}{\Gamma(k)\theta^k}\sum_{z=0}^{\infty}\frac{(-t/\theta)^z}{(z+k)z!}\right]\left[b_2+\Delta_2\right]\right)^i+\Delta_3^{-1}$$

$$p_{23}p_{12}\left(b_3+\Delta_3\right)\left(\left[t-\frac{t^{k+1}}{\Gamma(k)\theta^k}\sum_{z=0}^{\infty}\frac{(-t/\theta)^z}{(z+k)z!}\right]\left[b_3+\Delta_3\right]\right)^n\sum_{i=0}^{\infty}\left[i!(n+i+1)\right]^{-1}\left(-\left[t-\frac{t^{k+1}}{\Gamma(k)\theta^k}\times\right.\right. \quad (5\text{-}11)$$

$$\left.\left.\sum_{z=0}^{\infty}\frac{(-t/\theta)^z}{(z+k)z!}\right]\left[b_3+\Delta_3\right]\right)^i-p_{32}p_{21}\left(b_1-\Delta_1\right)^{n+1}\times\Delta_1^{-1}\left[t-\frac{t^{k+1}}{\Gamma(k)\theta^k}\sum_{z=0}^{\infty}\frac{(-t/\theta)^z}{(z+k)z!}\right]^n\sum_{i=0}^{\infty}\left[b_1-\Delta_1\right]^i$$

$$\times\left[i!(n+i+1)\right]^{-1}\left[t-\frac{t^{k+1}}{\Gamma(k)\theta^k}\sum_{z=0}^{\infty}\frac{(-t/\theta)^z}{(z+k)z!}\right]^i(-1)^i-\left(\left[t-\frac{t^{k+1}}{\Gamma(k)\theta^k}\sum_{z=0}^{\infty}\frac{(-t/\theta)^z}{(z+k)z!}\right]\left[b_2-\Delta_2\right]\right)^n$$

$$\times p_{32}p_{12}\Delta_2^{-1}\left(b_2-\Delta_2\right)\times\sum_{i=0}^{\infty}\left[i!(n+i+1)\right]^{-1}\left(-\left[t-\frac{t^{k+1}}{\Gamma(k)\theta^k}\sum_{z=0}^{\infty}\frac{(-t/\theta)^z}{(z+k)z!}\right]\left[b_2-\Delta_2\right]\right)^i-p_{23}p_{12}\Delta_3^{-1}$$

$$\left.\left(b_3-\Delta_3\right)^{n+1}\left[t-\frac{t^{k+1}}{\Gamma(k)\theta^k}\sum_{z=0}^{\infty}\frac{(-t/\theta)^z}{(z+k)z!}\right]^n\sum_{i=0}^{\infty}\left[i!(n+i+1)\right]^{-1}\left[\left(t-\frac{t^{k+1}}{\Gamma(k)\theta^k}\sum_{z=0}^{\infty}\frac{(-t/\theta)^z}{(z+k)z!}\right)\left(\Delta_3-b_3\right)\right]^i\right\}.$$

Similarly, the dynamic probability of false alarm is given by

$$P_{FA}(t)=\sum_{n=1}^{\infty}\left[2\left(p_{32}p_{21}+p_{32}p_{12}+p_{23}p_{12}\right)n!\right]^{-1}\left[\Gamma(nu)\right]^{-1}\Gamma(nu,\lambda_Z/2)\left\{p_{32}p_{21}\Delta_1^{-1}\left(b_1+\Delta_1\right)\right.$$

$$\left(\left[t-\frac{t^{k+1}}{\Gamma(k)\theta^k}\sum_{z=0}^{\infty}\frac{\left(-t/\theta\right)^z}{(z+k)z!}\right]\left[b_1+\Delta_1\right]\right)^n\sum_{i=0}^{\infty}\left[i!(n+i+1)\right]^{-1}\left(b_1+\Delta_1\right)^i\left[\frac{t^{k+1}}{\Gamma(k)\theta^k}\sum_{z=0}^{\infty}\frac{\left(-t/\theta\right)^z}{(z+k)z!}\right.$$

$$\left.-t\right]^i+p_{32}p_{12}\Delta_2^{-1}\left(b_2+\Delta_2\right)^{n+1}\left[t-\frac{t^{k+1}}{\Gamma(k)\theta^k}\sum_{z=0}^{\infty}\frac{\left(-t/\theta\right)^z}{(z+k)z!}\right]^n\sum_{i=0}^{\infty}\left[\frac{t^{k+1}}{\Gamma(k)\theta^k}\sum_{z=0}^{\infty}\frac{\left(-t/\theta\right)^z}{(z+k)z!}-t\right]^i$$

$$\times\left[b_2+\Delta_2\right]^i\left[i!(n+i+1)\right]^{-1}+p_{23}p_{12}\Delta_3^{-1}\left(b_3+\Delta_3\right)\left(\left[t-\frac{t^{k+1}}{\Gamma(k)\theta^k}\sum_{z=0}^{\infty}\frac{\left(-t/\theta\right)^z}{(z+k)z!}\right]\left[b_3+\Delta_3\right]\right)^n \quad (5\text{-}12)$$

$$\sum_{i=0}^{\infty}\left[i!(n+i+1)\right]^{-1}\left[\frac{t^{k+1}}{\Gamma(k)\theta^k}\sum_{z=0}^{\infty}\frac{\left(-t/\theta\right)^z}{(z+k)z!}-t\right]^i\left(b_3+\Delta_3\right)^i-p_{32}p_{21}\Delta_1^{-1}\left(b_1-\Delta_1\right)^{n+1}\left[t-\frac{t^{k+1}}{\Gamma(k)\theta^k}\right.$$

$$\left.\sum_{z=0}^{\infty}\frac{\left(-t/\theta\right)^z}{(z+k)z!}\right]^n\times\sum_{i=0}^{\infty}\left[i!(n+i+1)\right]^{-1}\left(\Delta_1-b_1\right)^i\left[t-\frac{t^{k+1}}{\Gamma(k)\theta^k}\sum_{z=0}^{\infty}\frac{\left(-t/\theta\right)^z}{(z+k)z!}\right]^i-p_{32}p_{12}\Delta_2^{-1}\left(b_2-\Delta_2\right)^{n+1}$$

$$\left[t-\frac{t^{k+1}}{\Gamma(k)\theta^k}\sum_{z=0}^{\infty}\frac{\left(-t/\theta\right)^z}{(z+k)z!}\right]^n\sum_{i=0}^{\infty}\left[i!(n+i+1)\right]^{-1}\left(-\left[t-\frac{t^{k+1}}{\Gamma(k)\theta^k}\sum_{z=0}^{\infty}\frac{\left(-t/\theta\right)^z}{(z+k)z!}\right]\left[b_2-\Delta_2\right]\right)^i-p_{23}p_{12}\Delta_3^{-1}$$

$$\left.\left(b_3-\Delta_3\right)^{n+1}\left[t-\frac{t^{k+1}}{\Gamma(k)\theta^k}\sum_{z=0}^{\infty}\frac{\left(-t/\theta\right)^z}{(z+k)z!}\right]^n\times\sum_{i=0}^{\infty}\left(\Delta_3-b_3\right)^i\left[i!(n+i+1)\right]^{-1}\left[t-\frac{t^{k+1}}{\Gamma(k)\theta^k}\sum_{z=0}^{\infty}\frac{\left(-t/\theta\right)^z}{(z+k)z!}\right]^i\right\}.$$

Fig. 5-3 shows the time-varying probability mass function of the number of CRs in the system. When the time increases, the most probable number of CRs in the network also increases. We can also understand the probability mass function spreads wider with the time. This reflects the randomness of *N(t)*, i.e. entropy, increases with time. By using (5-10), Fig. 5-4 demonstrates the probability of miss detection P_m (= 1 - P_d) is indeed a function of the number of collaborative CRs. P_m substantially drops from 10^{-4} to 10^{-7} when the number of CRs increases from 7 to 10. If

CRN ignores the dynamics of CRs and does not adapt the sensing parameters, the uncertainty of the reliability of spectrum sensing has very broad dynamic range. For example, when $N(t=1)$=5, $N(t=2)$=10, and $N(t=3)$=8, then the corresponding probabilities of miss detection at these three time instances are 10^{-3}, 10^{-7}, and 10^{-5}. Therefore, CRN cannot neglect the impacts of dynamic activities of CRs and should adapt the system parameters to meet the network operation requirements, e.g. the interference to the primary user constraint. The receiver operating characteristic (ROC) curve is an important performance evaluation for a detector. The ROC curves, by (5-11) and (5-12), for the energy-based cooperative spectrum sensing over the shadowed Nakagami-*m* fading channels are provided in Fig. 5-5. When the channel is better, e.g. smaller *m* or larger μ_Ω, the spectrum sensing yields more reliable decisions. By using (5-11) and (5-12), Fig. 5-6 shows the ROC curve for the spectrum sensing is not fixed but time-varying. This is because CRs join and leave the cooperation randomly. Thus, the performance of the cooperative spectrum sensing is also dynamically changing.

In order to seek for the spectrum opportunities without interfering to the licensed primary user, CRN not only has to intelligently learn the environments and adapt to the wireless transmission channels but also has to detect the primary users' activities and simultaneously combat the potential interferers. Furthermore, CRN its own network is dynamically changing because of the dynamic behaviors of the CR users. Therefore, CRN also has to adapt the system parameters

accordingly to guarantee the privileges of the primary users and also to optimize CRN its own system performance. The closed form expressions derived in this manuscript are analytically tractable. Thus, CRN can efficiently evaluate the performance metrics to adjust system parameters accordingly to achieve the goal as a self-learning, self-organizing, and self-healing overlay secondary network.

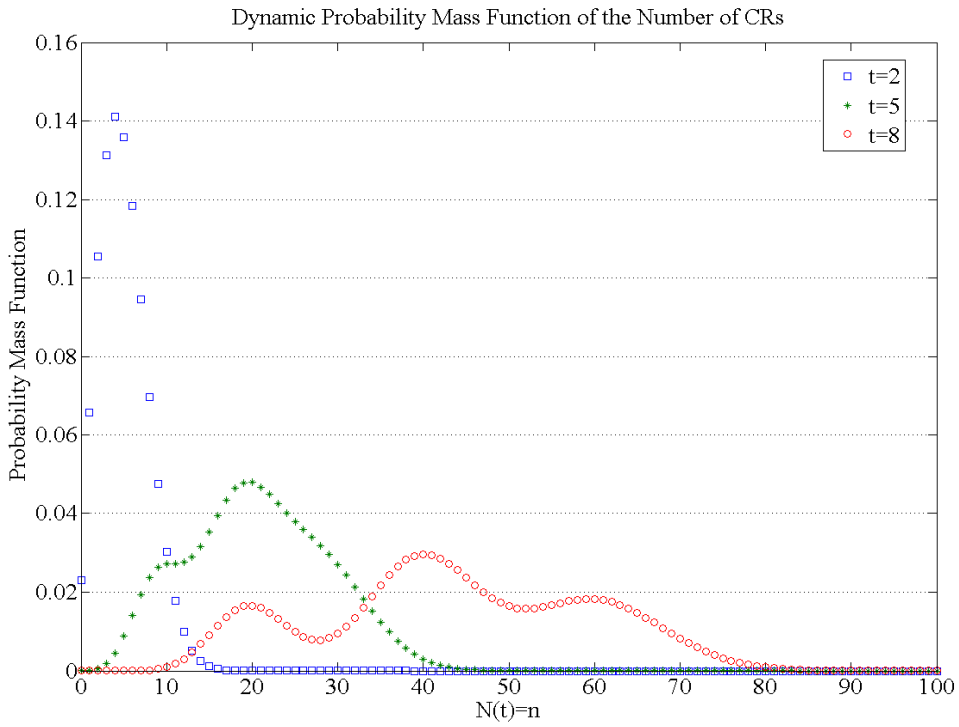

Fig. 5-3. Dynamic Probability Mass Function of the Number of CRs

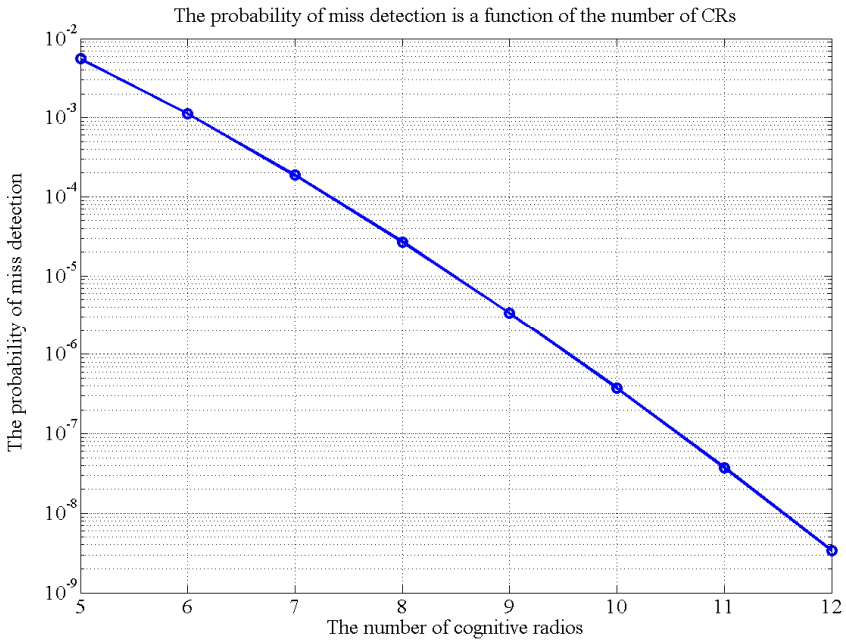

Fig. 5-4. Probability of Miss Detection is a Function of the Number of CRs

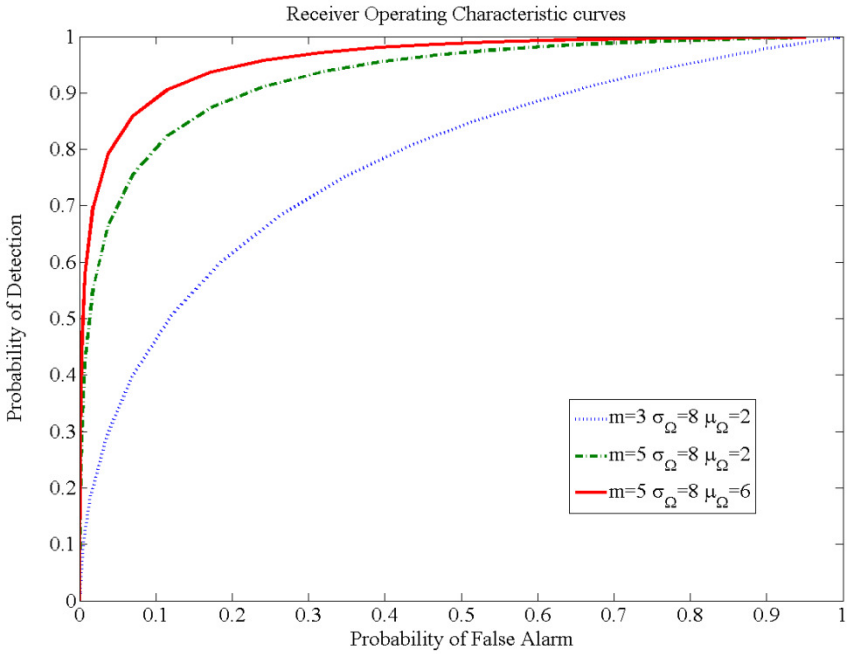

Fig. 5-5. ROC Curves for Shadowed Nakagami-*m* Fading Channels

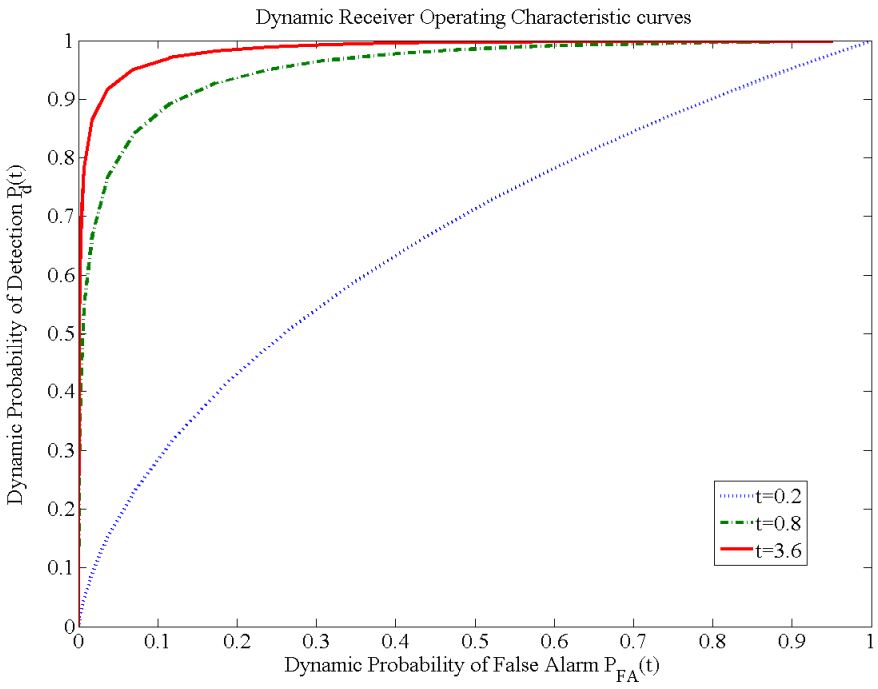

Fig. 5-6. Dynamic Receiver Operating Characteristic Curves

5.3 Summary

We study the dynamic activity effects on spatially distributed energy-based cooperative spectrum sensing in cognitive radio networks. We model the CR users' dynamics by a semi-Markov process with Cox arrival process and random departures. The associated probability mass function of the dynamic number of CRs in the system is derived. We also derive the probability of detection for the energy-based cooperative spectrum sensing in shadowed Nakagami-*m* fading channels by the well-approximated moment generating function

of Gamma-log-normal probability density function. Furthermore, the closed form expressions of the dynamic performance metrics, probability of detection and probability of false alarm, are also obtained. These analytical closed form expressions provide the framework to apply analytical optimization and numerical optimization techniques to efficiently guarantee the global optimality for the system design parameters without exhaustive search. This is essential for cognitive radio networks to real-time adapt the system parameters in the challenging dynamic scenarios which consist of the wireless links, dynamic activities of the primary users, and also the dynamic behaviors of CRs.

References

[5-1] FCC, "Spectrum Policy Task Force Report," FCC ET Docket No. 02-155, Nov. 2002.

[5-2] FCC, "Facilitating opportunities for flexible, efficient and reliable spectrum use employing cognitive radio technologies: Notice of proposed rule making and order," FCC ET Docket No. 03-108, Dec 2003.

[5-3] S. Haykin, "Cognitive radio: Brain-empowered wireless communications," *IEEE J. Sel. Areas Comm.*, vol. 23, no. 2, Feb. 2005.

[5-4] S. Haykin, D. J. Thomson, and J. H. Reed, "Spectrum sensing for cognitive radio,"

Proceedings of the IEEE, Vol. 97, No. 5, May 2009.

[5-5] K. B. Letaief and W. Zhang, "Cooperative communications for cognitive radio networks," *Proceedings of the IEEE*, Vol. 97, No. 5, May 2009.

[5-6] T. Yücek and H. Arslan, "A survey of spectrum sensing algorithms for cognitive radio applications," *IEEE Communications Surveys & Tutorials*, Vol. 11, No. 1, First quarter, 2009.

[5-7] I. F. Akyildiz, B. F. Lo, R. Balakrishnan, "Cooperative spectrum sensing in cognitive radio networks: A survey," *Physical Communication (Elsevier) Journal*, vol. 4, no. 1, pp. 40-62, March 2011.

[5-8] Y. Zeng and Y. C. Liang, "Eigenvalue-Based Spectrum Sensing Algorithms for Cognitve Radio," *IEEE Trans. Communications*, Vol. 57, NO. 6, Jun 2009.

[5-9] P. Pawelczak, K. Nolan, L. Doyle, S. Oh, and D. Cabric, "Cognitive Radio: ten years of experimentation and development," *IEEE Communication Magazine*, Mar. 2011.

[5-10] B. Wang and K. J. R. Liu, "Advances in Cognitive Radio Networks: a survey," *IEEE Journal of Selected Topics in Signal Processing*, Vol. 5, NO.1 Feb. 2011.

[5-11] M. Yacoub, *Foundations of Mobile Radio Engineering*. CRC Press, Inc., 1993.

[5-12] L. R. Rabiner, "A tutorial on hidden Markov Models and selected applications in speech recognition," *Proc. IEEE*, pp. 257-286, Feb. 1989.

[5-13] D. R. Cox and V. Isham, *Point Processes*. Chapman and Hall, 1980.

[5-14] A. L. E. Corral-Ruiz, F. A. Cruz-Perez, and G. Hernandez-Valdez, "Channel holding time in mobile cellular networks with heavy-tailed distributed cell dwell time," *in Proc. IEEE Wireless Commun. Netw. Conf. (WCNC)*, 2011.

[5-15] A. L. E. Corral-Ruiz, F. A. Cruz-Perez, and G. Hernandez-Valdez, "Channel holding time in mobile cellular networks with generalized coxian distributed cell dwell time," in *Procc. IEEE Intl. Sym. On Personal, Indoor and Mobile Radio Comm. (PIMRC)*, 2010.

[5-16] S. Pattaramalai, V.A. Aalo, and G. P. Efthymoglou, "Evaluation of call performance in cellular networks with generalized cell dwell time and call-holding time distributions in the presence of channel fading," *IEEE Transations on Vehicular Technology.*, vol. 58, no. 6, July 2009.

[5-17] R. G. Gallager, *Discrete Stochastic Processes*. Kluwer Academic Publishers, 1995.

[5-18] F. F. Digham, M. Alouini, and M. K. Simon, "On the energy detection of unkown signals over fading channels," *IEEE Trans. Communications*, Vol. 55, NO.1, Jan. 2007.

[5-19] M. Ho and G. Stüber, "Co-channel interference of microcellular systems on shadowed Nakagami fading channels," *Proc. IEEE Veh. Technol. Conf. (VTC'93)*, Secaucus, NJ, May 1993.

[5-20] M. K. Simon and M. Alouini, *Digital Communication over Fading Channels*. John Wiley

& Sons, 2005.

[5-21] M. Abramowitz and I. Stegun, *Handbook of Mathematical Functions With Formulas, Graphs, and Mathematical Tables*, National Bureau of Standards, U.S. Department of Commerce, Dec. 1972.

Chap 6
Applications in Public Safety Networks

The success of wireless communication technology has deeply influenced the human society. Emergency responders, such as policemen, fire fighters, and emergency medical service personnel, are extensively equipped with wireless laptops, handheld computers, mobile video cameras, smart phones, and etc. to improve their efficiency, visibility, and ability to immediately collaborate with central command, coworkers, and other agencies to prevent or respond to incidents. The wireless communication demands for public safety range from data communication, including messaging, email, web browsing, and database access, to multimedia wideband communications, such as voice, picture transfer, and video streaming. Hence, the high priority, reliability, security, data throughput rate, smooth streaming, etc requirements have to be satisfied [6-1], [6-2], and [6-3].

Video surveillance cameras are becoming important effective devices to extend the eyes and ears of public safety agencies. Examples include monitoring disaster conditions and telemedicine for emergency medical services. However, the allocated radio frequency spectrum for public safety use has become highly congested in many urban areas. Furthermore, the first responders

from different public safety agencies and cities often cannot communicate during the emergencies. This is primarily caused by incompatible wireless interfaces among different emergency responders from different jurisdictions. The high demands on interoperability, priority delivery, reliability, and low-latency with least interruptions pose great challenges in the public safety wireless network [6-4], [6-5].

On the other hand, the fixed spectrum allocation regulations have been shown to lead to the spectrum underutilization. Cognitive Radio (CR) is a promising candidate to the solution to the spectral congestion problem [6-6], [6-7]. Federal Communications Commission (FCC) defines CR as "*Cognitive Radio: A radio or system that senses its operational electromagnetic environment and can dynamically and autonomously adjust its radio operating parameters to modify system operation, such as maximize throughput, mitigate interference, facilitate interoperability, and access secondary markets.*" Meanwhile, more available wireless spectrum opportunities, hence larger effective transmit bandwidth by aggregation techniques, can supply the high throughput demand by the multimedia information streaming and also can provide the diversities for multicasting to prevent time-sensitive life-saving information from loss or delay. Therefore, cognitive radio network technologies can provide the physical foundation for public safety emergency networks through larger effective spectrum bandwidth to meet interoperability, priority delivery, reliability, low-latency with least interruptions, and etc requirements.

Spectrum sensing is one of the most challenging and crucial components in CR [6-8]. Several spectrum sensing schemes have been proposed. They can be classified into the following categories: energy detection, matched filter coherent detection, feature-based detection, and eigenvalue-based detection [6-9], [6-10]. Several literatures also provide sequential detection algorithms based on the Hidden Markov Models for the dynamic access networks [6-11], [6-12]. Among these spectrum sensing schemes, energy-based detection is most widely adopted in current CRN prototype system due to the simplicity and low computation cost [6-9]. Therefore, from the practical point of view, in this Chapter, we will focus on the energy-based detection scheme. In order to resolve the hidden primary user issue in fading and shadowing environments, the spatially distributed cooperative spectrum sensing methodologies have been proposed [6-13]. Through the spatially distributed cooperation, the spectrum sensing performance becomes more reliable. However, due to the dynamic number of CRs in a public safety network, the performance metrics, such as probability of detection and probability of false alarm, for spectrum sensing are correspondingly time varying.

6.1 User Dynamic

In the Public Safety community, the mobile terminals, such as the police cars, fire trucks, ambulances, and etc, will rush to the incident location when an incident occurs. Due to the geographical deployment of the police stations, fire departments, and hospitals, the mobile terminals arrive at the incident location at different times. Depending on the kind and severity of the incident and also the degree of severity of the event, the mobile terminals might not only come from the local corresponding facilities, but also come from the organizations in the neighbor cities or counties, see Fig. 6-1. If the level of the damage is extreme, such as unfortunate attacks of 9/11, Hurricane Katrina, the 2010 Haiti Earthquake, or Higashi Nihon Daishinsa (2011 March Japan Earthquake), the rescue teams from the other countries will also do their best to join as soon as possible. However, due to the physical distances, traffic conditions, preparation times, transportation times, and so on, the cognitive mobile terminals will appear in the incident location intermittently. The cognitive mobile terminals in the city which the incident happens will come first within a certain period of time and the cognitive mobile terminals from a neighbor city will come after within some following period of time.

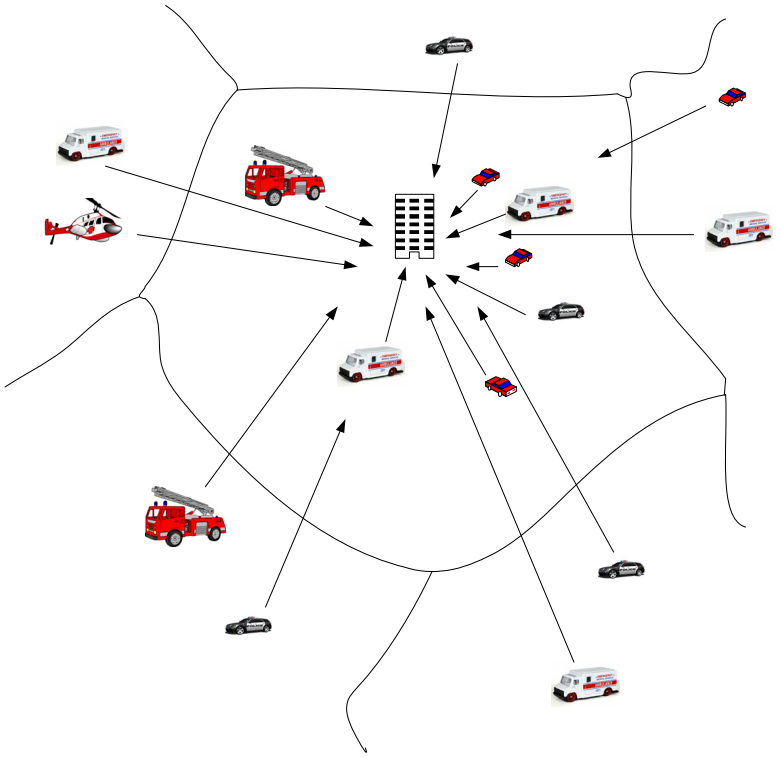

Fig. 6-1 Illustration of the Physical Distances between the Incident Place and Mobile Terminals in a Public Safety Network

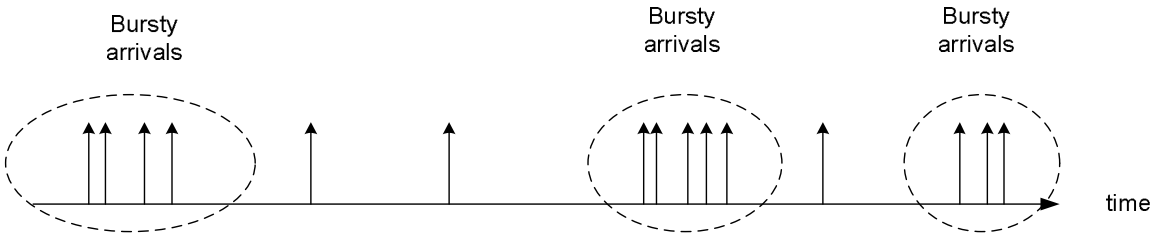

Fig. 6-2 Intermittent Bursty Arrivals

Due to the city/county/country physical distance, the cognitive mobile terminals arrive with alternating high arrival rate and low arrival rate, see Fig. 6-2. Therefore, we can model the arrival

process by a Hidden Markov Model (HMM) with two states, S_H and S_L, which are corresponding to a high arrival rate period and a low arrival rate period respectively. When they arrive, the rescue team members turn on the CR functionalities and hope to search for the available spectrum holes to communicate with each other. They will stay in the incident location for a certain period of time and then leave when they finish their tasks. For example, the persons coming from the ambulances will find the victims first, perform the immediate medical treatments if necessary, and carry the victims to the ER as soon as possible. Hence, the CRs carried by them will stay in the network for a certain period of time and then leave. We can model this behavior by a Pareto distribution [6-15], with two parameters x_m and α_m, where x_m models the time that they spend to find the victims and to perform the necessary immediate emergency medical treatments and α_m value is to model the urgency to leave. After they finish, they leave the place as soon as possible to carry the victims to the hospitals. For the police officers, they will arrive and stay to perform their duties, such as directing traffic in chaotic areas, maintaining the order, and so on. They do not leave like the ambulance people. Therefore, we can model their CRs as persistent CRs which stay in the network without leaving. Therefore, we can categorize the rescue teams into two types of CRs: (I) those that stay in the network without leaving are denoted as in the persistent mode; (II) those that stay in the network for a certain period of time and then leave as soon as possible are denoted as in the dynamic mode.

We can model the emergent dynamic behaviors of CRs and the dynamic number of cognitive mobile terminals at each time instance t, $\{N(t)\}$, as a hyper-semi-Markov process over infinitely countable state space as follows:

$$\{N(t) = n \mid t \in R,\ \mathrm{n} \in \{0, 1, 2, \ldots\}\}. \tag{6-1}$$

$\{N(t)\}$ can be viewed as a composite semi-Markov processes [6-14], as $\{N(t)\}=\{N_I(t)\}+\{N_{II}(t)\}$, where $\{N_I(t)\}$ is to model the dynamic number of type I CRs; $\{N_{II}(t)\}$ models the dynamic number of type II CRs. We will discuss $\{N_I(t)\}$ and $\{N_{II}(t)\}$ in the following subsections.

6.1.1 Type I: Persistent CRs

Due to the geographical deployment, the type I CRs intermittent arrivals can be modeled by a Hidden-Markov Model (HMM) with two states, $S_{p,1}$ and $S_{p,2}$ and the associated transition probabilities $\alpha_{p,1}$ and $\alpha_{p,2}$ as follows:

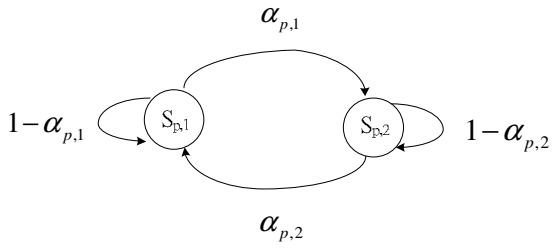

Fig. 6-3. Hidden Markov Model for Persistent CRs

At the low arrival rate periods, CRs join the network follows a Poisson process with rate $\lambda_{p,1}$. During the high arrival rate periods, the arrival process can be modeled as a Poisson process with arrival rate $\lambda_{p,2}$. Hence, the dynamic probability mass function for the number of Type I CRs can be derived as

$$P_{N_I(t)}(t,n) = \frac{t^n}{(\alpha_{p,1}+\alpha_{p,2})n!}\left[{\lambda_{p,1}}^n \alpha_{p,2} e^{-\lambda_{p,1}t} + {\lambda_{p,2}}^n \alpha_{p,1} e^{-\lambda_{p,2}t}\right], \quad \text{n=0,1,2,....} \quad (6\text{-}2)$$

6.1.2 Type II: Dynamic CRs

Similarly, because of the physical distance from the home department locations to the incident location, the type II CRs' arrival process can also be modeled by a HMM with two states, $S_{d,1}$ and $S_{d,2}$, which are associated with a high arrival rate, $\lambda_{d,1}$, and a low arrival rate, $\lambda_{d,2}$ respectively and with transition probabilities, $\alpha_{d,1}$ and $\alpha_{d,2}$ as illustrated in Fig. 6-4.

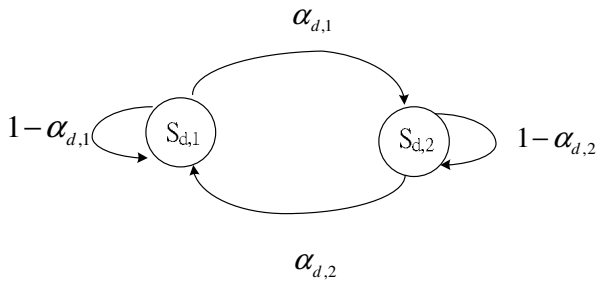

Fig. 6-4. Hidden Markov Model for Dynamic CRs

Given the time for Type II CRs staying in the cooperation following the Pareto distribution with two parameters, $x_m > 0$ and $\alpha_m > 0$, the time-varying probability mass function for the number of Type II CRs in the networks is given by, for $0 \le t < x_m$ and n=0, 1, 2, …,

$$P_{N_{II}(t)}(t,n) = \frac{t^n}{(\alpha_{d,1}+\alpha_{d,2})n!}\left[\lambda_{d,1}{}^n \alpha_{d,2} e^{-\lambda_{d,1}t} + \lambda_{d,2}{}^n \alpha_{d,1} e^{-\lambda_{d,2}t}\right]. \quad (6\text{-}3)$$

For $t \ge x_m$ and n=0,1, 2, …,

$$P_{N_{II}(t)}(t,n) = \frac{1}{(\alpha_{d,1}+\alpha_{d,2})n!}\left[\alpha_{d,2}\left(\frac{\lambda_{d,1}x_m}{1-\alpha_m}\left(x_m^{\alpha_m-1}t^{-\alpha_m+1}-1\right)\right)^n e^{\frac{-\lambda_{d,1}x_m}{1-\alpha_m}\left(x_m^{\alpha_m-1}t^{-\alpha_m+1}-1\right)}\right. \quad (6\text{-}4)$$
$$\left.+\alpha_{d,1}\left(\frac{\lambda_{d,2}x_m}{1-\alpha_m}\left(x_m^{\alpha_m-1}t^{-\alpha_m+1}-1\right)\right)^n e^{\frac{-\lambda_{d,2}x_m}{1-\alpha_m}\left(x_m^{\alpha_m-1}t^{-\alpha_m+1}-1\right)}\right].$$

6.1.3 Total Number of CRs

Therefore, we can obtain the dynamic probability mass function for the total number of CRs $N(t)$ in the network as follows. For $0 \le t < x_m$ and n=0, 1, 2, …,

$$P_{N(t)}(t,n)=\frac{t^n}{n!\left(\alpha_{p,1}+\alpha_{p,2}\right)\left(\alpha_{d,1}+\alpha_{d,2}\right)}\times\Big[\alpha_{p,2}\alpha_{d,2}e^{-\left(\lambda_{p,1}+\lambda_{d,1}\right)t}\left(\lambda_{p,1}+\lambda_{d,1}\right)^n+\alpha_{p,1}\alpha_{d,2}$$
$$e^{-\left(\lambda_{p,2}+\lambda_{d,1}\right)t}\left(\lambda_{p,2}+\lambda_{d,1}\right)^n+\alpha_{p,2}\alpha_{d,1}e^{-\left(\lambda_{p,1}+\lambda_{d,2}\right)t}\left(\lambda_{p,1}+\lambda_{d,2}\right)^n+\alpha_{p,1}\alpha_{d,1}e^{-\left(\lambda_{p,2}+\lambda_{d,2}\right)t}\left(\lambda_{p,2}+\lambda_{d,2}\right)^n\Big]. \quad (6\text{-}5)$$

For $t \ge x_m$ and n=0,1, 2, …,

$$P_{N(t)}(t,n)=\frac{(-1)^{n+1}}{n!\left(\alpha_{p,1}+\alpha_{p,2}\right)\left(\alpha_{d,1}+\alpha_{d,2}\right)\left(1-\alpha_m\right)}\Big\{\Big[\lambda_{p,1}t(1-\alpha_m)+\left(x_m{}^{\alpha_m-1}t^{-\alpha_m+1}-1\right)$$
$$\lambda_{d,1}x_m\Big]^n\alpha_{p,2}\alpha_{d,2}e^{-\left[\lambda_{p,1}t+\frac{\lambda_{d,1}x_m}{1-\alpha_m}\left(x_m{}^{\alpha_m-1}t^{-\alpha_m+1}-1\right)\right]}+\Big[\lambda_{p,2}t(1-\alpha_m)+\left(x_m{}^{\alpha_m-1}t^{-\alpha_m+1}-1\right)\lambda_{d,1}x_m\Big]^n$$
$$\alpha_{p,1}\alpha_{d,2}e^{-\left[\lambda_{p,2}t+\frac{\lambda_{d,1}x_m}{1-\alpha_m}\left(x_m{}^{\alpha_m-1}t^{-\alpha_m+1}-1\right)\right]}+[\lambda_{p,1}t(1-\alpha_m)+\lambda_{d,2}x_m\left(x_m{}^{\alpha_m-1}t^{-\alpha_m+1}-1\right)]^n\alpha_{p,2}\alpha_{d,1} \quad (6\text{-}6)$$
$$e^{-\left[\lambda_{p,1}t+\frac{\lambda_{d,2}x_m}{1-\alpha_m}\left(x_m{}^{\alpha_m-1}t^{-\alpha_m+1}-1\right)\right]}+[\lambda_{p,2}t(1-\alpha_m)+\lambda_{d,2}x_m\left(x_m{}^{\alpha_m-1}t^{-\alpha_m+1}-1\right)]^n\alpha_{p,1}\alpha_{d,1}$$
$$e^{-\left[\lambda_{p,2}t+\frac{\lambda_{d,2}x_m}{1-\alpha_m}\left(x_m{}^{\alpha_m-1}t^{-\alpha_m+1}-1\right)\right]}\Big\}.$$

Since the performance of spatially distributed cooperative spectrum sensing depends on the number of CRs in the network, we can obtain the dynamic performances in the following section based on the above time-varying probability mass function for the total number of CRs in the network.

6.2 Performance Analysis for Shadowed Nakagami-*m* Fading Channels

We consider that spatially distributed CRs form a local Public Safety Network to collaborate in sensing the spectrum utilization to seek the opportunities using available wireless channels to communicate in the disaster area. They randomly select one as the leader of the CRs as the fusion center. Each CR senses the spectrum and sends the collected local energy information through a dedicated error free channel, i.e., 700 MHz Public Safety frequency band, to the fusion center.

6.2.1 System Model

Consider the received signal at the *i*-th CR given by

$$H_0 : r_i(t) = n_i(t),$$
$$H_1 : r_i(t) = h_i(t)x_i(t) + n_i(t), \quad (6\text{-}7)$$

where $x_i(t)$ is the primary complex-valued signal waveform received at the i-th CR, $h_i(t)$ is a slow fading channel, and $n_i(t)$ is the additive white Gaussian noise (AWGN). H_1 is when the primary is using its own licensed band; H_0 means the licensed band is vacant. The i-th CR collects the energy by taking $M/2$ samples of the received waveform $r_i(t)$ both at the I and Q components respectively over a period of time T, and then takes the absolute values, squares, and sums the samples to yield the corresponding collected received signal energy statistic given by

$$y_i = \sum_{k=1}^{M/2} | r_i(k) |^2 . \quad (6\text{-}8)$$

Therefore, the collected energy statistic y_i is given by

$$H_0 : y_i \sim \chi_M^2,$$
$$H_1 : y_i \sim \chi_M^2(2\gamma_i), \quad (6\text{-}9)$$

where, under H_1, y_i has a noncentral chi-square distribution with noncentrality $2\gamma_i$ and M degrees of freedom and, under H_0, y_i has a central chi-square distribution with M degrees of freedom. Then all N CRs transmit the encoded collected energy statistics through a dedicated channel to the fusion center. The fused energy statistics is given by

$$Z = \sum_{i=1}^{N} y_i. \tag{6-10}$$

To make a spectrum sensing decision, the fusion center compares the energy statistic Z to a threshold λ_Z, and then declares $\hat{H}_0$ when $Z < \lambda_Z$ and declares $\hat{H}_1$ when $Z \geq \lambda_Z$. The probability of false alarm, $P(\hat{H}_1 \mid H_0, \gamma)$, and probability of detection, $P(\hat{H}_1 \mid H_1, \gamma)$, conditioned on the Signal-to-Noise Ratio (SNR), γ, are given by [6-16]

$$P_{FA|\gamma} = \frac{\Gamma(Nu, \lambda_Z/2)}{\Gamma(Nu)}, \tag{6-11}$$

$$P_{d|\gamma} = Q_{Nu}\left(\sqrt{2\gamma}, \sqrt{\lambda_Z}\right), \tag{6-12}$$

where $Q_M(a,b)$ is the generalized Marcum Q-function, $\Gamma(x,y)$ is the upper incomplete gamma function, $\Gamma(x)$ is the gamma function, u = TW is the time bandwidth product with T as the

observation time interval and W as the one-sided bandwidth. From (6-12), we know the conditional probability of false alarm is indeed independent of SNR, γ. Therefore, the average probability of false alarm over any fading channels is fully characterized by (6-12). The average probability of detection over a fading channel can be obtained by

$$P_d = \int_0^\infty Q_{Nu}\left(\sqrt{2\gamma}, \sqrt{\lambda_Z}\right) f_\gamma(\gamma) d\gamma. \qquad (6\text{-}13)$$

The detection threshold λ_Z can be decided under the Neyman-Pearson criterion. Under the given desired probability of false alarm, $P_{FA} = \alpha$, λ_Z can be determined and the average probability of detection can be calculated by (6-13).

6.2.2 Shadowed Nakagami-m Fading Channels

A composite shadowed fading wireless fading environment consists of multipath fading superimposed on shadowing. In this environment, the wireless receiver does not average out the envelope fading due to multipath but rather reacts to the instantaneous composite multipath/shadowed signal. This is often the scenario in congested downtown areas with slow pedestrians and vehicles [6-17]. In the Public Safety Networks, the CRs are carried by public

safety agencies and only moving slowly or even almost stationary around the disaster area. Therefore, we propose to model the wireless links for CRs in the Public Safety Networks by a composited shadowed Nakagami-*m* channel model introduced by Ho and Stöber [6-18]. This composite shadowed fading channel has the Gamma-log-normal probability density function as follows:

$$f(\gamma)=\int_0^{\infty}\left(\frac{m}{w}\right)^m\frac{\gamma^{m-1}}{\Gamma(m)}e^{-m\gamma/w}\frac{10}{\sqrt{2\pi}\ln(10)\sigma_\Omega w}\exp\left\{-\left[10\log_{10}(w)-\mu_\Omega\right]^2\Big/2\sigma_\Omega{}^2\right\}dw, \quad (6\text{-}14)$$

where *m* is the Nakagami-*m* parameter and μ_Ω and σ_Ω are the parameters for the log-normal shadowing. By [6-19], we can obtain the well approximated moment generating function for the Gamma-log-normal probability density function as

$$M_\gamma(s)\cong\frac{1}{\sqrt{\pi}}\sum_{j=1}^{N_p}H_{x_j}(1-10^{\left(\sqrt{2}\sigma_\Omega x_j+\mu_\Omega\right)/10}\times\frac{s}{m})^{-m}. \quad (6\text{-}15)$$

Therefore, after carrying out routine mathematical manipulations, the average probability of detection over the composite shadowed Nakagami-m fading channel can be obtained by

$$P_d = \sum_{k=0}^{\infty} \frac{(-1)^k \Gamma(m+k)\Gamma(Nu+k, \lambda_Z/2)}{k!\sqrt{\pi} m^{k+1} \Gamma(m)\Gamma(Nu+k)} \sum_{j=1}^{N_p} H_{x_j} 10^{\left(\sqrt{2}\sigma_\Omega x_j + \mu_\Omega\right)/10} \left(m - 10^{\left(\sqrt{2}\sigma_\Omega x_j + \mu_\Omega\right)/10}\right)^{-(m+k)}, \quad (6\text{-}16)$$

where x_j are the zeros of the N_p-order polynomial and H_{xj} are the weight factors of the N_p-order Hermite polynomial [6-20].

6.2.3 Dynamic Performance Analysis

The cooperative spectrum sensing performance is varying because of fading, shadowing, etc. On the other hand, since the number of CRs in CRN is also dynamically changing, the cooperative spectrum sensing performance is varying accordingly. The average probability of false alarm and the average probability of detection in the above subsections are under some fixed number of CRs in the cooperation. In this subsection, we consider the dynamic of the number of CRs in the network to analyze the dynamic performances. The dynamic probability of false alarm can be obtained by, for $0 \leq t < x_m$ and n=0, 1, 2, …,

$$P_{FA}(t)=\sum_{n=1}^{\infty}\frac{t^{n}\Gamma(nu,\lambda_{Z}/2)}{n!\left(\alpha_{p,1}+\alpha_{p,2}\right)\left(\alpha_{d,1}+\alpha_{d,2}\right)\Gamma(nu)}\Big[\alpha_{p,2}\alpha_{d,2}e^{-\left(\lambda_{p,1}+\lambda_{d,1}\right)t}\left(\lambda_{p,1}+\lambda_{d,1}\right)^{n}$$
$$+\alpha_{p,1}\alpha_{d,2}\times e^{-\left(\lambda_{p,2}+\lambda_{d,1}\right)t}\left(\lambda_{p,2}+\lambda_{d,1}\right)^{n}+\alpha_{p,2}\alpha_{d,1}e^{-\left(\lambda_{p,1}+\lambda_{d,2}\right)t}\left(\lambda_{p,1}+\lambda_{d,2}\right)^{n} \quad (6\text{-}17)$$
$$+\alpha_{p,1}\alpha_{d,1}e^{-\left(\lambda_{p,2}+\lambda_{d,2}\right)t}\left(\lambda_{p,2}+\lambda_{d,2}\right)^{n}\Big].$$

For $t \geq x_m$ and n=0,1, 2, …,

$$P_{FA}(t)=\sum_{n=1}^{\infty}\frac{(-1)^{n+1}\,\Gamma(nu,\lambda_{Z}/2)}{n!\Gamma(nu)\left(\alpha_{p,1}+\alpha_{p,2}\right)\left(\alpha_{d,1}+\alpha_{d,2}\right)(1-\alpha_{m})}\Big\{\alpha_{p,2}\alpha_{d,2}$$
$$[\lambda_{p,1}t(1-\alpha_{m})+\lambda_{d,1}x_{m}\left({x_{m}}^{\alpha_{m}-1}t^{-\alpha_{m}+1}-1\right)]^{n}e^{-\left[\lambda_{p,1}t+\frac{\lambda_{d,1}x_{m}}{1-\alpha_{m}}\left({x_{m}}^{\alpha_{m}-1}t^{-\alpha_{m}+1}-1\right)\right]}$$
$$+[\lambda_{p,2}t(1-\alpha_{m})+\lambda_{d,1}x_{m}\left({x_{m}}^{\alpha_{m}-1}t^{-\alpha_{m}+1}-1\right)]^{n}\alpha_{p,1}\alpha_{d,2}$$
$$e^{-\left[\lambda_{p,2}t+\frac{\lambda_{d,1}x_{m}}{1-\alpha_{m}}\left({x_{m}}^{\alpha_{m}-1}t^{-\alpha_{m}+1}-1\right)\right]}+[\lambda_{p,1}t(1-\alpha_{m})+\lambda_{d,2}x_{m}\left({x_{m}}^{\alpha_{m}-1}t^{-\alpha_{m}+1}-1\right)]^{n} \quad (6\text{-}18)$$
$$\alpha_{p,2}\alpha_{d,1}e^{-\left[\lambda_{p,1}t+\frac{\lambda_{d,2}x_{m}}{1-\alpha_{m}}\left({x_{m}}^{\alpha_{m}-1}t^{-\alpha_{m}+1}-1\right)\right]}+[\lambda_{p,2}t(1-\alpha_{m})+\lambda_{d,2}x_{m}\times$$
$$\left({x_{m}}^{\alpha_{m}-1}t^{-\alpha_{m}+1}-1\right)]^{n}\alpha_{p,1}\alpha_{d,1}e^{-\left[\lambda_{p,2}t+\frac{\lambda_{d,2}x_{m}}{1-\alpha_{m}}\left({x_{m}}^{\alpha_{m}-1}t^{-\alpha_{m}+1}-1\right)\right]}\Big\}.$$

Similarly, the dynamic probability of detection can be obtained by, for $0 \leq t < x_m$ and n=0, 1, 2, …,

$$P_d(t)=\sum_{n=1}^{\infty}\sum_{k=0}^{\infty}\frac{(-1)^k t^n\Gamma(m+k)\Gamma(Nu+k,\lambda_Z/2)}{n!k!\sqrt{\pi}m^{k+1}\Gamma(m)\Gamma(Nu+k)\left(\alpha_{p,1}+\alpha_{p,2}\right)\left(\alpha_{d,1}+\alpha_{d,2}\right)}\sum_{j=1}^{N_p}H_{x_j}10^{\left(\sqrt{2}\sigma_\Omega x_j+\mu_\Omega\right)/10}$$

$$\left(m-10^{\left(\sqrt{2}\sigma_\Omega x_j+\mu_\Omega\right)/10}\right)^{-(m+k)}\left[\alpha_{p,2}\alpha_{d,2}e^{-\left(\lambda_{p,1}+\lambda_{d,1}\right)t}\left(\lambda_{p,1}+\lambda_{d,1}\right)^n+\alpha_{p,1}\alpha_{d,2}e^{-\left(\lambda_{p,2}+\lambda_{d,1}\right)t}\right.$$

$$\left.\left(\lambda_{p,2}+\lambda_{d,1}\right)^n+\alpha_{p,2}\alpha_{d,1}e^{-\left(\lambda_{p,1}+\lambda_{d,2}\right)t}\left(\lambda_{p,1}+\lambda_{d,2}\right)^n+\alpha_{p,1}\alpha_{d,1}e^{-\left(\lambda_{p,2}+\lambda_{d,2}\right)t}\left(\lambda_{p,2}+\lambda_{d,2}\right)^n\right]. \quad (6\text{-}19)$$

For $t \geq x_m$ and n=0,1, 2, …,

$$P_d(t)$$

$$=\sum_{n=1}^{\infty}\sum_{k=0}^{\infty}\frac{(-1)^{n-k+1}\Gamma(m+k)\Gamma(Nu+k,\lambda_Z/2)}{n!k!\sqrt{\pi}m^{k+1}\Gamma(m)\Gamma(Nu+k)\left(1-\alpha_m\right)}\sum_{j=1}^{N_p}H_{x_j}10^{\left(\sqrt{2}\sigma_\Omega x_j+\mu_\Omega\right)/10}\left(m-10^{\left(\sqrt{2}\sigma_\Omega x_j+\mu_\Omega\right)/10}\right)^{-(m+k)}$$

$$\frac{1}{\left(\alpha_{p,1}+\alpha_{p,2}\right)\left(\alpha_{d,1}+\alpha_{d,2}\right)}\left\{\left[\lambda_{p,1}t(1-\alpha_m)+\lambda_{d,1}\,x_m\left({x_m}^{\alpha_m-1}t^{-\alpha_m+1}-1\right)\right]^n\alpha_{p,2}\alpha_{d,2}\right.$$

$$e^{-\left[\lambda_{p,1}t+\frac{\lambda_{d,1}x_m}{1-\alpha_m}\left({x_m}^{\alpha_m-1}t^{-\alpha_m+1}-1\right)\right]}+\left[\lambda_{p,2}t(1-\alpha_m)+\lambda_{d,1}x_m\left({x_m}^{\alpha_m-1}t^{-\alpha_m+1}-1\right)\right]^n e^{-\left[\lambda_{p,2}t+\frac{\lambda_{d,1}x_m}{1-\alpha_m}\left({x_m}^{\alpha_m-1}t^{-\alpha_m+1}-1\right)\right]}$$

$$\alpha_{p,1}\alpha_{d,2}+[\lambda_{p,1}t(1-\alpha_m)+\lambda_{d,2}x_m\left({x_m}^{\alpha_m-1}t^{-\alpha_m+1}-1\right)]^n\alpha_{p,2}\alpha_{d,1}e^{-\left[\lambda_{p,1}t+\frac{\lambda_{d,2}x_m}{1-\alpha_m}\left({x_m}^{\alpha_m-1}t^{-\alpha_m+1}-1\right)\right]}$$

$$\left.+\left[\lambda_{p,2}t(1-\alpha_m)+\lambda_{d,2}\,x_m\left({x_m}^{\alpha_m-1}t^{-\alpha_m+1}-1\right)\right]^n\alpha_{p,1}\,\alpha_{d,1}e^{-\left[\lambda_{p,2}t+\frac{\lambda_{d,2}x_m}{1-\alpha_m}\left({x_m}^{\alpha_m-1}t^{-\alpha_m+1}-1\right)\right]}\right\}. \quad (6\text{-}20)$$

The number of CRs is dynamic as we can understand in Fig. 6-5. As time goes by, the average number of CRs in the system increases. However, the associated probability mass function also spreads wider when the time increases. Therefore, the dynamic range of possible number of CRs in the system becomes larger such that the dynamic performance of the

cooperative spectrum sensing also has larger dynamic range. This means the PHY-layer spectrum sensing decisions might be reached with high reliability by many CRs or with low reliability by few CRs. Thus, there is the issue of how CRN should dynamically adapt the management protocols in the spectrum sensing level. The shadowed fading channels affect the spectrum sensing performances. In Fig. 6-6, we plots the the receiver operating characteristic (ROC) curves (P_d versus P_{FA}) for different combinations of Nakagami-*m* fading parameter, *m*, and log-normal shadowing parameters, μ_Ω and σ_Ω. Smaller *m* means more severe the fading effect, i.e., Nakagami-*m* fading degenerates to Rayleigh fading when *m* = 1. Since σ_Ω is typically observed between 5 to 12 dB in macrocellular applications and between 4 to 13 dB in microcellular applications, we use σ_Ω = 8 dB to generate the curves in Fig. 6-6. When the channels are more benign, the receiver yields better detection results. Fig. 6-7 shows the dynamic probability of false alarm under different $\alpha_{p,2}$ and $\alpha_{d,2}$. When time goes by, the more CRs are in the network to collaborate and the probability of false alarm drops significantly. As we can see, when both type I and type II CRs are more likely staying in the high arrival periods, the probability of false alarm becomes smaller and thus CRN is less probable to miss the opportunities to exploit the vacant band to enhance its own throughput. The red curve is the case when only type I CRs stay longer in high arrival rate periods; the green curve represents the case when only type II CRs stay longer in high arrival rate periods. When only one of the two types of

CRs stay longer in the high arrival rate periods, the red curve outperforms the green curve. Hence, the type I CRs are more influential compared to type II CRs. This is because type I CRs stay in the network but type II CRs would leave the cooperation after their jobs in the incident location are done.

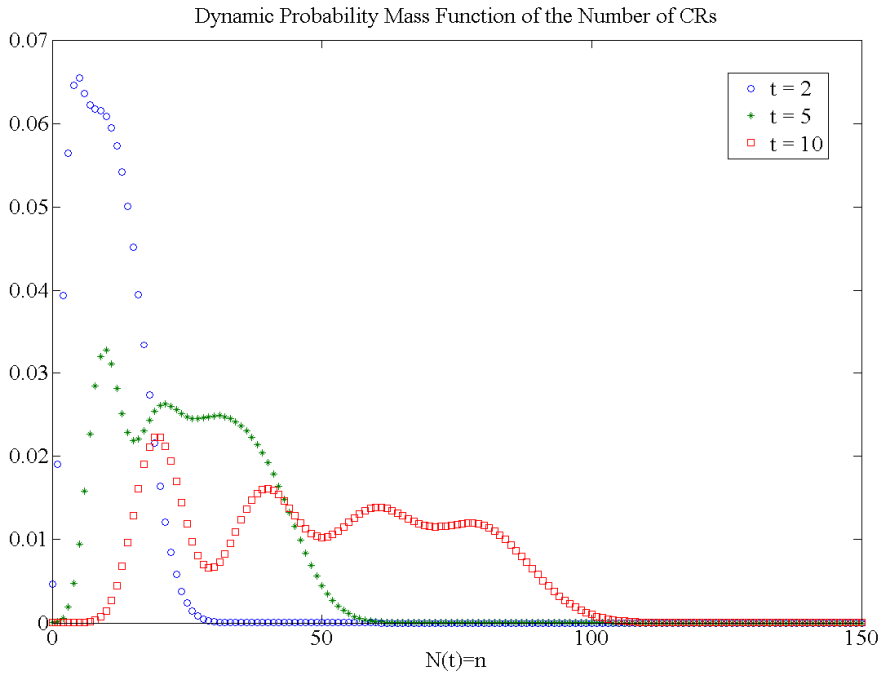

Fig. 6-5. $P_{N(t)}(n, t)$ at t = 2, 5, and 10.

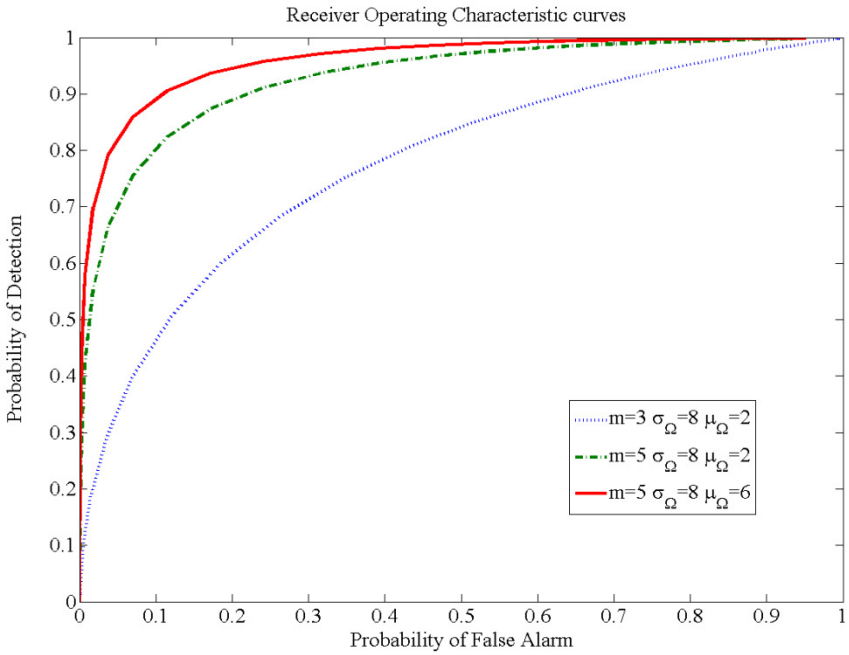

Fig. 6-6. Receiver Operating Characteristic Curves for Shadowed Nakagami-*m* Fading Channels

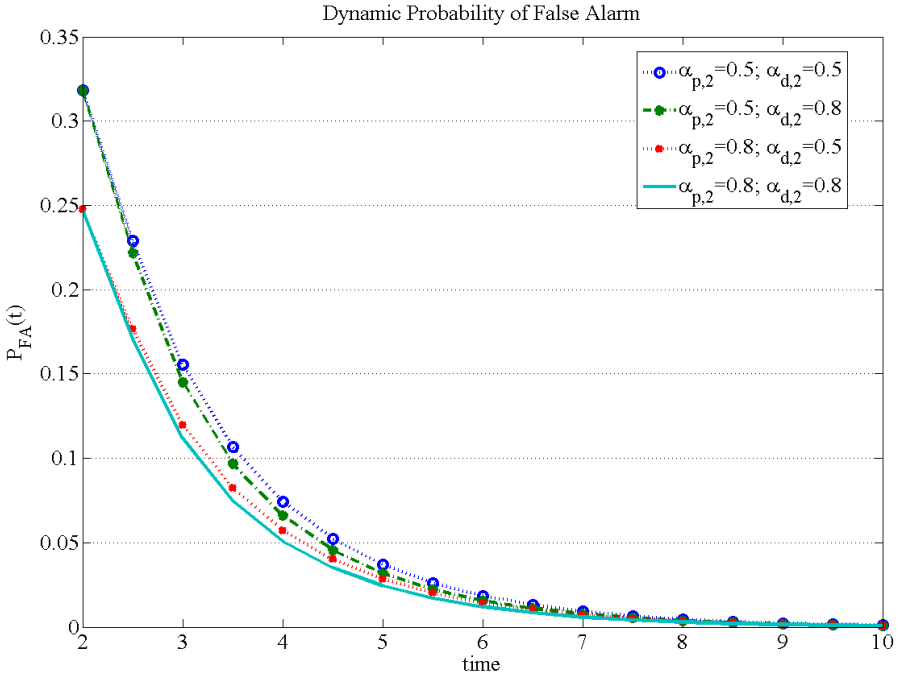

Fig. 6-7. Dynamic Probability of False Alarm with Different $\alpha_{p,2}$ and $\alpha_{d,2}$

6.3 Summary

In this Chapter, we modeled the emergent behaviors of CRs by a hyper-semi-Markov process and the performances for energy-based spectrum sensing over shadowed Nakagami-*m* fading channels were derived. The close forms of dynamic probability of false alarm and dynamic probability of detection were derived. These close-form expressions can provide the framework for the cognitive radio public safety network system to perform the online adaptation/learning.

References

[6-1] Ali Gorcin and Huseyin Arslan, "Public Safety and Emergency Case Communications: Opportunity from the Aspect of Cognitive Radio," In *IEEE Symposium on New Frontiers in Dynamic Spectrum Access Networks (DySPAN)*, Chicago, Illinois, October 14-17, 2008.

[6-2] D. Scaperoth, B. Le, T. W. Rondeau, D. Maldonado, and C. W. Bostian, "Cognitive Radio Platform Development for Interoperability," In *Military Communications Conference (MILCOM)*, Washington D.C., October 2006.

[6-3] John S. Powell, "Cognitive and Software Radio: A Public Safety Regulatory Perspective," In *National Public Safety Telecommunicastions Council Committee and Governing Board Meeting*, Washington D. C., June 14-15, 2004.

[6-4] "U.S. Department of Homeland Security, Public Safety Statement of Requirements for Communications and Interoperability," vol. 1, ver. 1.2, October 2006.

[6-5] P. Pawelczak, R. Venkatesha Prasad, L. Xia, I.G.M.M. Niemegeers, "Cognitive Radio Emergency Networks – Requirements and Designs," In *IEEE Symposium on New Frontiers in Dynamic Spectrum Access Networks (DySPAN)*, Baltimore, Maryland, November 8-11, 2005.

[6-6] S. Haykin, "Cognitive radio: Brain-empowered wireless communications," *IEEE J. Sel. Areas Comm.*, vol. 23, no. 2, Feb. 2005.

[6-7] Ekram Hossain, Dusit Niyato, and Zhu Han, *Dynamic Spectrum Access in Cognitive Radio Networks*, *Cambridge University Press,* 2009.

[6-8] B. Wang and K. J. R. Liu, "Advances in Cognitive Radio Networks: a survey," *IEEE J. of Sel. Topics in Sig. Proc.*, Vol. 5, NO.1 Feb. 2011.

[6-9] P. Pawelczak, K. Nolan, L. Doyle, S. Oh, and D. Cabric, "Cognitive Radio: ten years of experimentation and development," *IEEE Communication Magazine*, Mar. 2011.

[6-10] Y. Zeng and Y.C. Liang, "Eigenvalue-Based Spectrum Sensing Algorithms for Cognitve Radio," *IEEE Trans. Communications*, Vol. 57, NO. 6, Jun 2009.

[6-11] Z. Sun, G. Bradford, and J. N. Laneman, "Sequence Detection Algorithms for PHY-Layer Sensing in Dynamic Spectrum Access Networks," *IEEE Journal of Selected Topics in Signal Prorcessing*, Vol. 5, Feb. 2011.

[6-12] C. Ghosh, C. Cordeiro, D. Agrawal, and M. Rao, "Markov Chain Existence and Hidden Markov Models in Spectrum Sensing," *IEEE PerCom*, Mar. 2009.

[6-13] G. Ganesan and Y. Li, "Cooperative Spectrum Sensing in Cognitive Radio Networks," In *IEEE Symposium on New Frontiers in Dynamic Spectrum Access Networks (DySPAN)*, 2005.

[6-14] R. G. Gallager, *Discrete Stochastic Processes*. Kluwer Academic Publishers, 1995.

[6-15] A. L. E. Corral-Ruiz, F. A. Cruz-Perez, and G. Hernandez-Valdez, "Channel holding time in mobile cellular networks with heavy-tailed distributed cell dwell time," *in Proc. IEEE Wireless Commun. Netw. Conf. (WCNC)*, 2011.

[6-16] F. F. Digham, M. Alouini, and M. K. Simon, "On the energy detection of unkown signals over fading channels," *IEEE Trans. Communications*, Vol. 55, NO.1, Jan. 2007.

[6-17] H. Suzuki, "A statistical model for urban multipath propagation," *IEEE Trans. Commun.*, vol. COM-25, July 1977.

[6-18] M. Ho and G. Stüber, "Co-channel interference of microcellular systems on shadowed Nakagami fading channels," *Proc. IEEE Veh. Technol. Conf. (VTC'93)*, Secaucus, NJ, May 1993.

[6-19] M. K. Simon and M. Alouini, *Digital Communication over Fading Channels*. John Wiley & Sons, 2005.

[6-20] M. Abramowitz and I. Stegun, *Handbook of Mathematical Functions With Formulas, Graphs, and Mathematical Tables*, National Bureau of Standards, U.S. Department of Commerce, Dec. 1972.

Chap 7
Conclusions

In this dissertation, we study the cooperative spectrum sensing for the self-organizing dynamic overlay cognitive radio networks system. Dynamic spatial diversity is analyzed for when the number of CR users in the network is random. We derive the exact closed form expressions for dynamic probability of detection and dynamic probability of false alarm for cooperative spectrum sensing over different wireless links conditions. The long-term asymptotic performance metrics, probabilities of detection and false alarm, are also analyzed under these different scenarios.

We also investigate two promising CRN technologies applications: cellular wireless systems and public safety emergency network systems and derive the explicit performance expressions of cooperative spectrum sensing in these two application scenarios over practical composite Nakagami-*m* fading and log-normal shadowing channels in the dense-populated urban areas. These analytically tractable expressions enable the efficient optimization of system performance without costly exhaustive search. This capability is critical for CRN to operate in harsh dynamic application scenarios with the wireless links, the primary users' dynamics, and

the CRs' dynamics such that CRN can self-organize its own network and guarantee the privileges of the licensed primary users.